



Development of novel *Listeria monocytogenes* strains as
therapeutic agents for targeted tumor therapy

Entwicklung von neuen *Listeria monocytogenes* Stämmen
zur Anwendung in der Tumorthherapie

Doctoral thesis for submission to a doctoral degree
at the Graduate School of Life Sciences,
Julius Maximilian University Würzburg,
Section Infection and Immunity

submitted by

Martin Heisig

from

Fulda

Würzburg, 2009

Submitted on:

Members of the *Promotionskomitee*:

Chairperson: Prof. Dr. Thomas Müller

Supervisor (first): Prof. Dr. Werner Goebel

Supervisor (second): Prof. Dr. Ulf Rapp

Supervisor (third): PD. Dr. Ivaylo Gentshev

Day of Rigorosum:

Certificates were handed-out on:

Affidavit

(Eidesstattliche Erklärung)

I hereby declare that my thesis entitled

is the result of my own work. I did not receive any help or support from commercial consultants. All sources and / or materials applied are listed and specified in the thesis.

Furthermore, I verify that this thesis has not yet been submitted as part of another examination process neither in identical nor in similar form.

Würzburg
Date Signature

1	ABSTRACTS	1
1.I	Summary	1
1.II	Zusammenfassung	2
2	INTRODUCTION	4
2.I	Cancer	4
2.II	Current cancer therapy	4
2.III	Cancer and infection	5
2.III.1	Application of bacteria in cancer immunotherapy	5
2.III.2	Targeted cancer therapy using bacteria and viruses	7
2.III.2.a	Viral accumulation in tumors	7
2.III.2.b	Bacterial accumulation in tumors	8
2.III.2.c	Approaches in tumor therapy using targeted bacteria	10
2.III.2.d	Limitations of bacterial and viral use in tumor therapy	11
2.IV	Listeria monocytogenes	12
2.IV.1	Epidemiology and Pathogenesis	12
2.IV.2	Infection cycle	13
2.IV.3	Use of <i>L. monocytogenes</i> as targeted carrier	14
3	AIM OF STUDY	16
3.I	RNA delivery by <i>L. monocytogenes</i>	16
3.II	Improvement of <i>L. monocytogenes</i> tumor colonization	17
3.II.1	Antibody-mediated tumor targeting by <i>L. monocytogenes</i>	17
3.II.2	Evaluation of two <i>L. monocytogenes</i> mutants as tumor targeting vectors	19
4	MATERIAL	20
4.I	Bacterial strains	20

4.II	Plasmids	21
4.III	Oligonucleotide sequences	22
4.III.1	PCR primer	22
4.III.2	shRNA DNA oligomers	24
4.III.3	qRT-PCR primer	24
4.IV	Eukaryotic cell lines	25
4.V	Antibodies	26
4.VI	Buffers and solutions	26
4.VI.1	Media	26
4.VI.2	Buffers	27
4.VI.3	Solutions	28
4.VII	Animals	28
4.VIII	Consumables and chemicals	28
4.IX	Enzymes and special reagents	29
5	METHODS	30
5.I	Microbiology	30
5.I.1	General bacterial culture	30
5.I.2	Electrotransformation	30
5.I.3	Preparation of infection aliquots	31
5.I.4	Quick lysate of <i>L. monocytogenes</i>	31
5.II	Molecular biology	31
5.II.1	Isolation and purification of DNA	31
5.II.2	Agarose gel electrophoresis	32
5.II.3	Polymerase chain reaction (PCR)	32
5.II.3.a	Colony PCR	32
5.II.3.b	PCR for cloning	34
5.II.4	Site directed mutagenesis	34

5.II.5	Annealing of DNA oligomers for cloning	35
5.II.6	Enzymatic DNA modifications	36
5.II.6.a	DNA restriction	36
5.II.6.b	Ligation	36
5.II.6.c	Phosphorylation	37
5.II.6.d	Dephosphorylation	37
5.II.7	Construction of <i>L. monocytogenes</i> mutants	37
5.II.8	Analysis of bacterial growth kinetics	38
5.II.9	RNA analysis	38
5.II.9.a	RNA isolation with DNase digestion	38
5.II.9.b	RNA polyacrylamide gel electrophoresis	39
5.II.9.c	Reverse transcription of RNA	40
5.II.10	Quantitative Real Time-PCR (qRT-PCR)	40
5.II.11	Treatments of live <i>L. monocytogenes</i> for antibody coating	42
5.II.11.a	Coating	42
5.II.11.b	Crosslinking	42
5.II.11.c	Serum treatment of <i>L. monocytogenes</i>	42
5.II.12	Haematoxinilin Eosin staining	42
5.III	Protein analysis	43
5.III.1	Protein isolation	43
5.III.1.a	Cellular proteins	43
5.III.1.b	Secreted proteins	43
5.III.1.c	Membrane proteins	44
5.III.2	Polyacrylamide gel electrophoresis	44
5.III.3	Western blot analysis	45
5.IV	Eukaryotic cell biology	45
5.IV.1	General eukaryotic cell culture	45
5.IV.2	Infection assay using bacteria	45
5.IV.3	Treatment of eukaryotic cells using magnetic beads	46
5.IV.4	Quantitation of prodrug conversion <i>in vitro</i> (prodrug assay)	46
5.IV.5	Fluorescence imaging of GFP positive cells	47

5.IV.6	Immunofluorescence staining	47
5.IV.7	Flow cytometry	48
5.V	Animal experiments	48
5.V.1	General animal handling	48
5.V.2	Induction and measurement of tumor growth	48
5.V.3	Determination of the bacterial count in murine tissues	48
5.V.3.a	Bacterial load per gram organ mass	48
5.V.3.b	Bacterial load per cell population	49
5.V.4	Isolation of murine serum	49
6	RESULTS	50
6.I	Reduction of cell-membrane tension by <i>L. monocytogenes</i> virulence factor InlC and influence on cell-to-cell spread	50
6.I.1	Generation of <i>L. monocytogenes inlC</i> mutants	50
6.I.2	Influence of InlC on apical cell junctions and cell-to-cell spread by <i>L. monocytogenes</i>	50
6.II	RNA delivery into eukaryotic cells by <i>L. monocytogenes</i>	52
6.II.1	Integration of T7 RNA polymerase into the genome of <i>L. monocytogenes</i>	52
6.II.1.a	Generation of T7 RNA polymerase integration vector and genomic integration	52
6.II.1.b	Cloning of stabilized expression vectors for RNA delivery	52
6.II.1.c	Analysis of the trimmed RNA delivery strain	53
6.II.2	shRNA delivery	55
6.II.2.a	Cloning of SMAC/DIABLO shRNA delivery vector	55
6.II.2.b	Purification and analysis of small RNAs	56
6.III	Protein A mediated antibody coating of <i>L. monocytogenes</i>	58
6.III.1	Characterization of bacterial antibody coating	58
6.III.1.a	Quantitation and specificity of antibody binding	58
6.III.1.b	Kinetics of antibody coating	60
6.III.2	Antibody-mediated internalization of <i>L. monocytogenes in vitro</i>	61

6.III.2.a	Evaluation of optimal antibody concentrations for antibody-mediated internalization	61
6.III.2.b	Comparison of bacterial internalization into isogenic cell lines	62
6.III.2.c	Influence of cell density and bacterial MOI during infection on antibody-mediated internalization	64
6.III.2.d	Adherence, internalization and replication of protein A expressing <i>L. monocytogenes</i>	65
6.III.2.e	Cetuximab-mediated internalization into human cancer cell lines	68
6.III.2.f	Antibody-mediated internalization of prodrug-converting <i>L. monocytogenes</i>	69
6.III.3	Mechanistic insights into antibody-mediated internalization	71
6.III.3.a	Antibody-mediated internalization of Lm-spa ⁺ using fluorescent antibodies	71
6.III.3.b	Coating beads with fluorescent antibodies	73
6.III.3.c	Antibody-mediated internalization of Dynabeads®	75
6.III.4	Examination of antibody-mediated tumor targeting <i>in vivo</i>	76
6.III.4.a	Generation of a xenograft tumor model using cell lines overexpressing HER2/neu	76
6.III.4.b	Antibody-mediated bacterial tumor targeting <i>in vivo</i>	79
6.III.4.c	Investigation of the non-functionality of antibody-mediated targeting <i>in vivo</i>	80
6.III.4.d	Covalent crosslinking of antibodies to protein A on the surface of viable Lm-spa ⁺	82
6.III.4.e	Crosslinking partially prevents the effect of murine serum on antibody-mediated internalization	84
6.III.4.f	Tumor targeting of Lm-spa ⁺ crosslinked to antibodies	86
6.IV	Bacterial colonization of murine organs after infection using different <i>L. monocytogenes</i> mutants	88
6.IV.1	Colonization pattern of <i>L. monocytogenes</i> Δhpt mutants in a murine tumor model	88
6.IV.1.a	The Δhpt mutant in a xenograft mouse tumor model	89
6.IV.1.b	Attenuation of <i>L. monocytogenes</i> Δhpt	90
6.IV.1.c	The $\Delta aroA \Delta hpt$ mutant in a xenograft mouse tumor model	90
6.IV.2	Colonization pattern of <i>L. monocytogenes</i> $\Delta inIGHE$ mutants in a murine tumor model	91
6.IV.2.a	The $\Delta inIGHE$ mutant in a xenograft mouse tumor model	91
6.IV.2.b	The $\Delta aroA \Delta inIGHE$ mutant in a xenograft mouse tumor model	92
7	DISCUSSION	93

7.I	Influence of InIC on apical cell junctions and cell-to-cell spread by <i>L. monocytogenes</i>	93
7.II	RNA delivery into eukaryotic cells by <i>L. monocytogenes</i>	94
7.III	Protein A mediated antibody coating of <i>L. monocytogenes</i>	97
7.IV	Bacterial colonization of murine organs after infection using different <i>L. monocytogenes</i> mutants	104
8	REFERENCES	106
9	APPENDIX	120
9.I	Abbreviations	120
9.II	Publications	122
9.III	Curriculum Vitae	123
10	ACKNOWLEDGMENTS	124

1 Abstracts

1.1 Summary

Despite marked progress in development and improvement of cancer therapies the rate of cancer related death remained stable over the last years. Especially in treating metastases alternative approaches supporting current therapies are required. Bacterial and viral vectors have been advanced from crude tools into highly sophisticated therapeutic agents detecting and treating neoplastic lesions. They might be potent enough to fill in this therapeutic demand.

In this thesis *Listeria monocytogenes* was investigated as carrier for targeted bacterial cancer therapy. One part of the study focussed on modification of a functional bacterial mRNA delivery system. Genomic integration of T7 RNA polymerase driving mRNA production allowed reduction to an one-plasmid-system and thereby partially relieved the growth retardation exerted by mRNA delivery. Importantly the integration allowed metabolic attenuation of the mRNA delivery mutant potentially enabling *in vivo* applications. Further expansion of the bacterial RNA delivery system for transfer of shRNAs was examined. Bacterial mutants producing high amounts of RNA containing shRNA sequences were constructed, however a functional proof of gene silencing on delivery in eukaryotic cell lines was not achieved.

The second part of this thesis focussed on increasing tumor colonization by *Listeria monocytogenes in vivo*. Coating bacteria with antibodies against receptors overexpressed on distinct tumor cell lines enabled specific bacterial internalization into these cells *in vitro*. Optimization of the bacterial antibody coating process resulted in an up to 10^4 -fold increase of intracellular bacteria. Combination of this antibody-mediated targeting with the delivery of prodrug-converting enzymes showed a cytotoxic effect in cell lines treated with the corresponding prodrug. Since incubation in murine serum completely abrogated antibody-mediated bacterial internalization the antibodies were covalently linked to the bacteria for application in xenografted tumor mice. Bacteria coated and crosslinked in this manner showed enhanced tumor targeting in a murine tumor model demonstrating antibody-mediated bacterial tumor targeting *in vivo*. Independent of antibody-mediated tumor targeting the intrinsic tumor colonization of different *Listeria monocytogenes* mutants was examined. *Listeria monocytogenes* $\Delta aroA \Delta inlGHE$ colonized murine melanoma xenografts highly efficient, reaching up to 10^8 CFU per gram of tumor mass 7 days post infection.

Taken together the presented data shows highly promising aspects for potential bacterial application in future tumor therapies. Combination of the delivery systems with antibody-mediated- and intrinsic bacterial tumor targeting might open novel dimensions utilizing *Listeria monocytogenes* as therapeutic vector in targeted tumor therapy.

1.II Zusammenfassung

Die Weiterentwicklung der Therapiemöglichkeiten bei Krebserkrankungen hat trotz deutlicher Fortschritte nicht zu einer grundsätzlichen Verringerung der krebsbedingten Sterberate geführt. Besonders in der Behandlung von Metastasen werden alternative Therapieansätze zur Unterstützung der etablierten Standardmethoden benötigt. Insbesondere bakterielle und virale Vektoren wurden von groben Werkzeugen zu hochtechnischen therapeutischen Instrumenten verfeinert und könnten in der Zukunft diese therapeutische Lücke schliessen.

In dieser Arbeit wurden verschiedene Aspekte der Anwendung von *Listeria monocytogenes* in der bakteriellen Tumorthherapie untersucht. Im ersten Teil der Arbeit wurde das bereits publizierte System zur bakteriellen Übertragung von mRNAs modifiziert. Die genomische Integration der T7 RNA Polymerase, welche die mRNA herstellt, erlaubte die Reduktion der Plasmidzahl und verringerte die Stoffwechselbelastung auf die RNA-übertragenden Bakterien. Diese Integration erlaubte zum ersten Mal die metabolische Attenuation von RNA-übertragenden *Listerien* und ermöglicht damit den *in vivo* Einsatz dieser Stämme. Als Erweiterung zur bakteriellen mRNA Übertragung wurde die Übertragung von shRNAs untersucht. Obwohl große Mengen an bakteriellen RNAs nachgewiesen wurden, die die shRNA Sequenz enthielten, konnte nach Infektion eukaryotischer Zellen mit diesen Bakterienmutanten keine funktionale Genregulation nachgewiesen werden.

Im zweiten Teil dieser Arbeit wurde mit verschiedenen Methoden die Kolonisierung von Tumoren durch *Listeria monocytogenes* verbessert. Durch Beladung der Bakterien mit Antikörpern gegen Rezeptoren, die auf bestimmten Tumorzellen überexprimiert werden, wurde die bakterielle Internalisierung in diese Zelllinien ermöglicht. Durch Optimierung des Antikörper-Beladungsprozesses konnte die Antikörper-vermittelte bakterielle Internalisierung auf das 104 fache der Kontrollen gesteigert werden. In Verbindung mit der Übertragung von Enzymen, die Medikamentenvorstufen in cytotoxische Medikamente umwandeln, konnten in Zellen, die mit der Medikamentenvorstufe inkubiert wurden, zytotoxische Effekte beobachtet werden. Da aber die Behandlung Antikörper-beladener Bakterien mit murinem Serum die spezifische Internalisierung vollständig verhindert, wurden die Antikörper für die Anwendung in Xenograft Tumormäusen kovalent an die Bakterien gebunden. Auf diese Weise behandelte Bakterien zeigten eine verbesserte Tumorzielsteuerung bei Beladung mit tumorbindenden Antikörpern. Unabhängig von der Antikörper-vermittelten Tumorzielsteuerung wurde die Tumorkolonisation verschiedener *Listeria monocytogenes* Mutanten untersucht. Insbesondere *Listeria monocytogenes* $\Delta aroA$ $\Delta inlGHE$ kolonisierte Melanom-Xenograft Tumoren sehr effizient und erreicht bis zu 10^8 CFU pro Gramm Tumormasse.

Zusammengefasst zeigt diese Arbeit verschiedene vielversprechende Aspekte der

bakteriellen Tumorthherapie, die möglicherweise in Zukunft angewandt werden können. Durch Verbindung der RNA-Transfersysteme mit Antikörper-vermittelter- und intrinsischer Tumorzielsteuerung können neue Möglichkeiten für den Einsatz von *Listeria monocytogenes* als therapeutischer Vektor geschaffen werden.

2 Introduction

2.1 Cancer

Cancer is one of the ten leading causes of death worldwide (WHO, 2008). In developed countries approximately 20-25 % of disease related death toll is caused by transformed tissue (Jemal et al., 2007; WHO, 2008). In spite of highly advanced therapeutics and chemotherapeutic drugs, cancer related death rate has remained stable over the last years (Jemal et al., 2007). Although the standard therapies including surgery, radiation- and chemotherapy are constantly being improved, additional novel approaches are needed. Life prolonging therapies are available for treatment of many types of primary tumors, but metastases are still a major therapeutic problem. There is a great demand for specific treatments for metastases which are responsible for around 90% of cancer related deaths (Weinberg, 2006).

Almost every tissue in the human body can be transformed into neoplastic lesions and progress into malignancy. Prostate and breast, together with lung and bronchus are the most affected organs in humans (Jemal et al., 2009; Jemal et al., 2007). Tissue transformation is caused by unrestricted cellular proliferation together with a loss of endogenous and exogenous homeostatic regulation (Hanahan and Weinberg, 2000). Cells initiating neoplastic growth have to acquire several characteristics, while others have to be lost during transformation. The most popular list of those was expressed by Hanahan and Weinberg in 2000 (Hanahan and Weinberg, 2000). Cells transforming into neoplastic lesions need self-sufficiency in growth signals, insensitivity to anti-growth signals, evade apoptosis, promote angiogenesis and require a limitless replicatory potential together with a loss of homeostatic regulation of cell division.

2.11 Current cancer therapy

Treatment of cancer is a complex task, because the differences between healthy cells and tumor cells are minimal (Klausner, 1999; Ratain and Relling, 2001). Metastases and resistance of cancer cells to chemotherapeutic agents make therapeutic interventions less efficient and decrease the chance of complete patient recovery (Di Nicolantonio et al., 2005). The occurrence of side effects during chemotherapy often limits drug application and leads to application of suboptimal dosages in the treatment regimen or premature treatment discontinuation (Huang and Ratain, 2009; Schrama et al., 2006). These limitations led to the development of novel therapeutic approaches supporting current therapies including strategies using microorganisms.

2.III Cancer and infection

Almost one hundred years ago Ellermann and Bang and a few years later Peyton Rous were the first to describe a virus causing neoplastic transformations in chicken (Ellermann and Bang, 1908; Rous, 1910, , 1911). Several decades later scientists finally accepted these initial findings and today many more viruses like HPV, HBV, HHV-8 or HTLV-1 have been proven to initiate tissue transformation (reviewed in Javier and Butel, 2008; Klein and Silverman, 2008). In addition to viral agents, bacteria like *Helicobacter pylori* have been shown to promote tissue transformation (reviewed in Ferreira et al., 2008). Other microbial pathogens or parasites, which promote chronic inflammations, also are believed to be involved in tissue transformation (Huang et al., 2007; Klein and Silverman, 2008). It is estimated that about 20% of worldwide cancer incidence is caused by infections (Parkin, 2006). Despite the potential of some microorganisms to induce or promote tumor growth, viruses and bacteria have also been investigated for their application in tumor diagnosis and therapy.

At the end of the 19th century, Busch, Fehleisen and Richter were the first to describe the enhanced survival of cancer patients infected with *Streptococcus pyogenes* and *Serratia marcescens* (Busch, 1866; Fehleisen, 1882; Richter, 1896). The American surgeon Coley was the first to investigate these observations in detail for cancer treatment (Coley, 1896; Coley, 1991). Although the mechanism of action was unclear at this time, these applications represent the first reports of bacterial anti-cancer therapies. At the same time an initial report on tumor regression after rabies virus vaccination was published (de Pace, 1912). It took four to five decades until first clinical trials using different viruses and bacteria were performed (Carey et al., 1965; Huebner et al., 1956; Southam and Moore, 1952; Webb et al., 1966). The beneficial outcome of these approaches was marginal, leading to a reduction in microbial cancer therapy research for the next decades. Given the immense potential of genetic manipulation of microorganisms, these therapeutic approaches have reemerged and are at present being intensively investigated. Alternative cancer therapies using microorganisms can be classified based on their mechanism of action. Immunologic approaches aim on the induction of specific or non-specific immune responses to tumors, while targeted approaches utilize the specific accumulation of microorganisms in tumor tissue for tumor disruption.

2.III.1 Application of bacteria in cancer immunotherapy

Cancer immunotherapy is based on the induction of potent immune response directed

against tumor tissue finally resulting in tumor regression (Guinn et al., 2007). In addition to immediate effects, the generation of an immunologic memory is required for prevention of cognate tumors.

An efficient immunologic anti-tumor response is composed of a wide variety of cellular and humoral components of the immune system (IS). Parts of the innate IS like macrophages, natural killer cells (NK) and neutrophils as well as parts of the adaptive IS like cytotoxic and helper T-cells are required to jointly interact against neoplastic lesions. In different mouse models, the cellular rather than the humoral immune responses caused rejection and regression of transplanted tumors (Rosenberg, 2001). Although the intrinsic humoral immune response seems to be rather unimportant in animal models, the therapeutic application of antibodies showed significant successes in clinical studies (Reichert et al., 2005).

In addition to cell transfers and vaccinations using peptides or DNA, several microorganisms have been used in immunologic cancer therapies. Initial approaches, based on the nonspecific induction of inflammation were performed by Coley, more than a hundred years ago; nevertheless the initial formulation consisting of inactivated bacteria is still in use for cancer treatment (Coley, 1896; Tang et al., 1991). The most prominent example of bacterial immunotherapy is the treatment of superficial bladder cancer using *Mycobacterium bovis* BCG (BCG) (reviewed in Lockyer and Gillatt, 2001; Morales et al., 1976). Application of viable BCG into the bladder leads to infiltration of macrophages and T-cells and is followed by a massive secretion of cytokines (Chakrabarty, 2003). The resulting inflammation prevents disease progression and reduces tumor recurrence (Lockyer and Gillatt, 2001). Several studies indicate inflammation as the main- but not sole cause for therapeutic effect of BCG as induction of inflammation alone is less efficient in therapy (Kleef and Hager, 2006; Lockyer and Gillatt, 2001).

In addition to non-specific immune-stimulation by bacterial agents intracellular bacteria have been used for delivery of tumor antigens to elicit a directed immune response. The specificity of therapy is determined by the choice of the tumor associated antigen (TAA), as the distinction in between cancer cell and healthy cell is made on presence or absence of this TAA (Lewis et al., 2003; Wang and Rosenberg, 1999). If a non-specific antigen is chosen and the immune tolerance broken, severe autoimmune reactions may occur (Selvaraj et al., 2008).

Bacteria have been used as therapeutic cancer vaccines for surface presentation or secretion of TAAs to prime T-cells against cancer antigens. Genetically modified strains of *L. monocytogenes* and *Salmonella enterica* sp. have been evaluated for delivery of heterologous antigens (Gentschev et al., 2000). Initially it was shown, that both strains were able to initiate an immune response in mice against heterologous model antigens, preventing tumor growth after challenge with cancer cells expressing these antigens (Paglia et al., 1998;

Schafer et al., 1992). The bacterial carriers displayed an intrinsic adjuvant effect, which could be boosted by additional delivery of cytokines (reviewed in Vassaux et al., 2006).

In the group of Yvonne Paterson endogenous TAAs like HER2/erbB2, PSA or virally originating E7 were fused to the highly immunogenic listeriolysin and used as bacterial cancer vaccines. After immunization, potent immune responses against the TAA were induced in mice preventing tumor growth after challenge and reducing tumor load under therapeutic conditions (reviewed in Paterson and Maciag, 2005). Using attenuated *Salmonella enterica* serovar Typhimurium strains, similar results were obtained on secretion of the melanoma TAA NY-ESO-1 or PSA (Fensterle et al., 2008; Nishikawa et al., 2006).

Use of bacteria as carrier for heterologous antigen presentation in cancer therapy has shown promising results in animal models and the transfer into clinical applications is currently underway. Completely different characteristics of bacteria and viruses are used making them shuttles for tumor targeted delivery of therapeutic agents as discussed in the next section.

2.III.2 Targeted cancer therapy using bacteria and viruses

One of the major challenges in cancer treatment is the distinction between healthy and transformed cells. Commonly applied chemotherapy acts systemic on every cell of a patients body, usually leading to cytotoxic effects in all rapidly dividing cells (Brown and Giaccia, 1998). Although most cancer cells are more sensitive to chemotherapeutics, severe side effects often limit the application of cytotoxic drugs and lead to the premature discontinuation of treatment (Huang and Ratain, 2009; Schrama et al., 2006). Limitation of cytotoxic effects to the tumorsite or metastases would limit the side-effects and make the application of more potent drugs possible.

Targeted cancer therapies use TAAs or other parameters correlating with neoplastic transformation as target structure to restrict therapies to the tumorsite and metastases. Using bacteria or viruses in targeted cancer therapy utilizes the differential colonization behavior of these pathogens in cancer bearing patients. Some organisms or viruses intrinsically accumulate in neoplastic tissues after systemic infection and could be used as therapeutic agents. Once these pathogens have reached the tumor tissue, they selectively replicate, accumulate, and elicit locally restricted cytotoxic effects optimally leading to a lasting tumor regression.

2.III.2.a Viral accumulation in tumors

Accumulation of bacterial- as well as viral strains has been shown in transformed tissue after systemic infection. Several viruses depend during their infection cycle to some degree on

activated RAS pathways, which are activated in many human tumors (Barbacid, 1987; Sears and Nevins, 2002). While the vaccinia virus is able to infect many cell lines in tissue culture, efficient intracellular multiplication takes place only if the mitogen-activated protein kinase (MAPK) pathway is activated (Andrade et al., 2004; de Magalhaes et al., 2001). Other members of the poxviridae require a delicate balance of MAPK activation and inactivation for virus multiplication (Wang et al., 2004). The viral infection behavior can also be influenced by intracellular signalling. The Reovirus depends on an activated RAS pathway for efficient infection (Coffey et al., 1998).

Interferons are involved in mediation of growth inhibitory signals as well as the cellular antiviral response (Stark et al., 1998). Interferon non-responding cells have acquired a growth advantage combined with a higher susceptibility to viral infections. The vesicular stomatitis virus (VSV) is especially sensitive to interferon and was used for tumor treatment experiments based on selective replication in interferon non-responding tumors (Belkowsky and Sen, 1987; Stojdl et al., 2000).

Other viruses were genetically engineered to selectively target tumor cells or replicate in tumors. An adenovirus was genetically altered to be dependent on cellular upregulation of E2F with concurrent p53 downregulation (Bischoff et al., 1996; McCormick, 2003). In a different approach, a dependence of the viral multiplication on the G1-S-phase checkpoint was incorporated into an adenoviral strain by mutating the E1A early viral protein (Heise et al., 2000). Different deletions and modifications were made in herpes simplex virus type 1 (HSV-1) limiting replication selectively to dividing cells (Mineta et al., 1994; Mineta et al., 1995).

In addition to modification of endogenous viral proteins, some viruses were equipped with heterologous proteins for cancer targeting. In the fiber and envelope proteins of an adenovirus and a sindbis virus, the antibody binding domains derived from *Staphylococcus aureus* protein A were inserted to enable viral coating with immunoglobulins (Ohno et al., 1997; Volpers et al., 2003). Using different antibodies bound to the viral particles these viruses were enabled to infect cancer cell lines in an antibody-dependent manner.

2.III.2.b Bacterial accumulation in tumors

Bacterial carriers have been investigated with respect to their tumor targeting capacity as well, though the reasons for increased tumor colonization differ from those of viral carriers. Bacterial accumulation is related to a great extent to the metabolic and physical properties of tumor tissue rather than the presence or absence of the surface receptors involved in the viral tumor targeting. Commonly tumor growth proceeds faster than the vascularization system is able to build up a sufficient network of supporting vessels (Fukumura and Jain,

2007). In addition the vascular architecture in tumors is often disorganized leading together with the elevated interstitial tissue pressure to a suboptimal blood flow. The resulting shortage of sufficient oxygen and nutrients leads to hypoxic and necrotic regions in tumor areas remote from the vessels (Fukumura and Jain, 2007). The lack of oxygen in anoxic areas and the reprogramming of immune cells prevents efficient immune responses leading to immunological sanctuaries (Brown and Giaccia, 1998; Espey, 2006; Lambin et al., 1998). The listed characteristics differ between healthy and tumor tissue and are discussed as reasons facilitating bacterial accumulation in tumors after systemic infection (reviewed in Brown, 1999; Ryan et al., 2006; St Jean et al., 2008).

Obligate anaerobic bacteria like *Clostridia* are unable to bear oxygen in their vegetative form and only spores are tolerant to aerobic conditions (Paredes et al., 2005). On systemic infection of humans with *Clostridia* spores, germination followed by replication is restricted to anaerobic areas of the body (Carey et al., 1965; Lambin et al., 1998). Different *Clostridia* species have been investigated as tumor-accumulating therapeutic vectors since the initial reports published in 1947 (Malmgren and Flanigan, 1955; Parker R. C. et al., 1947). *Clostridium histolyticum*, *Clostridium butyricum*, *Clostridium sporogenes*, *Clostridium acetobutylicum* and even *Clostridium tetani* have been employed as targeting vectors yielding varying therapeutic efficiencies (reviewed in Wei et al., 2008a). Recently an attenuated strain of *Clostridium novyi* devoid of its α -toxin, showed promising tumor targeting properties in several animal models (Dang et al., 2001).

Other obligate anaerobic bacteria belonging to the apathogenic *Bifidobacteria* were used for targeted delivery into tumor tissue. *Bifidobacterium bifidum* showed lasting but locally restricted growth in hypoxic tumor areas while being eliminated after 24-48h in blood, bone marrow, muscle, liver, spleen, kidney and lung (Kimura et al., 1980). Several other species of this genus were examined in detail and especially *Bifidobacterium longum* is currently used in cancer gene therapy (Fujimori et al., 2002; Yazawa et al., 2001).

Various other facultative anaerobic bacteria have also been shown to accumulate in tumor tissue after systemic infection. *Vibrio cholerae*, different *Salmonella enterica* serovars and *Escherichia coli* were used as targeted carriers in various cancer therapy approaches (Cunningham and Nemunaitis, 2001; Nemunaitis et al., 2003; Pawelek et al., 1997; Stritzker et al., 2007; Toso et al., 2002; Yu et al., 2004). The reason for bacterial tumor accumulation by facultative anaerobes, with exception of *Salmonella enterica* serovar typhimurium, is currently unknown. As indicated at the beginning of this chapter, several properties of tumor tissue are discussed as reason for bacterial accumulation, but only recently the mechanism of tumor accumulation by a facultative anaerobic bacterium has been proposed. Chemotaxis for ribose, serine and aspartate was pinpointed as cause for tumor colonization of *S. typhimurium* (Kasinskas and Forbes, 2006; Kasinskas and Forbes, 2007). Mutants lacking

the corresponding chemotaxis receptors were shown to colonize only distinct regions of tumor cell cylindroids *in vitro* (Kasinskas and Forbes, 2007).

Tumor accumulation of *S. typhimurium* was artificially enhanced by chemical mutagenesis resulting in a leucine and arginine auxotroph mutant (Zhao et al., 2005). Organ colonization of this mutant strain was shown to be limited to tumor tissue, as the amino acid supply in other tissues was not sufficient for bacterial replication. *In vivo* passaging in tumor bearing mice further improved tumor cell invasion and caused tumor regression in nude mice (Zhao et al., 2006). In a different approach, bacterial tumor targeting was synthetically improved by expression of tumor specific single-chain-antibodies (scFv) bound to the bacterial surface. Expression of a scFv directed against the carcinoembryonic antigen (CEA) led to a doubling of bacterial counts in tumor tissue compared to bacteria without scFV expression (Bereta et al., 2007). In addition to preferential tumor colonization after systemic infection, several studies were performed by injecting the bacteria into solid tumors to increase bacterial tumor colonization. Using this technique colonization of liver and spleen, commonly colonized after systemic infection, can be reduced (Sasaki et al., 2006).

Depending on bacterial strains, animal tumor models and the examined time points, the ratio of bacterial tumor- to healthy tissue colonization differs a lot. Initial studies using *S. typhimurium* reported a 250- to 9000-fold higher bacterial count in tumor tissue than in the liver two to four days after systemic infection (Pawelek et al., 1997). Similar ratios were found using scFv guided *S. typhimurium* (Bereta et al., 2007). In xenografted tumor mice *S. choleraesuis* was found to colonize tumors 1.000 to 100.000 fold better than liver and spleen (Lee et al., 2004; Lee et al., 2005). The higher these ratios of bacterial titers are between colonization of healthy tissues and tumors, the better these strains can be employed for therapeutic purposes.

2.III.2.c Approaches in tumor therapy using targeted bacteria

Once the bacteria and viruses are enriched in the tumors, antitumor effects are to be initiated for therapy. Several bacterial and viral strains intrinsically cause oncolysis, while others have been genetically manipulated to destroy tumor cells. Beside direct cytotoxic effects, bacteria and viruses have been used for tumor targeted delivery. Using tumor targeted carriers, gene therapy, suicide-gene therapy, immuno-gene therapy, anti-angiogenic approaches or gene silencing have been achieved (reviewed in Wei et al., 2008b).

Historically, bacterial induced tumor lysis was shown for the first time in xenografted tumor mice by injection of *Clostridium histolyticum* spores into tumor tissue (Parker R. C. et al., 1947). Clostridial secretion of kininases, proteases, peptidases, nucleases and

phospholipase A resulted in liquefaction of the tumor center (Brantner and Schwager, 1979, , 1980; Fischer et al., 1975; Haller and Brantner, 1979; Mose et al., 1972; Schmidt et al., 2006). In addition oncolysis was shown in experiments using *Bifidobacterium adolescentis*, but not on application of *Bifidobacterium longum* (Fujimori, 2006; Kimura et al., 1980; Wang et al., 1999). This strain was used for delivery of prodrug-converting enzymes in transplanted as well as autochthonous tumors in rats. On intratumoral injection of 10^8 prodrug-converting bacteria followed by systemic application of the prodrug, regression of tumor growth was observed (Sasaki et al., 2006). Using attenuated *Salmonella typhimurium* VPN2009 for delivery of carboxypeptidase G2, profound bacterial colonization and prodrug conversion was observed in xenografted murine tumors. Cytotoxic effects of the converted prodrug led to significant tumor regression in murine tumor models (Friedlos et al., 2008). In addition to applications in suicide gene therapy, *S. typhimurium* has been employed for delivery of the pro-apoptotic Fas ligand (FasL). Tumor colonization with simultaneous FasL expression by the bacterial carriers resulted in marked tumor regression and less aggressive metastatic spread in the tumor mice (Loeffler et al., 2008).

Delivery of an eukaryotic expression cassette encoding endostatin, an angiogenesis inhibitor, was accomplished using *B. longum*, *B. adolescentis* and *S. choleraesuis*. The different approaches were able to induce endostatin expression in tumor tissue, reduce tumor vascularization and growth but failed in curing the tumors (Lee et al., 2004; Li et al., 2003; Xu et al., 2006).

2.III.2.d Limitations of bacterial and viral use in tumor therapy

Although targeted bacterial and viral cancer therapy approaches have been intensively studied and reached first clinical trials, several disadvantages still limit the broad clinical application of these carriers. Clearly one of the major problems in targeted therapies is the cancer targeting itself. Only by using the obligate anaerobic *Clostridia* as a carrier, high numbers of bacteria colonize the tumor tissue. The second bacterial strain of strictly anaerobic bacteria used in targeted cancer therapy, the *Bifidobacteria*, show much lower tumor colonization. Bacterial titers of some *Clostridia* reach 10^8 - 10^9 CFU/g tumor mass, in comparison to the highest published titers of *Bifidobacteria* which range between 10^5 to 10^6 CFU/g (Sasaki et al., 2006; Wei et al., 2008b). Published anti-tumor effects of *Bifidobacteria* therefore often relied on intratumoral injection of the carrier bacterium, avoiding intrinsic bacterial targeting. The tumor lysis syndrome is another common problem of *Clostridia* and several oncolytic viruses on application in cancer therapy. After successful tumor breakdown, there is a mass of cell debris, electrolytes and carrier particles released into the surrounding tissue leading to severe clinical symptoms (reviewed in Tiu et al., 2007). Another critical

issue on application of *Clostridia* is the obligate need for anoxia for spore germination. Obligate anaerobic bacteria are unable to colonize small metastases as long as these are sufficiently supplied with oxygen. They are unable to trigger their cytotoxic effects, even in the well oxygenized outer rim of solid tumors, and that is probably the reason why tumors often regrow from cells of the outer rim following clostridial tumor therapy (Minton, 2003; Nuyts et al., 2002; Wei et al., 2008a).

The facultative anaerobic carriers of the genera *Salmonella*, *Escherichia* or *Listeria* are basically able to grow in the whole tumor including the outer rim, but the application of these bacteria has other downsides. Noninvasive *E. coli* strains in cancer therapy are limited to extracellular delivery of therapeutic agents but e.g. suicide-gene therapy requires intracellular bacteria. The invasive *Salmonella* and *Listeria* mutants currently under investigation show low tumor to liver infection ratios. Ratios range between 100:1 to 100.000:1 of bacterial tumor to liver titers and average ratios below 10.000:1 are reported (Forbes et al., 2003; Kim et al., 2009; Lee et al., 2005; Low et al., 1999; Pawelek et al., 1997). Especially the presence of the highly immunogenic LPS on the bacterial surface poses an additional problem on application of gram-negative bacteria and the amount of LPS has to be reduced when using gram-negative carrier bacteria. This is the reason why many gram-positive bacteria are investigated for use in tumor therapy. These described limitations in the various approaches are the reasons why clinical use of targeted bacterial tumor therapy is still in early trial phases.

2.IV *Listeria monocytogenes*

2.IV.1 Epidemiology and Pathogenesis

Listeria monocytogenes is a pathogenic gram-positive bacterium, commonly found in environmental, human and animal samples (Seeliger et al., 1965; Vazquez-Boland et al., 2001). Frequent occurrence in spoiled food products like raw milk and meat results in broadly spread immune memory in the human population (Hof, 2003; Schuchat et al., 1991). Though severe pathologic symptoms are rather rare on infections of healthy individuals, *L. monocytogenes* may cause encephalitis, septicemia and stillbirth in immuno-compromised humans. Especially pregnant women, elderly people and patients suffering from leukemia or AIDS are prone to develop severe listeriosis on *L. monocytogenes* infection (Hof, 2003; Vazquez-Boland et al., 2001).

Following ingestion of contaminated food, bacteria surviving the gastric acid reach the intestinal tract. After active crossing of the epithelial cell layer, the bacteria enter into lymphatic and blood vessels and are carried to liver and spleen, where they are taken up by

resident macrophages (Ebe et al., 1999; Marco et al., 1992; Pron et al., 1998). Bacteria evading the killing by macrophages spread to proximate cells and replicate particularly in hepatocytes. During early infection, neutrophils are recruited mediating destruction of infected hepatocytes (Mackaness, 1962; Rogers and Unanue, 1993). Later mononuclear cells and lymphocytes mediate granuloma formation confining infected cells. Finally the infection is cleared by infiltrating IFN γ -activated macrophages and CD8⁺ lymphocytes (Gregory and Liu, 2000; Harty et al., 1992; Kaufmann, 1993; Mielke et al., 1988; Vazquez-Boland et al., 2001). If *L. monocytogenes* is not cleared from liver and spleen, a secondary release of bacteria into the blood stream leads to infection of brain and placenta leading to severe pathologic symptoms (Cossart, 2002).

2.IV.2 Infection cycle

L. monocytogenes is a facultative intracellular bacterium entering non-phagocytic cells via the zipper mechanism. Active invasion was shown for various different cell types including epithelial-, endothelial- and neuronal cells and also for fibroblasts and hepatocytes (Drams et al., 1998; Drevets et al., 1995; Gaillard et al., 1987; Guzman et al., 1995; Kuhn et al., 1988; Wood et al., 1993). *L. monocytogenes* is taken up by phagocytic cell types like macrophages and neutrophils (Hamon et al., 2006; Mackaness, 1962).

Following cell invasion, the bacteria lyse the acidifying phagosome using Listeriolysin O (LLO) and replicate within the cytosol using nutrients acquired from the host cell (Beauregard et al., 1997; Gaillard et al., 1987; Joseph and Goebel, 2007; Joseph et al., 2006). Actin polymerisation at one bacterial cell pole pushes *L. monocytogenes* through the cytosol in an undirected manner. Polar expression of ActA leads to recruitment of the Arp2/3 complex via VASP mediating the generation of actin fibers (Cossart and Lecuit, 1998; Domann et al., 1992; Kocks et al., 1992). When the bacterium is propelled against the host cell membrane, a protrusion into the adjacent cell with the bacterium at the tip develops. The protrusion becomes a secondary endosome which is rapidly lysed by the bacterial phospholipase C (PlcB) and LLO (Vazquez-Boland et al., 2001). Once the bacteria arrive inside the host cell cytosol the replication cycle starts over again.

Active bacterial invasion into non-phagocytic cells is mediated by two proteins of the internalin family. Internalin A (InlA) interacts with epithelial cadherin (E-cadherin) and is mainly responsible for the initial crossing of the intestinal barrier following ingestion (Mengaud et al., 1996). Interaction with transiently exposed E-cadherin on enterocytes of intestinal villi mediates bacterial invasion into these epithelial cells (Pentecost et al., 2006). Internalin B (InlB) is able to interact with two different cellular receptors. MET/HGFR (mesenchymal-epithelial transition factor / hepatocyte growth factor receptor) and the

complement receptor gC1qR represent the main InIB receptors and invasion is enhanced by interactions with glucosaminoglycans (Braun et al., 2000; Jonquieres et al., 2001; Shen et al., 2000). The interaction of InIB and MET is important for infection of hepatocytes allowing colonization of the murine liver following infection (Khelef et al., 2006; Shen et al., 2000).

Several additional internalins have been described to be involved in the bacterial infection and colonization process *in vivo*. *L. monocytogenes* harbouring deletions in the three membrane bound internalins InIG, H and E (InIG/H/E) shows reduced virulence *in vivo* following oral infection (Raffelsbauer et al., 1998). In contrast *inIG/H/E* deletions leads to an upregulation of InIA/B resulting in an hyperinvasive bacterial phenotype *in vitro* (Bergmann et al., 2002).

In addition to these cell wall associated internalins the secreted internalin C (InIC) was found to be involved in the late phase of *L. monocytogenes* infection *in vitro* (Engelbrecht et al., 1996). The LD₅₀ of *L. monocytogenes* Δ *inIC* is elevated 50-fold in mice in comparison to wildtype bacteria on i.v. infection, indicating an important function in bacterial pathogenicity. The molecular mechanisms how InIC increased pathogenicity remained unclear till today.

2.IV.3 Use of *L. monocytogenes* as targeted carrier

L. monocytogenes has been attenuated by deletions of different virulence genes like *actA*, *actA mpl plcB*, *actA plcB* or *actA inIB* (Angelakopoulos et al., 2002; Brockstedt et al., 2004; Dietrich G. et al., 1998; Wallecha et al., 2009). In targeted tumor therapy, bacterial virulence factors are desirable for efficient tumor colonization, and hence other attenuations have been made for this application. In the past, genes involved in bacterial amino acid metabolism or cell wall synthesis were deleted to attenuate the bacteria while simultaneously keeping all virulence factors functional (Dougan et al., 1987; Stritzker and Goebel, 2004; Stritzker et al., 2004; Thompson et al., 1998). But even the knockout of non-virulence genes like the *dal*, *dat* genes involved in the generation of D-alanine for cell-wall synthesis can render the bacteria unsuitable for targeted tumor therapy. As the *dal dat* deletion leads to an almost complete abrogation of intracellular replication *in vitro* and the mutant is cleared *in vivo* in less than two days post infection, this attenuation is inappropriate for the desired application (Thompson et al., 1998).

Bacterial attenuation by deletion of the *aroA* and *aroB* genes, involved in the aromatic amino acid metabolism, leads to a significant reduction of pathogenicity, too. The LD₅₀ in mice is increased more than five orders of logarithmic magnitude despite of the bacteria still being able to infect, replicate and spread (Stritzker and Goebel, 2004; Stritzker et al., 2004). Using attenuated *L. monocytogenes* mutants, several systems for delivery of functional molecules into eukaryotic cells were developed (Dietrich G. et al., 1998; Loeffler et al., 2006; Pilgrim et

al., 2003; Schoen et al., 2005; Stritzker et al., 2008). *L. monocytogenes* were used for delivery of prokaryotic and eukaryotic expression cassettes into the cytosol of different cell lines. In the mouse model different delivery systems were proven functional in delivery of the heterologous antigens (Loeffler et al., 2006). Colonization of tumor tissue using these *L. monocytogenes* mutants has not been published so far. Experiments investigating tumor colonization of *L. monocytogenes* Δ aroA in xenografted tumor mice following i.v. infection were done, but the overall bacterial numbers reached only a maximum of 10^6 CFU per gram of tumor mass (Fensterle, personal communication; Heisig, unpublished data). These bacterial titers are too low for efficient therapeutic delivery approaches, as the amount of delivered cargo is too small.

3 Aim of study

The use of bacteria in targeted tumor therapy requires several criteria to be met by the carrier bacterium. An absolute prerequisite for utilization of pathogenic strains as carriers, the strains have to be adequately attenuated to avoid disease outbreak. Apart from this, two main factors will influence the later therapeutic outcome. On the one hand, the bacterial tumor colonization especially in relation to colonization of healthy organs is crucial for efficiency and circumvention of side effects. On the other hand, the therapeutic component delivered as payload significantly influences the anti-tumor effects.

This PhD thesis focused on characterization and improvement of the two latter aspects of bacterial tumor therapy. Different approaches for enhancement of bacterial tumor colonization were analyzed. In addition to the improvement of bacterial titers in tumor tissue, the delivery of functional RNAs as potential therapeutic component was investigated. As future goal, a combination of both would potentially allow tumor therapeutic applications using *L. monocytogenes*.

3.1 RNA delivery by *L. monocytogenes*

The delivery of functional mRNAs by *L. monocytogenes* into mammalian cell lines was shown for the first time in 2005 (Schoen et al., 2005). The T7RNAP based delivery system was encoded on two plasmids harbouring the polymerase gene and the expression cassette respectively. Expression of the T7RNAP was under the control of the *actA* promotor, resulting in strongly enhanced expression following phagosomal escape of the bacteria. The T7RNAP transcribed an EGFP gene preceded by a viral ribosome entry site. Following mRNA expression and release into the eukaryotic cytosol, the host cell translated the mRNA into functional proteins. *In vitro* this RNA delivery resulted in significant EGFP production already 4h p.i. (Schoen et al., 2005). *In vivo*, the RNA delivery by non-attenuated *L. monocytogenes* was used for delivery of heterologous antigens (Loeffler et al., 2006). The application of RNA delivering bacteria in targeted tumor therapy was not researched until now, as the amount of bacteria needed for initial tumor colonization exceeded the LD₅₀ in mice. In addition, it proved to be impossible to attenuate the RNA delivering strains by *aroA* deletion (Pilgrim, personal communication). Beside the inability for aromatic amino acid production the *aroA* mutant was devoid of a functional electron carrier, therefore dependent on anaerobic energy generation (Stritzker et al., 2004). Presumably the overall energy demand exerted by the two expression plasmids and the highly active T7RNAP was too high to be covered by the *aroA* mutant. Consequently, one goal of this study was increasing the growth rate efficiency by integration of the T7RNAP gene into the genome of

L. monocytogenes. The copy number reduction from plasmid- to genomic expression reduced the amount of active T7RNAP molecules consuming energy. Following this integration, the RNA delivery system was encoded on a single plasmid additionally reducing the growth retardation. The final aim of this approach was the attenuation of the one-plasmid RNA delivery strain for application *in vivo*.

In addition to the established delivery systems of nucleic acids encoding proteins or heterologous antigens, *L. monocytogenes* was sought to be engineered as carrier for small interfering RNA (siRNA) mediating gene silencing. Silencing of gene expression by RNA interference (RNAi) was initially discovered in *C. elegans* on injection of double stranded RNAs (Fire et al., 1998). Though these siRNAs offer promising opportunities in gene therapy the application of siRNA is difficult *in vivo* (Takeshita and Ochiya, 2006). The challenging problem of silencing specificity has been solved and therefore the remaining main problem of siRNA treatment in living organisms is the targeted delivery to the site of disease because of RNA degradation *in vivo* (Carthew and Sontheimer, 2009; Kurreck, 2009; Takeshita and Ochiya, 2006). Currently, the only siRNA therapies investigated for clinical application are performed in easily accessible organs like the eyeball, liver and lung (Fattal and Bochot, 2006; Thomas et al., 2007). Expansion of therapeutic use to other organs depends on the development of novel delivery systems in addition to the current viral and chemical methods. Delivery of siRNAs by intracellular bacteria represents one possible approach, but the bacteria would have to synthesize these siRNAs prior to delivery. For application of *L. monocytogenes* in siRNA, a shRNA expression cassette was designed connecting the RNA sense- and antisense strand with a short linker sequence. This expression cassette was placed under control of the T7RNAP promotor for timed expression in the host cell cytosol. The aim of this project was to test the feasibility of shRNA delivery by *L. monocytogenes* for future applications.

3.II Improvement of *L. monocytogenes* tumor colonization

3.II.1 Antibody-mediated tumor targeting by *L. monocytogenes*

Tumor-specific epitopes have been used as targets in cancer therapy in various of therapeutic approaches (reviewed in Neller et al., 2008; Schietinger et al., 2008). In addition to these mainly immune based approaches, extracellular tumor associated antigens (TAAs) offer a possible targeting structure for direct guidance of therapeutic agents.

A *L. monocytogenes* mutant expressing cell-wall anchored *S. aureus* protein A, which

enabled bacterial immunoglobulin binding was constructed and characterized (Frentzen, 2008). Coating of *L. monocytogenes* expressing protein A (*L. monocytogenes* Δ aroA/trpS Δ inlAB int::P_{hly}-spa + pFlo-trpS, Lm-spa⁺) with an antibody recognizing a TAA, enables bacteria to bind cancer cells expressing the corresponding antigen. Initial *in vitro* experiments investigating the functionality of antibody-mediated cell targeting were performed using bacteria coated with Trastuzumab. Trastuzumab (® Herceptin) is a humanized monoclonal antibody directed against the HER2/neu protein which is clinically used for therapy of HER2/neu overexpressing metastatic breast cancer (reviewed in Hudis, 2007). HER2/neu is overexpressed in approximately 30% of all breast cancer patients making it a valid TAA (McCann et al., 1991; Thor et al., 1989; Venter et al., 1987).

Infection experiments performed in the human breast cancer cell line SK-BR-3, showed the proof of principle for antibody-mediated cancer cell internalization of Lm-spa⁺ as shown in figure 3.1.

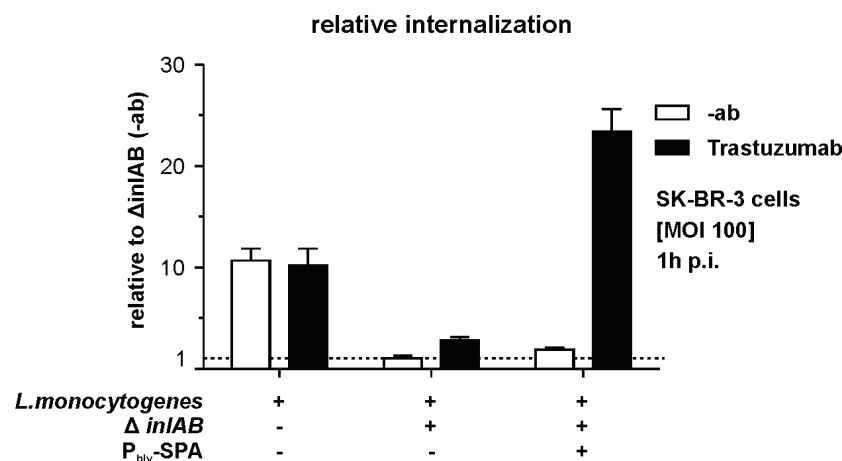


figure 3.1: Relative internalization of *L. monocytogenes* mutants into SK-BR-3 cells following incubation with and without Trastuzumab (Frentzen, 2008; modified)

In comparison to uncoated bacteria, the Trastuzumab coated *L. monocytogenes* expressing protein A internalized about 20-fold better into this cell line. The amount of intracellular bacteria was even twice as high as the wildtype bacteria. As expected, no difference between coated and uncoated bacteria was observed when protein A negative strains were examined.

These promising results laid the groundwork for further improvement and expansion of the antibody-mediated tumor targeting as examined in this study. Several aspects of the delivery were to be examined in detail. First of all, the specificity of the approach had to be tested with cell lines expressing the antibody ligand in comparison to the isogenic ligand-negative cell line. With a functional system, several parameters were to be optimized to increase the bacterial internalization rate specifically. Finally, the application of antibody-mediated

targeting was to be investigated *in vivo* in tumor bearing mice.

3.II.2 Evaluation of two *L. monocytogenes* mutants as tumor targeting vectors

Two *L. monocytogenes* mutants were examined with regards to their colonization and accumulation behavior in tumors.

The mutant carrying a deletion in the putative hexose phosphate transporter *hpt* was found to show decreased liver colonization in ICR mice following systemic infection (Chico-Calero et al., 2002). The inability to take up phosphorylated hexoses results in a sustained bacterial growth disadvantage in liver cells as these sugars are the predominant carbohydrates in hepatocytes. In applications utilizing the bacteria for tumor targeted delivery of toxic agents, the reduction of liver colonization would be beneficial for reduction of adverse reactions. Consequently the *hpt* mutant was examined in a murine melanoma model regarding tumor colonization and tumor to liver ratio.

The invasion properties of different internalin mutants published earlier were examined and it was found that the *L. monocytogenes* mutant comprising deletions of the internalins G, H and E showed a distinct invasion increase into a murine melanoma cell line as shown in figure 3.2 (Bergmann et al., 2002; Duechs, 2007).

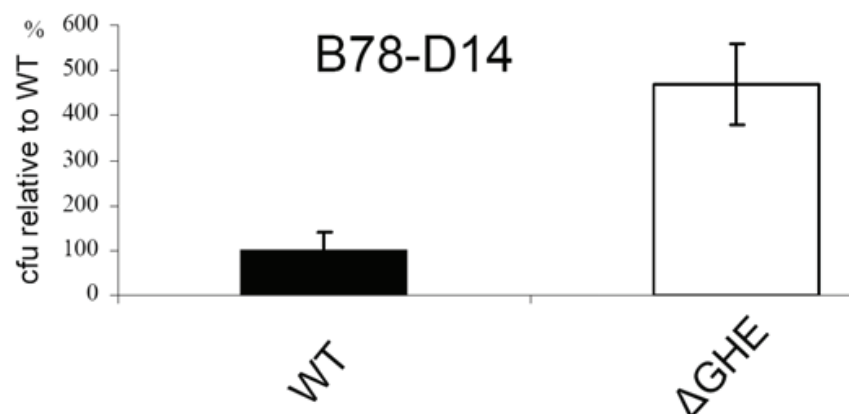


figure 3.2: Invasion of *L. monocytogenes* EGD wildtype and the corresponding internalin G/H/E deletion mutant into the murine B78/D14 melanoma cell line (Duechs, 2007)

Deletion of $\Delta inIGHE$ leads to pronounced upregulation of the two major internalins A and B resulting in a hyper invasive phenotype of this mutant (Bergmann et al., 2002). This evidence encouraged investigation of tumor colonization by this mutant in murine tumor models.

Enhancing tumor targeting on the one hand and delivery on the other hand was intended to improve key bacterial properties involved in tumor therapy. Generation of *L. monocytogenes* strains harbouring both attributes might allow future therapeutic use.

4 Material

4.1 Bacterial strains

name	relevant genotype	source
<i>L. monocytogenes</i> EGDe	wildtype	Jürgen Kreft
<i>L. monocytogenes</i> EGDe $\Delta trpS$ x pFlo-trpS	deletion of <i>trpS</i>	(Pilgrim et al., 2003)
<i>L. monocytogenes</i> EGDe $\Delta trpS/\Delta int::P_{actA^-}$ -T7RNAP x pFlo-trpS	deletion of <i>trpS</i> , genomic substitution of <i>int</i> by P_{actA^-} - T7RNAP	this study
<i>L. monocytogenes</i> EGDe $\Delta aroA$	deletion of <i>aroA</i>	(Stritzker and Goebel, 2004)
<i>L. monocytogenes</i> EGDe $\Delta trpS/\Delta aroA/\Delta int::P_{actA^-}$ -T7RNAP x pFlo-trpS	deletion of <i>aroA</i> , <i>trpS</i> ; genomic substitution of <i>int</i> by P_{actA^-} -T7RNAP	this study
<i>L. monocytogenes</i> EGD Δhpt	deletion of <i>hpt</i>	(Chico-Calero et al., 2002)
<i>L. monocytogenes</i> EGD $\Delta aroA$ Δhpt	deletion of <i>aroA</i> , <i>hpt</i>	this study
<i>L. monocytogenes</i> EGD $\Delta inlGHE$	deletion of <i>inlGHE</i>	(Raffelsbauer et al., 1998)
<i>L. monocytogenes</i> EGD $\Delta aroA$ $\Delta inlGHE$	deletion of <i>aroA</i> , <i>inlGHE</i>	this study
<i>L. monocytogenes</i> EGDe $\Delta trpS$ $\Delta aroA \Delta inlA \Delta inlB$ x pFlo-trpS (Lm- spa^-)	deletion of <i>aroA</i> , <i>trpS</i> , <i>inlA</i> , <i>inlB</i>	(Frentzen, 2008)
<i>L. monocytogenes</i> EGDe $\Delta trpS$ $\Delta inlA \Delta inlB \Delta int::P_{hly}$ -spa x pFlo-trpS (Lm- $aroA^+ spa^+$)	deletion of <i>trpS</i> , <i>inlA</i> , <i>inlB</i> ; genomic substitution of <i>int</i> by <i>spa</i>	(Frentzen, 2008)
<i>L. monocytogenes</i> EGDe $\Delta trpS$ $\Delta aroA \Delta inlA \Delta inlB \Delta int::P_{hly}$ -spa x pFlo-trpS (Lm- spa^+)	deletion of <i>aroA</i> , <i>trpS</i> , <i>inlA</i> , <i>inlB</i> ; genomic substitution of <i>int</i> by <i>spa</i>	(Frentzen, 2008)

table 4.1: Bacterial strains

4.II Plasmids

name	relevant properties	source
pFlo-trpS	<i>trpS</i> expression cassette with P _{trpS}	(Pilgrim et al., 2003)
pLSV101-IntAB-P _{actA} -T7RNAP	vector for genomic substitution of <i>int</i> by P _{actA} -T7RNAP	this study; (Heisig, 2005)
pLSV101-Δ <i>aroA</i>	plasmid for <i>aroA</i> deletion	(Stritzker and Goebel, 2004)
pCSAI	vector harbouring a T7RNAP expression cassette under control of the <i>actA</i> promotor, stabilized in <i>trpS</i> deficient <i>L. monocytogenes</i>	(Schoen et al., 2005)
pCSA-IRES/EGFP	vector harbouring an EGFP expression cassette with a viral IRES element under control of the T7RNAP promotor, stabilized in <i>trpS</i> deficient <i>L. monocytogenes</i>	this study
pCSA-IRES/FCUI	vector harbouring a FCUI expression cassette with a viral IRES element under control of the T7RNAP promotor, stabilized in <i>trpS</i> deficient <i>L. monocytogenes</i>	this study
pCSB1	RNA delivery vector harbouring a EGFP expression cassette under control of the T7RNAP promotor	(Schoen et al., 2005)
pCSB-IRES/EGFP	vector harbouring an EGFP expression cassette with a viral IRES element under control of the T7RNAP promotor	(Heisig, 2005)
pCSB-IRES/FCUI	vector harbouring a FCUI expression cassette with a viral IRES element under control of the T7RNAP promotor	(Heisig, 2005)
pCSB-shSmac	RNA delivery vector harbouring an anti-SMAC/DIABLO shRNA expression cassette under control of the T7RNAP promotor	this study

table 4.2: Bacterial plasmids

4.III Oligonucleotide sequences

4.III.1 PCR primer

name	sequence [5' -> 3']	application
aroA check 3'	GTCTGCTTCGATAGCTAGAGC	detection of <i>L. monocytogenes aroA</i>
aroA check 5'	GCTTAACACGATTCTTGCAGC	
aroA check -1	CAGGCAAATTAGCTGATACCG	detection of <i>L. monocytogenes aroA</i>
aroA check -4	AATCCCACGAGCAAGTTCAGC	
aroB check 3'	GCTAAATCGAAATCCAGTCCG	detection of <i>L. monocytogenes aroB</i>
aroB check 5'	CGTTCCGTGTGTATGAAGAC	
b-actin 3' mouse	TGGATGGCTACGTACATGGCTGGG	detection of murine β - actin
b-actin 5' mouse	TTCTTTGCAGCTCCTTCGTTGCCG	
GFP check 3'	GCCATGTGTAATCCCAGCAGC	detection of <i>gfp</i>
GFP check 5'	CCAACACTTGTCCTACTTTTCG	
hpt check 3'	CTCCTGCTATTATGGGTGTCC	detection of <i>L. monocytogenes hpt</i>
hpt check 5'	CTCGCAACGATTAAACATGCC	
InlA check 3'	GCTCTAAGTTAGTGAGTGCGG	detection of <i>L. monocytogenes inlA</i>
InlA check 5'	CTTCAGGCGGATAGATTAGGG	
InlB check 3'	TGCTTTTTCGGTCGTTTCCGC	detection of <i>L. monocytogenes inlB</i>
InlB check 5'	AGGACCTAAGTTGCTCAAGG	
InlC check 3'	ACCATCTACATAACTCCCACC	detection of <i>L. monocytogenes inlC</i>
InlC check 5'	AGCTGAGAGTATTCAACGACC	
InlE check 3'	CGCTAATAGTATCCGGTGCAA	detection of <i>L. monocytogenes inlE</i>
InlE check 5'	TGCTCGGAAAAGCGGATGTAA	
InlG check 3'	TCGGTTCTTGTAGCAGAGCTT	detection of <i>L. monocytogenes inlG</i>
InlG check 5'	TGGGTAAATGCAAGTCATGGG	
InlH check 3'	GCAAGTGGGCTAACATCACTA	detection of <i>L. monocytogenes inlH</i>
InlH check 5'	ATGGTAACTGCTATTCTCGGG	
Integrase check -1	GATGAATATGTAGAAGATGGT	detection of <i>L. monocytogenes int</i>
Integrase check -4	CTTATACATACTCAGAGGATG	
Integrase screen 3'	CGATGAACAAACCCTAATCCGC	detection of <i>L. monocytogenes int</i>
Integrase screen 5'	GAAAAGCTAACAGCCTTGTGCC	
LSV3	AGTACCATTACTTATGAG	screening of mcs in pLSV101
LSV-4380 rev	AGGGTTTTCCCAGTCACG	

name	sequence [5' -> 3']	application
Myko check 5'	ACTCCTACGGGAGGCAGCAGTA	detection of mycoplasma
Myko check 3'	TGCACCATCTGTCACTCTGTTAACCTC	
pFLO 5'	CAGGAAACAGCTATGACCATG	screening of mcs in pFlo and derivates
pFLO IRES 3'	CCATTGTATGGGATCTGATCT	
pLVTHM mcs 3'	GCAAAAAGCAGCATAACTTCG	screening of mcs in pLVTHM and derivates
pLVTHM mcs 5'	AGGAATTCGAACGCTGACGTC	
pSP0 mcs 3'	ACACGAACCGTCTTATCTCCC	screening of mcs in pSP0 and derivates
pSP0 mcs1 check 5'	GATACCTGTCCGCCTTTCTCC	
PtrpsS end 3'	TAGGGACGAACGGTTATCCGC	detection of <i>aroA</i>
Tet R end 5'	CCAGCCAACTAATGACAATGA	
trpS check gen 3'	AAGCAACTCGTGGTAACATCG	detection of genomic <i>trpS</i> in <i>Lm</i>
trpS check gen 5'	TATCTGAATTAGTCGGCCTGC	
trpS check int 3'	CACTAGAATCGGTCACAGCGC	detection of <i>L. monocytogenes trpS</i>
trpS check int 5'	CGAACATGCTATTACGGTTCC	
trpS end 5'	AGAAAAAGCAGCTCGCGTGGC	
InIC gen 1 5'	GGATGGTATACTATACAAGCG	detection of genomic <i>inIC</i> copy in <i>Lm</i>
InIC gen 4 3'	GTCGATCAATCTTACTTCACG	
InIC mut2 170 5'	CTATTCGTAATAATGCATTAAAAAGTATTGTG	mutagenesis of <i>inIC</i> (K173A, additional introduction of NsiI site)
InIC mut2 170 3'	CACAATACTTTTTAATGCATTATTACGAATAG	
InIC mut2 204 5'	GGTGGACTAACTGCACTTAAGAAAGTTAACTGG	mutagenesis of <i>inIC</i> (R204A, additional introduction of AflIII site)
InIC mut2 204 3'	CCAGTTAACTTTCTTAAGTGCAGTTAGTCCACC	
InIC bef start BamHI 5'	TAAATAGGATCCGAGTGAGGTGTAATATGGGG	amplification of <i>inIC</i>
InIC start2 BamHI 5'	AAGTACGGATCCAGAGTATTCAACGACCAACG	
InIC aft end Cfr9I 3'	GTTTCTCCCGGGGGTAACCTTATACGAATAAACG	

table 4.3: PCR primer

4.III.2 shRNA DNA oligomers

name	sequence [5' -> 3']	application
sh LDHA1 s	CCGGACCCCTCTAAAGGATCAGCTGATTTATTCAAGAGATA AATCAGCTGATCCTTTAGATTTTTTCCCGGGG	silencing of LDH A subunit
sh LDHA1 as	GATCCCCCGGGAAAAATCTAAAGGATCAGCTGATTTATCTC TTGAATAAATCAGCTGATCCTTTAGAGGGGT	
sh LDHB1 s	CCGGACCCCGGGCAACAGTTCCAAACAATAATTCAAGAGAT TATTGTTTGGAAGTGTGCTTTTTTCCCGGGG	silencing of LDH B subunit
sh LDHB1 as	GATCCCCCGGGAAAAAGGCAACAGTTCCAAACAATAATTC AAGAGATTATTGTTTGGAAGTGTGCGGGGT	
Smac shRNA BamHI/XmaI s	TTTTTTCCTAGGCCCGTCTTATTTACGTCGTCAATTCAAGA GATTGACGACGTAAATAAGACTTTTTGGATCCTTTTTT	silencing of SMAC/DIABLO
Smac shRNA BamHI/XmaI as	AAAAAAGGATCCAAAAAGTCTTATTTACGTCGTCAATCTCTT GAATTGACGACGTAAATAAGACGGGGCCTAGGAAAAAA	

table 4.4: shRNA DNA oligomers

4.III.3 qRT-PCR primer

name	sequence [5' -> 3']	application
shSmac RT (F)	CAGCCAACTCAGCTTCCTTT	quantitation of SMAC/DIABLO mRNA amount
shSmac RT (R)	CAATCTCTTGAATTGACGACGTA	
RpoB RT (F)	AAGTAACTGGCGGAATCGATA	quantitation of <i>rpoB</i> mRNA amount as housekeeping gene in <i>L. monocytogenes</i>
RpoB RT (R)	GGAATCCATAGATGGACCGTT	
Hprt2 RT (F)	TGACACTGGCAAAACAATGCA	quantitation of HPRT mRNA amount as eukaryotic housekeeping gene
Hprt2 RT (R)	GGTCCTTTTCACCAGCAAGCT	
b-actin RT (F)	GCTCGTCGTCGACAACGGCTC	quantitation of β -actin mRNA amount as eukaryotic housekeeping gene
b-actin RT (R)	CAAACATGATCTGGGTCATCTTCT	

table 4.5: qRT-PCR primer

4.IV Eukaryotic cell lines

name	origin	propagation medium	source
4T1	<i>Mus musculus</i> - mammary gland tumor	RPMI + 10% FCS + 1% L-Glutamin	Institut für med. Strahlenkunde und Zellforschung, Universität Würzburg
4T1-erbB2	4T1 derivate	DMEM + 10% FCS	Phil Darcy (Kershaw et al., 2004)
B16	<i>Mus musculus</i> - melanoma	RPMI + 10% FCS + 1% L-Glutamin	Institut für med. Strahlenkunde und Zellforschung, Universität Würzburg
B16-Ova	B16 derivate	RPMI + 10% FCS + 1% L-Glutamin + 40µl/ml G418 (50µg/ml)	Jürgen Hess, responsif GmbH, Erlangen
B78-D14	B16 derivate	RPMI + 10% FCS + 1% L-Glutamin + 8µl/ml G418 (50µg/ml) + 1µl/ml Hygromycin (50µg/ml)	Jürgen Becker, Hautklinik, Universität Würzburg
COS-1	<i>Cercopithecus aethiops</i> - kidney fibroblast	RPMI + 10% FCS + 1% L-Glutamin	Institut für Mikrobiologie, Universität Würzburg
J774	<i>Mus musculus</i> - macrophage sarcoma	DMEM + 10% FCS	Institut für Mikrobiologie, Universität Würzburg
SKOV3	<i>Homo sapiens</i> – mammary gland carcinoma	McCoy + 10% FCS	ATCC Promochem
SKBR3	<i>Homo sapiens</i> – ovary carcinoma	McCoy + 10% FCS	ATCC Promochem

table 4.6: Eukaryotic cells line

4.V Antibodies

name	recognized antigen	source
α -serum albumin	murine serum albumin [native], polyclonal rabbit	Abcam, ab34807
α -serum albumin	murine serum albumin [denatured], polyclonal rabbit	Abcam, ab19196-2
Trastuzumab (Herceptin)	HER2/neu, humanized	Universitätsklinikum Würzburg
Trastuzumab-AlexaFluor 488	HER2/neu, humanized	labeled using Invitrogen 'APEX Alexa Fluor® 488 Antibody Labeling Kit'
Cetuximab (Erbix)	EGFR, chimeric mouse/human	Universitätsklinikum Würzburg
α -GFP	green fluorescent protein, rabbit polyclonal	Santa Cruz, sc-8334
α -human-Cy5	goat polyclonal to human IgG - H&L	Abcam, ab6561
pan macrophage	α F4/80, rat monoclonal, clone BM8	Acris Antibodies GmbH

table 4.7: Antibodies

4.VI Buffers and solutions

4.VI.1 Media

name	composition	
BHI	37 g	brain heart infusion broth
	ad 1l	desalted water
SOC	20 g	bacto – tryptone
	5 g	bacto-yeast extract
	0.5 g	NaCl (sodium chloride)
	2.5 ml	KCl (1M) (potassium chloride)
	20 ml	glucose (1M)
	ad 1l	desalted water

table 4.8: Cultivation media

4.VI.2 Buffers

name (source)	composition	
3,5 x SMHEM	952 mM	glucose
	3,5 mM	MgCl ₂ (magnesium chloride)
	7 mM	HEPES pH 7,2
	solvent :	desalted water
DNA loading dye (Roche labFAQs)	250 mg	bromphenol blue
	250 mg	xylene cyanol
	33 ml	Tris-HCl (150mM, pH 7.6)
	60 ml	glycerol
	7 ml	desalted water
SDS PAGE sample buffer (Roche labFAQs)	10 ml	Tris-HCl (1.5 M, pH 6.8)
	6 ml	SDS (20%)
	30 ml	glycerol
	15 ml	β-mercaptoethanol
	1.8 mg	bromphenol blue
	ad 100 ml	desalted water
Oligo annealing buffer (tronolab.epfl.ch)	100 mM	CH ₃ COOK (potassium acetate)
	30 mM	HEPES (pH 7.4)
	2 mM	(CH ₃ COO) ₂ Mg
	solvent :	desalted water
MACS buffer (Miltenyi biotech)	0.5 g	bovine serum albumin
	4 ml	EDTA (25 mM)
	ad 50 ml	PBS adjust to pH 7.2
PEG lysis buffer (Chomczynski and Rymaszewski, 2006)	60 g	PEG 200
	until pH > 13.3	KOH (2 M) (potassium hydroxide)
	ad 100 ml	desalted water
PBST	0.05%	Tween 20
	solvent :	PBS
PBSt	0.02%	Tween 20
	solvent :	PBS
		adjust to pH 7.4

table 4.9: Buffers

4.VI.3 Solutions

name	solvent	applied concentration	
		E.coli	L. monocytogenes
Ampicillin	desalted water	100 µg/ml	
Tetracycline	50% EtOH p.A.	20 µg/ml	5 µg/ml
Erythromycin	EtOH p.A.	300 µg/ml	5 µg/ml
Menaquinone (vitamin K ₂)	EtOH p.A.		50µg/ml

table 4.10: Solutions

4.VII Animals

All animals were bought from Harlan-Winkelmann (Germany) and housed in the animal facility of the Institut für medizinische Strahlenkunde und Zellforschung or the Biozentrum, Universität Würzburg. Balb/c (OlaHsd), Balb/c SCID (JHanHsd-Prkdc), C57BL/6 (JOlaHsd) and Foxn1 nu/nu mice (Hsd: Athymic) were used for experiments.

4.VIII Consumables and chemicals

name	manufacturer
chemicals	Sigma-Aldrich, Applichem, Roth, Difco
kits	Qiagen, Fermentas, Ambion, Miltenyi, Amersham, Finnzymes
cell culture media / reagents	Gibco, PAN
other reagents	Thermo Scientific, Pierce
plastic consumables	Nunc, Greiner Bio-One, Millipore, Bio-Rad, Braun, Sarstedt, Amersham, Schleicher & Schuell

table 4.11: Consumables and chemicals

4.IX Enzymes and special reagents

name	manufacturer
restricion endonucleases, ligase, phosphorylase, kinase	Fermentas
polymerases	Genecraft, Finnzymes, Stratagene
Agarose, dNTPs, molecular weight marker	Invitrogen

table 4.12: Enzymes

5 Methods

5.1 Microbiology

5.1.1 General bacterial culture

All bacterial strains were cultivated in Brain Heart Infusion broth (BHI) at 37°C unless mentioned otherwise. All liquid overnight cultures were inoculated from a single colony. For harvesting bacterial cultures in defined growth phases, cultures were inoculated from overnight cultures. Addition of antibiotics was performed as required for maintenance of plasmids. Induction of *prfA* regulated genes *in vitro* was performed by addition of 1% Amberlite XAD to the bacterial cultures.

5.1.2 Electrotransformation

E.coli and *L. monocytogenes* are intrinsically not competent, therefore DNA transformation has to be facilitated by physical techniques. Different methods are available for transformation, but the mediation of DNA uptake by application of an electrical field is the most efficient. Therefore this method was used by default as described below.

An *E.coli* culture of 50 ml was grown to $OD_{600nm} = 0,6-0,8$ and chilled on ice for at least 15 min. Bacteria were pelleted at $3,345 \times g$ for 15 min at 4°C and serially washed in 50~, 25~ and 10 ml 10% glycerol. Finally bacteria were resuspended in 500 µl 10% glycerol and stored in aliquots at -80°C until transformation.

L. monocytogenes is a gram⁺ bacterium with a strong cell wall, which impedes efficient DNA uptake. Partial digestion of the cell wall permits the electrotransformation, albeit at a much lower efficiency than *E.coli*.

L. monocytogenes culture of 50 ml was grown to $OD_{600nm} = 0,6-0,8$ and Penicillin G was added to a final concentration of 5 µg/ml. The Bacteria were incubated for an additional hour and subsequently chilled on ice for at least 15 min. Bacteria were pelleted at $3,345 \times g$ for 15 min at 4°C and washed twice with 5 ml of 3,5 x SMHEM buffer. Finally bacteria were resuspended in 500 µl 3,5 x SMHEM buffer and stored in aliquots at -80°C until transformation. 1-5 µl of DNA was mixed with 100 µl electrocompetent bacteria and pulsed with the Micropulser Electroporator. Immediately after transformation bacteria were mixed with 1 ml of SOC medium and incubated without antibiotics. The duration of this interim incubation before plating on antibiotic agar plates was dependent on the resistance gene and the transformed bacterium (see table 5.1).

	E.coli	L. monocytogenes
Ampicillin	1 h	not applied
Erythromycin	3 h	6 h
Tetracycline	1 h	2 h

table 5.1

5.1.3 Preparation of infection aliquots

Bacterial cultures of 50 ml were grown to $OD_{600nm} = 1,0$ for wildtype bacteria and $OD_{600nm} = 0,8$ for $\Delta aroA$ mutants. Bacteria were chilled on ice at least for 15 min and pelleted at $3,345 \times g$ at $4^{\circ}C$. Bacteria were then washed twice in 0,9 % sodium-chloride solution and finally resuspended in 10 ml 0,9 % sodium-chloride / 20 % glycerol. Aliquots were stored at $-80^{\circ}C$.

After a minimum of 24h cold storage, three aliquots were thawed and the bacterial titer was determined by plating serial dilutions. The calculated mean value of the three aliquots was later on used as bacterial titer for infection experiments.

5.1.4 Quick lysate of *L. monocytogenes*

A single picked bacterial colony or the pellet of 20 μl overnight (o/n) culture were vortexed with 100 μl PEG lysis buffer and heated to $80^{\circ}C$ for 10 min. 1 μl of the crude lysate served as template for PCR screening.

5.II Molecular biology

After generation of new DNA constructs, all modified sequences were confirmed by sequencing. *In silico* cloning was performed with VectorNTI advance 10 (Invitrogen, USA).

5.II.1 Isolation and purification of DNA

All DNA isolations were performed with commercial Qiagen Kits. Plasmid DNA from gram⁻ and gram⁺ bacteria was isolated with Qiagen Plasmid Kits (QIAGEN Plasmid Kit). Genomic DNA was isolated from 2ml o/n culture with the Qiagen DNAeasy Blood & Tissue Kit (QIAGEN DNeasy Blood & Tissue Kit). Gel elution and DNA purification was performed with the QIAquick PCR Purification Kit (QIAquick PCR Purification Kit). All preparations were performed according to manufacturers protocols.

5.II.2 Agarose gel electrophoresis

DNA is charged negatively because of the phosphate residues in the sugar-phosphate backbone. Therefore DNA migrates in a constant electric field towards the positive pole. DNA was separated in size by electrophoresis in 0,5 x TBE agarose gels. DNA was mixed with loading dye and inserted into pockets of the agarose gels. The density of agarose gels was adjusted to the expected size of DNA fragments. For fragments below 500bp 2% agarose gels were used, for fragments between 500bp and 3Kbp 1% gels were used and larger DNA fragments were separated in 0.5% gels. For staining of DNA Ethidium bromide was added at a final concentration of 0,45µg/ml. DNA bands were visualized under UV-light.

5.II.3 Polymerase chain reaction (PCR)

Polymerase chain reaction was used to amplify specific DNA sections for screening or cloning purposes. *Taq* DNA polymerase was used for screening of bacterial clones, as it has no 3'->5' exonuclease (proofreading) activity. For cloning of DNA, DNA polymerases with proofreading activity like *Pfu* DNA polymerase and Phusion *Taq* were used.

The PCR can be divided into three parts: the first part being the denaturation of the double stranded DNA template into single stranded DNA. In the annealing phase specific DNA oligomers (primers), flanking the sequence to be amplified with their 3' ends directed towards this sequence, bind to the DNA and serve as an initiation point for the polymerase. Finally the polymerase elongates the primer until the template strand ends or it falls off spontaneously. Cycling of these three steps was performed 30-35 times depending on the initial amount of DNA template used.

Phusion *Taq* polymerase amplifies approximately 4kb of DNA per minute from an abundant template like plasmid DNA, and 2kb from genomic DNA. common *Taq* polymerase amplifies 1kb per minute, *Pfu* polymerase *only* 0,5kb per minute. Therefore the elongation time was chosen suitable for the expected product.

5.II.3.a Colony PCR

Colony PCR was performed for screening of bacterial colonies after cloning, plasmid insertion or mutagenesis. Gram⁻ bacteria like *E.coli* do not have a rigid cell wall, therefore these bacteria can be lysed during PCR to release sufficient DNA as template. Parts of a bacterial colony and the components for the PCR reaction were transferred into the PCR reaction tube. A typical PCR for screening of colonies was performed according to the following protocol:

	amount
10 x buffer	2,0µl
dNTPs	10pmol
primer 1	1pmol
primer 2	1pmol
template	picked colony
<i>Taq</i> DNA polymerase	1u
H ₂ O	ad 19µl
final volume	19

table 5.2 PCR reaction composition

no	duration [sec]	temperature	cycling	step
1	180	94°C		initial denaturation
2	60	94°C	30 - 35	cyclic denaturation
3	30	48 - 60°C		primer annealing (temperature depending on polymerase, buffer and primer)
4	15 -	72°C		elongation (duration depending on polymerase and amplicon length)
5	45 -	72°C		final elongation (at least three fold longer than elongation time)

table 5.3 Standard PCR protocol

5.II.3.b PCR for cloning

For cloning of DNA fragments the accuracy of the amplified sequence is crucial. Therefore for cloning purposes DNA was amplified with DNA polymerases capable of proof reading. *Pfu* DNA polymerase and Phusion *Taq* were used following three protocols:

<i>Pfu</i> DNA polymerase		Phusion <i>Taq</i> DNA polymerase	
	amount		amount
10 x buffer	5,0µl	5 x HF buffer	10,0µl
dNTPs	10pmol	dNTPs	10pmol
primer 1	1pmol	primer 1	1pmol
primer 2	1pmol	primer 2	1pmol
template	1,0µl	template	1,0µl
polymerase	0,5u	polymerase	0,5u
H ₂ O	ad 50µl	H ₂ O	ad 50µl
final volume	50	final volume	50

table 5.4 *Pfu* / Phusion PCR reaction composition

<i>Pfu</i> DNA polymerase				Phusion <i>Taq</i> DNA polymerase			
no	duration [sec]	temperature	cycling		duration [sec]	temperature	cycling
1	180	94°C		initial denaturation	30	98°C	
2	60	94°C		cyclic denaturation	10	98°C	
3	30	48 - 60°C	30 - 35	primer annealing	20	51 - 63°C	30 - 35
4	30 -	72°C		elongation	15 -	72°C	
5	90 -	72°C		final elongation	45 -	72°C	

table 5.5 *Pfu* / Phusion PCR protocol

5.II.4 Site directed mutagenesis

Exchange of single nucleotides was performed by site directed mutagenesis. Genes to be mutated were cloned in small plasmid vectors like puc18 for subsequent mutagenesis. A special PCR was performed with this plasmid as template, which amplifies the full plasmid with mutating primers. The two primers were located on the nucleotides to be mutated and reverse complementary. The base exchange is performed in a PCR with linear amplification using these mutating primers. The PCR conditions for site directed mutagenesis differ from the common PCR protocols (table 5.6 and table 5.7).

<i>Pfu</i> DNA polymerase	
	amount [μ l]
10 x buffer	5,0 μ l
dNTPs	10pmol
primer 1	1pmol
primer 2	1pmol
template	1,0 μ l
polymerase	0,5u
H ₂ O	ad 50 μ l
final volume	50

**table 5.6 Site directed mutagenesis
reaction composition**

no	duration [sec]	temperature	cycling	step
1	30	95°C		initial denaturation
2	30	95°C	18	cyclic denaturation
3	60	55°C		primer annealing (temperature depending on polymerase, buffer and primer)
4	600	68°C		elongation (duration depending on polymerase and amplicon length)

table 5.7 Site directed mutagenesis reaction protocol

After the amplification of the plasmid strands, the strands annealed spontaneously to dsDNA. After the PCR, 1 μ l of the restriction enzyme *DpnI*, which specifically cleaves methylated DNA, was added into the reaction tube. The template plasmid, isolated from *E.coli* and therefore bearing methylations, was digested, leaving only mutated dsDNA in the reaction. Direct transformation of this reaction mixture into electrocompetent *E.coli* yielded clones which were screened for the mutated sequences.

5.II.5 Annealing of DNA oligomers for cloning

For cloning of small artificial DNA sequences (<120 nucleotides) encoding multiple cloning sites or shRNAs, the desired sequences were ordered as complementary single strand oligomers. For later insertion into a plasmid vector, the single strand sequences were not completely complementary but had specific overhangs. At their ends after annealing, non-complementary bases remained, building distinct restriction site overhangs. The oligomers

were ordered lyophilized and reconstituted in H₂O to a final concentration of 100pmol/μl. In a first step 2μl of two oligomers were mixed in annealing buffer, heated for 5min to 95°C, 10 min to 70°C and then cooled down slowly at 0.1°C/sec to room temperature (RT). The single stranded complementary oligomers were thereby annealed to double stranded oligomers which can be phosphorylated for subsequent cloning.

5.II.6 Enzymatic DNA modifications

5.II.6.a DNA restriction

DNA restriction digests for specific assembly of DNA sequences were performed with purified type II endonucleases. These enzymes cut DNA at characteristic palindromic sequences of 4-8 bp length.

DNA restriction digestion was performed with approximately 1-2μg of purified DNA. One enzyme digestion reactions were performed in 20μl volume with 5-10u restriction enzyme. Simultaneous double digestion reactions were performed in 30μl volume with 5-10u of each restriction enzyme. The digestion buffers were chosen as recommended by the manufacturer (Fermentas restriction digestion). The digestion reaction was performed for 2-3h at 37°C unless noted otherwise.

5.II.6.b Ligation

The connection of the sugar-phosphate backbones of two double stranded DNAs is called ligation. Ligases catalyze the bond between the 3'-Hydroxylgroup of one DNA to the 5'-Phosphate of another. In ligation reactions usually one DNA fragment, most often the vector, was dephosphorylated before the reaction to prevent the religation of the empty vector.

	volume [μl]
vector DNA	1,00
insert DNA	11,75
ligase buffer (10 x)	1,50
ligase (1u/μl)	0,75
final volume	15

table 5.8 Ligation reaction composition

Ligation was performed at 16°C or at RT for 2-3h. Purified DNA fragments to be ligated were used to adjust the volume of the ligation reaction to 15μl. Unless mentioned otherwise, the 3- to 5-fold amount of plasmid with respect to the amount of insert was used in one reaction.

5.II.6.c Phosphorylation

DNA oligomers were supplied in the unphosphorylated form by the manufacturer. For direct cloning of ordered oligomers after annealing, they were phosphorylated to allow ligation.

	volume [μ l]
annealed oligomers (20pmol/ μ l)	5,0
water	12,0
T4 polynucleotide kinase buffer (10 x)	2,0
T4 polynucleotide kinase (10u/ μ l)	1,0
final volume	20

**table 5.9 Phosphorylation reaction
composition**

Phosphorylation was performed for 30min at 37°C and enzyme was inactivated for 10min at 70°C.

5.II.6.d Dephosphorylation

The dephosphorylation of 5' phosphate of the plasmid vector was performed before ligation to prevent religation of the empty vector.

Purified and digested vector DNA was dephosphorylated in the buffer supplied by the manufacturer. Into 50 μ l of purified plasmid DNA, the calf intestine alkaline phosphatase (CIAP) and the corresponding buffer were added and the mixture was incubated for 1h at 37°C.

5.II.7 Construction of *L. monocytogenes* mutants

Genomic insertions and deletions in *L. monocytogenes* were performed by homologous recombination using a modified protocol of (Wuenschel et al., 1991).

For deletions of specific genomic sequences, flanking upstream and downstream regions of about 300-500bp were amplified by PCR and cloned into the plasmid pLSV101. The plasmid pLSV101 was a shortened derivative of the published pLSV1 integration vector (kindly

provided by Thilo Fuchs, ; Wuenscher et al., 1991). Functional moieties on the plasmid were a gram^- origin of replication for propagation and cloning purposes in *E.coli*, an erythromycin resistance cassette for positive selection on plasmid carrying clones and a temperature sensitive gram^+ origin of replication. The gram^+ origin of replication allowed propagation of the plasmid only at incubation temperatures of about 30°C and lower, at higher temperatures the plasmid was lost by gram^+ bacteria like *L. monocytogenes*.

Plasmid pLSV101 with integrated homologous regions was transformed into the parental *L. monocytogenes* strain and clones were screened for plasmid presence after incubation at 30°C. An overnight culture of the positive clone was plated in serial dilutions on selective agar plates and incubated at 42°C. In this step, only bacteria with the integrated plasmid can survive because their antibiotic resistance cassette is stably inserted, while bacteria harbouring the plasmid outside the chromosome are thinned out as they can not replicate the plasmid at this elevated temperature. The insertion of the plasmid occurs by homologous recombination. Bacterial clones were screened for genomic plasmid insertion by PCR. Bacteria with integrated plasmid were serially passaged in medium without erythromycin selection at RT and screened periodically for resistance loss. Bacterial clones without antibiotic resistance had a second homologous recombination event which cut out the integrated plasmid. If this event took place at the second flanking region, the plasmid together with the gene to be deleted has been cut out of the genome and a mutant was generated.

Genomic insertions and replacements were performed with the same technique but with the gene to be inserted cloned in between the genomic flanking regions comprised in the integration plasmid.

5.II.8 Analysis of bacterial growth kinetics

Measurement of bacterial growth was assessed in autoclaved BHI medium. Bacterial starter cultures were grown overnight at 37°C and 180 rpm. The cultures were diluted 1:500 in 50ml fresh medium with required supplements like antibiotics. Bacterial growth was assessed by measuring absorption of the growth culture at 600 nm using a photometer at regular intervals.

5.II.9 RNA analysis

5.II.9.a RNA isolation with DNase digestion

For RNA isolation, the bacterial strains or mammalian cells were cultured under the required

conditions, pelleted and shock frozen in liquid nitrogen. RNA was isolated using Qiagen Kit according to manufacturers protocols with some modifications. Samples of *L. monocytogenes* were resuspended in 350 µl RLT buffer (Qiagen RNeasy Mini Kit) and transferred into a matrix D shredder tube (QBioGene). Bacteria were crushed three times for 45 sec in a Fast Prep FP120 shredder at level 6.5 with incubations on ice in between. After crushing the supernatant was mixed with 250 µl ethanol and transferred on the RNA isolation column and RNA was isolated as described by the manufacturers protocol (QIAGEN RNeasy Mini Kit). Eukaryotic RNAs were isolated as described by the manufacturers protocol (QIAGEN RNeasy Mini Kit). Contaminating DNA was digested on column with the Qiagen RNase-free DNase Set (QIAGEN RNase-free DNase Set). After RNA isolation, the presence of residual DNA contaminations was assessed by PCR with genomic housekeeping primers. PCR is not functional with RNA as template, therefore the reaction yielded a product only on presence of DNA. Residual DNA was digested with the Ambion DNA-free kit as described by the manufacturers protocol (Ambion DNA-free).

RNAs shorter than ~150 nucleotides were isolated following an abridged protocol. After cell lysis, the bacteria were mixed with 1 volume (~350 µl) of 2-propanol and transferred on a RNA isolation column. The flowthrough containing the small RNAs was precipitated with addition of 2 volumes (~700 µl) of 2-propanol and transferred on a second RNA isolation column. The first column was isolated as described in the manufacturers protocol. The column containing the small RNAs was washed twice with 500 RPE buffer, residual buffer was removed in an additional centrifugation step and the RNA was eluted using RNase free water.

5.II.9.b RNA polyacrylamide gel electrophoresis

The quality of the isolated RNA was determined by RNA polyacrylamide gel electrophoresis. TBE buffered urea gels were used to separate the RNA. Gels were prepared after following protocol.

	amount
acrylamide:bisacrylamide solution (19:1), 40%	7,5 ml
urea	7.2 g
10x TBE buffer	1.5 ml

table 5.10 RNA acrylamide gel composition

Components were mixed until the urea was completely dissolved. The solution was heated to 60°C and water was added to a final volume of 15 ml to facilitate dissolution. 60µl of

ammonium persulphate (10% w/v) and 15µl Temed were added to the mixture to activate the polymerization process and gels were cast.

Before electrophoretic separation of RNA, the gel was prerun without samples for 30min at 300V in 1 x TBE buffer.

RNA was mixed with 2 x RNA loading buffer (for urea polyacrylamide gels) and separated at 300V for 3h. Gels were fixed for 5 min in 50% ethanol, washed once in dH₂O and stained in 1 x TBE with 10µl of ethidium bromide stock solution (10mg/ml) for 5 min. Bands were visualized using UV light.

5.II.9.c Reverse transcription of RNA

For quantitation of relative mRNA amounts by qRT-PCR the RNA was transcribed into complementary DNA. Reverse transcription was performed with M-MuLV reverse transcriptase. Bacterial cDNA was generated using random hexamers and eukaryotic cDNA using oligo (dT)₁₈ primers. Transcription was performed with 0.5µg of total RNA using first strand cDNA synthesis kit as described by the manufacturer (Fermentas first strand cDNA synthesis kit).

5.II.10 Quantitative Real Time-PCR (qRT-PCR)

Transcriptional expression of genes was quantified by comparing amounts of the mRNA of interest with the mRNA of housekeeping genes in the same sample. mRNA was reversely transcribed as described in 5.II.9.c and cDNA was used as template for the qRT-PCR reaction. For gene expression analysis in eukaryotic samples the expression of the Hypoxanthine-guanine phosphoribosyltransferase gene (HPRT; primer: Hprt2 RT (F) & Hprt2 RT (R)) and the β -actin gene (ACTB; primer: b-actin RT (F) & b-actin RT (R)) were used as housekeeping controls. Transcriptional analysis in *L. monocytogenes* was performed in relation to the RNA polymerase beta subunit expression (rpoB; primer: RpoB RT (F) & RpoB RT (R)).

qRT-PCR was performed on the Rotorgene2000 using Finnzymes DyNAmo™ HS SYBR® Green qPCR Kit as described in the manual (see table 5.11) (Finnzymes DyNAmo™ HS SYBR® Green qPCR Kit). The included SYBR-green is a dye intercalating into dsDNA and

no	duration [sec]	temperature	cycling	step
1	900	95°C		initial denaturation, activation of hot start polymerase
2	10	94°C	40	cyclic denaturation
3	20	56°C		primer annealing, fluorescence acquisition (temperature depending on used oligos)
4	30	72°C		elongation
5	300	72°C		
6	600	25°C		
7		70-95°C		melt curve

table 5.11 Standard qRT-PCR protocol

The optimal annealing temperature was evaluated once for each primer using a PCR with a gradient in the annealing temperature and protocols as described in 5.II.3.a.

qRT-PCR data was analyzed using Rotor-Gene Analysis Software V4.6.70. All reactions were performed in triplicate. After the qRT-PCR run, the melting curve of the samples was examined to confirm the amplification of a single fragment. If the melting curve of samples amplified with the same primer pair differed, the qRT-PCR was repeated with elevated annealing temperature. On occurrence of multiple maxima in the melt curve of one sample the reaction was repeated with adjusted conditions, too. The threshold for quantitation was set in the logarithmic fluorescence graph just above the lag phase. The software then calculated the intersection point between the fluorescence curve of each sample and this threshold line. This value was called the Ct-value and relative mRNA amounts were calculated by elevating 2 by the power of the Ct values. These calculated values were linear variables representing the initial mRNA amount in each sample. The later the fluorescence in the sample was detected, the higher these values were, corresponding to a low amount of initial cDNA portion. The differences in the amount of template for cDNA synthesis and the applied amount for qRT-PCR reaction were compensated by dividing the amount of specific mRNA by the amount of a housekeeping mRNA for each sample.

5.II.11 Treatments of live *L. monocytogenes* for antibody coating

5.II.11.a Coating

Coating of *L. monocytogenes* was performed with bacterial infection aliquots which were diluted and washed in PBS (pH=8,2). Unless mentioned otherwise 1×10^8 CFU were incubated in 100µl PBS (pH=8,2) for 45min with 2-3µg of antibody. The antibody loading was performed at 23°C under vigorous shaking in a benchtop thermoshaker (500rpm). After the incubation 900µl PBS (pH=8,2) were added and the bacteria were pelleted for 2' and 16.000 x g. The supernatant was removed and the bacteria were again resuspended to a final volume of 1ml in PBS (pH=8,2).

5.II.11.b Crosslinking

Crosslinking of antibodies to SPA on the surface of *L. monocytogenes* was carried out with dimethyl pimelinediimidate dihydrochloride (DMP). Unless mentioned otherwise freshly prepared DMP in PBS (pH 8.2) was added to a final concentration of 0,65 mg/ml to the antibody coating reaction and incubated under vigorous shaking for 45 min at RT. The bacteria were washed with 900µl PBS (pH 8.2) and the crosslinking procedure was repeated for additional 45 min with a freshly prepared DMP stock solution at a final concentration of 0,65 mg/ml. The bacteria were washed twice with 900µl PBS (pH 8.2) and resuspended at a final volume of 1ml in PBS (pH=8,2).

5.II.11.c Serum treatment of *L. monocytogenes*

Bacteria were incubated with serum after antibody coating and crosslinking as described below. The bacteria were pelleted for 2min at 16.000 x g and RT and the supernatant was discarded. 100µl freshly isolated murine or human serum was added and the bacteria were incubated in a thermoshaker at 23°C with 500rpm for 45min. The bacteria were washed twice with PBS (pH=8,2) and finally the volume was adjusted to 1ml with PBS (pH=8,2).

5.II.12 Haematoxinilin Eosin staining

Mouse organs were fixed in buffered 4% paraformaldehyde solution for 24h at 4°C. Organs were stored in 50% ethanol until paraffin embedding and sectioning. Staining of sections for was performed with Haematoxinilin Eosin (H/E). This staining colors the structures in purple-blue and pink and allows a general overview of the tissue structure of the section. Tissues

were cut in 4-5 μm thick slices and mounted on a microscope slide. The H/E staining protocol is shown in table 5.12. After staining, tissue sections were mounted in Entellan and analysed microscopically

step	reagent	incubation time
1	Xylol I	10 min
2	Xylol II	10 min
3	Ethanol I	2-5 min
4	Ethanol II	2-5 min
5	Ethanol III	2-5 min
6	70 % Ethanol	5-10 min
7	dH ₂ O	5 min
8	Haematoxinilin	0,5-2 min
9	Tap Water	5-10 min

table 5.12: H/E staining protocol

step	reagent	incubation time
10	dH ₂ O	2-5 min
11	Eosin	0,5 - 1 min
12	dH ₂ O	2-5 min
13	70 % Ethanol	3 min
14	Ethanol I	3 min
15	Ethanol II	5 min
16	Ethanol III	5 min
17	Xylol I	10 min
18	Xylol II	10 min

5.III Protein analysis

5.III.1 Protein isolation

5.III.1.a Cellular proteins

Cultures of gram negative bacteria or suspensions of eukaryotic cells were pelleted and resuspended in Laemmli buffer (Laemmli, 1970). The buffer volume was chosen to concentrate the bacterial sample hundredfold and the eukaryotic cells to a final concentration of 10^8 cells/ml. The crude protein extracts were denatured for 5-10 min at 100°C and stored at -20°C.

Cultures of *L. monocytogenes* were pelleted, resuspended in 500 μl PBS and shredded as described in 5.II.9.a to lyse the bacteria. Tubes were centrifuged briefly and supernatant containing the lysed bacteria was mixed with Laemmli buffer and denatured for 5-10 min at 100°C and used for further analysis.

5.III.1.b Secreted proteins

Secreted proteins were isolated from culture supernatant by precipitation. Bacterial cultures were pelleted and 40 ml of supernatant were removed without disturbing the pellet. This supernatant was centrifuged again for 20 min at 3345 x g and 4°C. 20ml supernatant were mixed with 10% TCA and incubated on ice o/n for precipitation. After centrifugation for 1h at

4000rpm at 4°C, the liquid was decanted and the tube was rinsed with 1ml acetone. Following the drying of the tube walls they were rinsed thoroughly with 200µl Laemmli buffer (Laemmli, 1970). The tube was incubated on a rotator for 10-20 min to increase the protein yield. If the buffer color changed to yellow, indicating a low pH, 1µl of saturated Tris was added to adjust the pH. The protein samples were denatured for 5-10 min at 100°C and stored at -20°C for further use.

5.III.1.c Membrane proteins

The rigidity of the gram positive cell wall of *L. monocytogenes* allows a simple protocol for extraction of membrane proteins in this bacterium. The bacterial cultures were pelleted and resuspended in Laemmli buffer (Laemmli, 1970). After boiling for 5-10 min the protein extracts were centrifuged at 16.000 x g for 2 min at RT and supernatant containing the membrane proteins was used for further experiments.

5.III.2 Polyacrylamide gel electrophoresis

The isolated proteins were resuspended and boiled in Laemmli buffer containing β-mercaptoethanol and sodium-dodecylsulfate (SDS). Thereby secondary to quaternary structure was destroyed and binding of dodecyl-residues mediated a negative charge of different proteins.

Proteins were separated in size by polyacrylamide gel electrophoresis (SDS-PAGE). SDS gels were cast in Mini-Protean cells (BioRad) as described in table 5.13.

	separation gel [ml]			stacking gel [ml]
	5%	10%	12,5%	
Acrylamide/Bisacrylamide 40%	2,7	5	6,5	1,1
dH ₂ O	14,4	12,1	10,6	7,55
Tris-Cl	2,5 [3M pH 9,0]			1,25 [1M pH 6,8]
20% SDS	0,1			0,05
TEMED	0,02			0,01
10% APS	0,2			0,1

table 5.13: SDS-polyacrylamide gel composition

Separation of proteins smaller than 50kDa was performed on 12,5% separation gels, proteins up to a size of approximately 100kDa were separated on 10% gels and larger proteins on 5% gels. SDS-PAGE was performed in 0,5 x TBE buffer at 180V for 1h or until

the blue dye reached the end of the gel. Protein detection was performed by Western blot analysis or by coomassie staining with Bradford-Coomassie-Kit (Pierce).

5.III.3 Western blot analysis

After SDS-PAGE, the gels were equilibrated for 10 min in Towbin buffer at 4°C and proteins were transferred on nitrocellulose membranes by western blotting. Semi-dry blotting technique was performed at 25 V for 30-100 min depending on size of the target protein. Protein transfer and approximate protein amounts on the membrane were confirmed by Ponceau red staining. The membranes were washed with distilled water and blocked in PBS / 5 % milk with shaking for 45 min at RT. Primary antibodies were diluted in PBS/milk 1:1000 to 1:5000 and incubated o/n at 16°C or for 2h at RT. Following incubation membranes were washed three times for 10 min with PBS/0,05 % Tween 20 and incubated with horseradish-peroxidase labeled secondary antibodies for 2 h at RT. Membranes were washed again for three times and western blots were developed using ECL Western Blotting detection kit (GE Healthcare).

5.IV Eukaryotic cell biology

5.IV.1 General eukaryotic cell culture

Eukaryotic cell lines were maintained at 37°C under 5 % CO₂ atmosphere. Media containing 10 % FCS and 2 mM L-glutamine were used for propagation. Cells were passaged every 2-3 days at 1:1 to 1:10 ratios in the respective growth media as described in table 4.6.

5.IV.2 Infection assay using bacteria

Between 1×10^4 and 2×10^5 eukaryotic cells per well were seeded at least 16h before infection experiments. The cell density was chosen depending on the cell size, growth rate and the timepoints to be investigated after infection. Prior to infection, cells were washed once with medium lacking FCS and bacteria were diluted in the same medium. Infection was performed in a volume of 500µl per well for 1h at 37°C. The timepoint of bacterial addition to the cells was termed 0 h post infection (p.i.). 1 h p.i. the supernatants containing the bacteria were discarded and 1 ml of medium containing 100 µg/ml gentamicin was added to kill the extracellular bacteria. After 1 h, the supernatant was substituted with medium containing 10 µg/ml gentamicin. Intracellular CFU was determined by lysing the cells in 1 ml 0.1 % triton X-100 and plating serial dilutions on agar plates.

The number of adherent / early invasive bacteria was determined by washing infected cells five times with PBS and plating the cells lysed in 0.1 % triton X-100 in serial dilutions. Infection experiments for determination of CFUs were performed in triplicates for each bacterial strain and repeated three times.

1/10 of each sample was plated, so the counted CFU had to be multiplied by 10 to acquire the final bacterial count per sample. If no bacterial colonies were detected after infection, the CFU was artificially set on 1, to allow calculation of strain differences.

5.IV.3 Treatment of eukaryotic cells using magnetic beads

Eukaryotic cells were seeded in 24 well plates at a density of 1.2×10^5 cells per well at least 16h before incubation with magnetic beads. Immediately before bead treatment, cells were washed once with medium lacking FCS, treatment was performed in 500µl volume of the same medium.

5µl protein A coated Dynabeads® (Invitrogen) were removed from a carefully mixed stock vial and the liquid phase was aspirated while holding the beads close to a magnet. Following washing using 100µl PBSt the beads were incubated in 100µl PBSt with addition of antibodies. Approximately 1µg of unlabeled antibodies was added, fluorescently labeled antibodies were diluted 1:30. Following 10 min incubation at 23°C in a benchtop shaker at 800rpm in the dark, the beads were washed twice using 100µl PBSt. Following removal of the supernatant the beads were finally resuspended in 30µl PBSt and 5µl of this suspension was used for treatment of one well in a 24 well plate.

5.IV.4 Quantitation of prodrug conversion *in vitro* (prodrug assay)

Delivery of prodrug-converting enzymes was quantified indirectly through conversion of prodrugs into cytotoxic drugs. The viability of infected eukaryotic cells was used to grade delivery efficiency after infection with and without prodrug addition. Eukaryotic cells were infected in duplicates as described in 5.IV.2 but with some modifications. Following infection the eukaryotic cells were not lysed, but instead detached from the well by trypsin addition 4 h p.i. and the duplicates were pooled.

The cells were diluted to 2.5×10^4 cells/ml and 100µl was transferred into 96 well plates prepared with gentamycin and prodrug suspension. Gentamycin was used at a final concentration of 10µg/ml, while the prodrug 5-FC was used at a final concentration of 1mM.

Each strain was dispensed in triplicate in wells with and without prodrug and the plates were incubated at 37°C under a 5% CO₂ atmosphere. At 3 d, 5 d and 7 d post prodrug addition the

number of viable eukaryotic cells in each well was determined in a MTT viability assay. Therefore the culture medium was substituted by 100 μ l of MTT solution. Viable cells quantitatively convert in their mitochondria water soluble MTT dye into the non water soluble formazan. 2-4 h after MTT addition the supernatant was discarded and 100 μ l of 10% HCl in 2-propanol was added resolving the precipitated dye. The absorption at 405 nm subtracted by the reference wave length of 650 nm was measured photometrically and used for quantitation of formazan conversion.

5.IV.5 Fluorescence imaging of GFP positive cells

Eukaryotic cells were seeded in 24 well plates with disinfected glass coverslips on the bottom of the wells. Cells were infected in duplicates as described in 5.IV.2 with the exception that the eukaryotic cells were not lysed after infection. At the investigated timepoints, coverslips with attached cells were mounted upside-down in Mowiol on microscopic slides. The slides were stored in the dark at RT and observed by immunofluorescence microscopy.

5.IV.6 Immunofluorescence staining

Eukaryotic cells were seeded and infected on glass coverslips. Following treatment using bacteria or magnetic beads, coverslips were washed three times by dipping them consecutively into three petridishes filled with PBS. Cells were fixed in 4% paraformaldehyde solution for 10 min at RT and washed again as described before. Following fixation, cells were either permeabilized using 1% Triton X100 for 1h at RT or directly blocked using 10% of serum of the same species as the primary antibody. Blocking was performed for 1h at RT. Following washing, cells were incubated with the fluorescently labeled primary antibody at an dilution of 1: 500 for 2h at RT in the dark. Again the coverslips were washed three times, dried on a papertowel and mounted using mowiol or Slowfade antifade reagent (Invitrogen). Samples were examined using a confocal laser scanning microscope (Leica).

5.IV.7 Flow cytometry

Detached cell after treatment were washed once in FACSFlow sheat fluid (BD, Germany) and approximately 1×10^6 cells were stained in a volume of 50 μ l FACSFlow. Cells were incubated with primary antibody for 1 h at 4°C, washed once with FACSFlow and spinned down for 2 min at 200 x g. Antibodies were diluted 1:50 up to 1:300 for use. Incubation with secondary antibody was performed for 30 min at 4°C in the dark. Cells were washed before analysis in a FacsCalibur (BD, Germany).

5.V Animal experiments

5.V.1 General animal handling

Animals were housed in the animal facility of the MSZ. Animals were purchased aged 5-9 weeks from Harlan Winkelmann, Germany and housed for at least one week before commencing the experiments. Mice were sacrificed by cervical dislocation or decapitation and all experiments were conducted according to the german animal protection guidelines.

5.V.2 Induction and measurement of tumor growth

Xenograft tumor growth was induced by injection of cells into each flank of shaven abdominal skin. Cells were washed twice in PBS prior to injection. 1×10^4 to 5×10^6 cells were injected subcutaneously in a volume of 50 μ l using Omnican insulin syringes with 0.3 x 12 mm needles. Tumor diameters were measured using a caliper and volume was calculated using the formula:

$$V_{\text{tumor}} = \frac{\pi}{6} \cdot a \cdot b^2 \quad \left| \quad a > b \right. \quad \begin{array}{l} V_{\text{tumor}} > \text{tumor volume [mm}^3\text{]} \\ a, b > \text{orthogonal tumor diameters [mm]} \end{array}$$

5.V.3 Determination of the bacterial count in murine tissues

5.V.3.a Bacterial load per gram organ mass

Mice were infected with bacteria by intravenous (i.v.) injection into one lateral tail vein. At different timepoints p.i. mice were sacrificed and organs were removed aseptically. Bacterial organ load per gram was determined by weighing the organs followed by plating serial dilutions of the ground organs. Organs were sheared in Whirl-Paks (Nasco, USA) and diluted in 0.1 % Triton X-100.

5.V.3.b Bacterial load per cell population

Mice were i.v. infected as described in 5.V.3.a and organs removed at distinct timepoints post infection. Weight was determined before organs were cut into small pieces. Enzymatic digestion followed for 30-45 min at 37°C using 500 u/ml DNase and 2 µg/ml dispase in 5 ml MACS buffer. After digestion the suspension was pipetted several times using a 10 ml glass pipette for further disruption. The cell suspension was filtered consecutively using 70 µm and 40 µm cell strainers. Cell numbers were determined after tenfold dilution in Trypane blue (Sigma-Aldrich, Germany) using a counting chamber. One part of the suspension was removed and stored at 4°C until plating in serial dilutions. The rest of the cells was incubated for 1 h at 37°C with 100 µg/µl gentamicin. Again one aliquot was removed for further plating and the remnant was separated in a macrophage enriched and depleted cell population using MACS Kit (Miltenyi Biotech, Germany). The cells were incubated with primary antibody directed against F4/80 for 20 min at 4°C. 10µl of anti-IgG antibody conjugated with magnetic beads per 10⁶ cells was added and the suspension was incubated for 10 min. The cells were finally separated using the MACS columns in a magnetic field. Different eukaryotic cell fractions were counted in a counting chamber and plated in serial dilutions together with the temporarily stored fractions. The CFU was normalized to the number of plated eukaryotic cells.

5.V.4 Isolation of murine serum

Murine blood was drawn into a serum vial and incubated on ice for 45 min. After centrifugation for 2 min at 16000 x g at RT, the supernatant serum was transferred in fresh tubes and stored -20°C for further use.

6 Results

6.1 Reduction of cell-membrane tension by *L. monocytogenes* virulence factor InlC and influence on cell-to-cell spread

6.1.1 Generation of *L. monocytogenes inlC* mutants

To further investigate which of the specific InlC amino acid residues is responsible for binding to distinct cellular proteins different InlC mutants were generated. Amino acids at position 173 (K) and/or 204 (R) were exchanged to alanine to examine the protein-protein interactions.

InlC was amplified using genomic DNA of *L. monocytogenes* EGD as template. Primers InlC start2 BamHI 5' and InlC aft end Cfr9I 3' were used for amplification of this fragment which was ligated into the pUC18 vector following BamHI and Cfr9I restriction digestion. The insert of 909bp was mutated using the primers InlC mut2 170 5' and InlC mut2 170 3' in single site mutagenesis. The basepairs 419 to 421 were exchanged from AAG to GCA resulting in a K173A exchange in the final InlC protein. Another mutation was performed using primers InlC mut2 204 5' and InlC mut2 204 3'. The basepairs 511 to 514 were exchanged from AGA to GCA resulting in a R204A exchange in the final InlC protein. The mutated *inlC* genes were inserted into the BamHI and Cfr9I restriction sites of the plasmid pLSV101 and used for generation of genomic mutants as described in 5.II.7. Mutants comprising either of the single mutations and a double mutant strain were generated and verified by sequencing.

A control strain was generated by reconstituting *L. monocytogenes* $\Delta inlC$ with the wildtype *inlC* gene. For this purpose *inlC* was amplified of genomic DNA of *L. monocytogenes* EGD using primers InlC bef start BamHI 5' and InlC aft end Cfr9I 3'. The 1413bp fragment was ligated into pLSV101 following BamHI and Cfr9I restriction digestion. The reconstituted *inlC* *L. monocytogenes* mutant was generated as described in 5.II.7 and verified by sequencing.

6.1.2 Influence of InlC on apical cell junctions and cell-to-cell spread by *L. monocytogenes*

Already in the original publication describing InlC for the first time, InlC was thought to be involved in the intercellular spreading of *L. monocytogenes* (Engelbrecht et al., 1996). Using mutants generated in this work as described in 6.1.1, the distinct molecular functions of InlC during the infection process of *L. monocytogenes* were resolved in the lab of Keith Ireton (Rajabian et al., 2009). The major results of this publication are reported in this paragraph.

Yeast two-hybrid experiments revealed the interaction of InlC with Tuba, a protein involved in

regulation of the actin cytoskeleton. Tuba contains four SH3 domains located at the N-terminus mediating Dynamin binding, and two domains close to the C-terminus, responsible for interaction with N-WASP (Salazar et al., 2003). A Bar domain enables interaction with lipid bilayers, especially curvature-sensing and curvature-generation (Cestra et al., 2005).

Interaction of InIC with Tuba SH3 domain 6 (SH36) was shown in immunoprecipitation experiments using purified Tuba-fragments or InIC (Rajabian et al., 2009). On incubation of GST-tagged InIC with lysates of Caco-2 BBE1 cells, Tuba was immunoprecipitated. Interactions of InIC with Tuba isoforms of 150 and 180 kDa were detected. Using GST-tagged Tuba SH3 domains one to four or the single SH36 domain, InIC precipitation was examined. Only the Tuba SH36 domain bound InIC from lysates of Caco-2 BBE1 cells infected with the *L. monocytogenes* wildtype strain. The SH3 domains one to four mediated no protein-protein interaction with InIC.

The distinct InIC amino acids responsible for interaction with tuba were examined by generation of single amino acid exchanges in the InIC SH36 domain. The putative interacting RxxK motif at position 170 to 173 of InIC was disrupted by exchange of a conserved Lysin residue by Alanin in the *L. monocytogenes* *InIC.K173A* mutant.

On comparison of cell-to-cell spreading of the novel *InIC.K173A* mutant with an *inIC* knockout strain and the *L. monocytogenes* wildtype in Caco-2 BBE1 cells, spreading of the novel mutant resembled the $\Delta inIC$ mutant. This indicated the importance of the InIC RxxK motif for InIC function.

N-WASP, a key protein involved in regulation of the actin cytoskeleton, interacts with the Tuba SH36 domain. The influence of InIC on this known interaction partner was analyzed. *In vitro* wildtype InIC efficiently displaced N-WASP from Tuba SH36, while InIC.K173A failed to do so. Along the same line additional evidence of InIC acting by N-WASP displacement from Tuba was obtained on knockdown of either Tuba or N-WASP. This RNAi mediated knockdown restored the reduced protrusion formation of *L. monocytogenes* $\Delta inIC$ in Caco-2 BBE1 cells to wildtype level.

As Tuba is involved in regulation of cellular membrane tension the influence of InIC on this protein function was examined. Membrane tension was graded microscopically by measuring the membrane linearity (Otani et al., 2006). Only the infection with *L. monocytogenes* wt lowered the membrane tension of Caco-2 BBE1 cells. Using the $\Delta inIC$ - or the *inIC.K173A* mutant had no influence on membrane linearity. A similar reduction of membrane tension was observed on treatment of Caco-2 BBE1 cells using siRNA for silencing of Tuba or N-WASP.

Taken together these results indicate involvement of InIC in bacterial spreading by reduction of membrane tension.

6.II RNA delivery into eukaryotic cells by *L. monocytogenes*

6.II.1 Integration of T7 RNA polymerase into the genome of *L. monocytogenes*

6.II.1.a Generation of T7 RNA polymerase integration vector and genomic integration

For integration of the T7RNAP under control of the *actA* promotor into the genome of *L. monocytogenes*, the plasmid pLSV101-IntAB-P_{actA}-T7RNAP was generated. The *actA* promotor was chosen for regulation of polymerase expression because this promotor is strongly upregulated after arrival of *L. monocytogenes* in the host cell cytosol leading to a high transgene expression (Vazquez-Boland et al., 2001). Integration into the bacterial genome was performed according to Wuenscher et al., 1991 using the plasmid pLSV101 (Wuenscher et al., 1991). Homologous regions required for integration were placed adjacent to the genomically integrated phage A118 integrase / recombinase gene LMO02332 (Loessner et al., 2000). Upon knockout of this gene, the phage presumably loses the capability to re-enter into lytic cycle and therefore the integrated gene can not be lost following insertion. The integration vector backbone pLSV101-IntAB has been generated before as published (Heisig, 2005).

In between the homologous regions, *NcoI* and *SacI* restriction sites are located which were used for insertion of the T7RNAP gene. The functional T7-RNA polymerase expression cassette under control of *actA* promotor (P_{actA}) was cut out of pCSA1 by restriction digestion using *PstI* and *SacI*. The plasmid pLSV101-IntAB was linearized using *SacI* and sticky DNA ends of vector and insert were blunted using Klenow DNA polymerase. Following blunt end ligation and transformation, clones were screened by PCR using primers LSV-4380 rev and LSV3. The final integration vector pLSV101-IntAB-P_{actA}-T7RNAP was confirmed by sequencing.

The integration plasmid was electroporated into *L. monocytogenes* EGDe $\Delta trpS$ and a homologous insertion/replacement was performed as described in 5.II.7. Flanking regions of the genomic insertion were confirmed by sequencing a PCR fragment generated using primers integrase check -1 and integrase check -4.

6.II.1.b Cloning of stabilized expression vectors for RNA delivery

For reduction of the RNA delivery system to a system encoded on a single plasmid, the T7RNAP expression cassette was cloned into the stabilized pCSA1 plasmid (Schoen et al.,

2005). For evaluation of functionality of the system, an expression cassette mediating EGFP expression and an expression cassette encoding FCUI expression was cloned. The inserted cassettes were generated by digestion of pCSBI and pCSB-IRES-FCUI using *Pst*I and *Sac*I followed by agarose gel extraction of the P_{T7}-IRES-EGFP and P_{T7}-IRES-FCUI fragments. The stabilized vector backbone was generated from the plasmid pCSA1. pCSA1 was digested with *Pst*I and *Sac*I likewise and the backbone lacking the T7RNAP gene was purified using agarose gel extraction. The backbone was ligated with both fragments, respectively and after transformation, the plasmids were confirmed by sequencing. Sequencing of the newly generated plasmid pCSA-PT7-IRES-EGFP was performed using primers Screen H1 EPK-anti' and 'pFLO IRES 3' while plasmid pCSA-PT7-IRES-FCUI was sequenced using Screen H1 EPK-anti and Fcui Seq 2. Vector maps of the newly generated plasmids are depicted in figure 6.1.

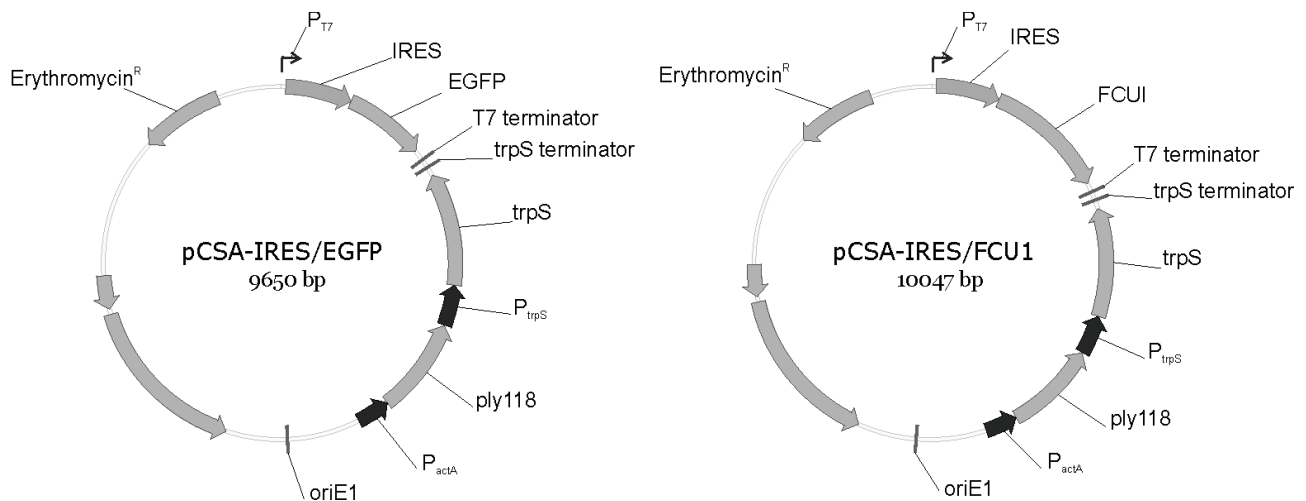


figure 6.1: Vector map of pCSA-IRES-EGFP and pCSA-IRES/FCUI

6.II.1.c Analysis of the trimmed RNA delivery strain

Integration of the T7RNAP into the genome of *L. monocytogenes* resulted in generation of a trimmed RNA delivery strain labeled *L. monocytogenes* $\Delta trpS$ $\Delta int::PactA$ -T7RNAP x pFlo-*trpS*. This strain was attenuated by *aroA* deletion as described in Stritzker *et al.* resulting in *L. monocytogenes* $\Delta trpS$ $\Delta aroA$ $int::PactA$ -T7RNAP x pFlo-*trpS* (Stritzker and Goebel, 2004). Growth kinetics of both strains was analyzed in BHI medium at 37°C (figure 6.2).

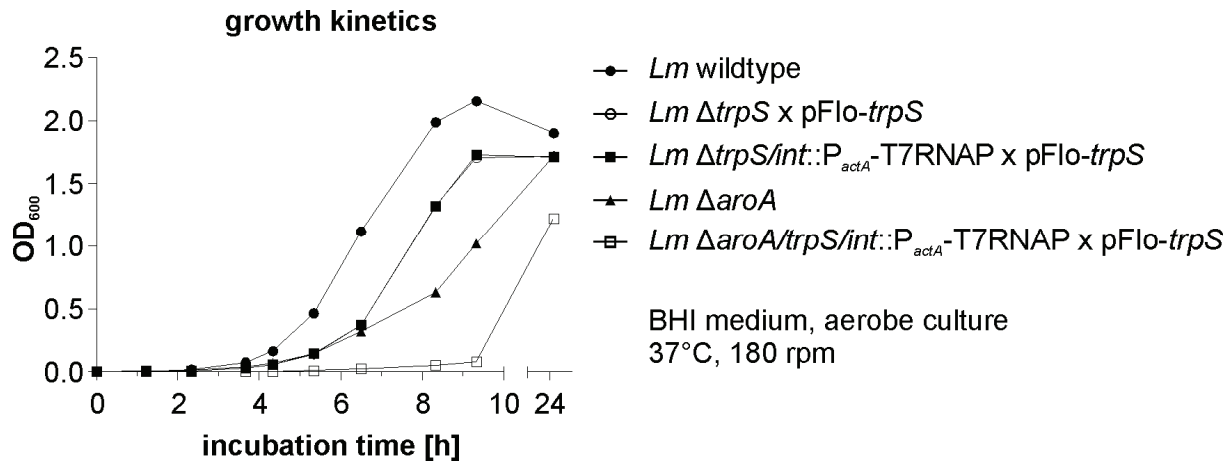


figure 6.2: Growth kinetics of the novel strains in BHI medium

Integration of the T7RNAP (■) into *L. monocytogenes* $\Delta trpS$ x pFlo-*trpS* (○, concealed by ■) did not alter growth kinetics in comparison to the parental strain, when no additional T7RNAP driven expression cassette was present. The $\Delta aroA$ -attenuated strain *L. monocytogenes* $\Delta trpS \Delta aroA/int::P_{actA}$ -T7RNAP x pFlo-*trpS* (□) likewise without T7RNAP driven expression cassette showed severe growth retardation. In comparison to the $\Delta aroA$ -attenuated strain without integration (▲) replication rate was strongly reduced on T7RNAP integration. This attenuated strain was not investigated further as transformation of plasmids containing T7RNAP driven expression constructs was not realizable. Addition of 50µg/ml menaquinone was not sufficient to revert the growth attenuation in this strain (data not shown).

RNA delivery of EGFP encoded on one plasmid was examined by flow cytometry. Infection of COS-1 cells was performed *in vitro* using *L. monocytogenes* $\Delta trpS$ x pCSAI x pCSBI and *L. monocytogenes* $\Delta trpS \Delta int::P_{actA}$ -T7 RNA pol x pCSA-IRES/EGFP at an MOI of 100 in comparison to uninfected cells. Following infection, cells were detached by trypsinisation and fluorescence was analyzed by flow cytometry. The relative percentage of GFP expressing cells is shown in figure 6.3.

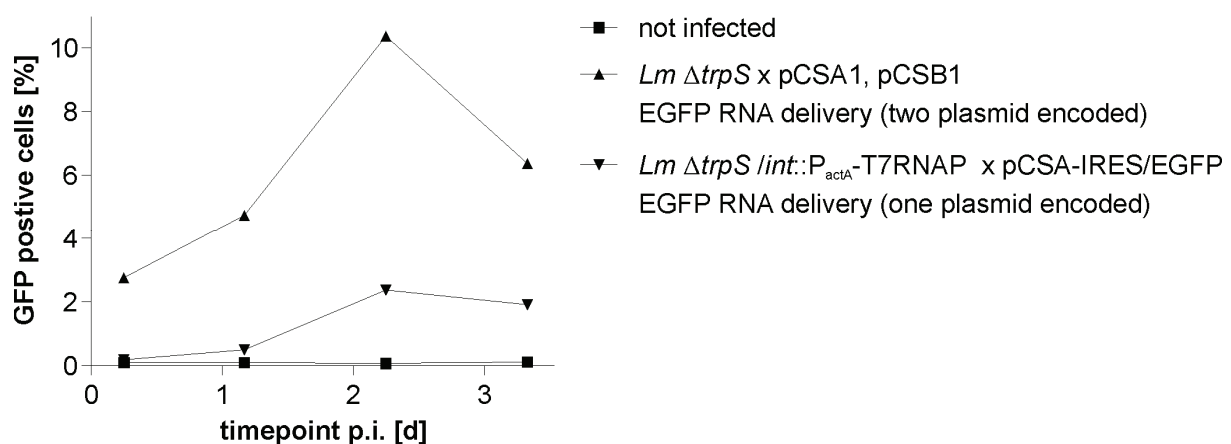


figure 6.3: Flow cytometric analysis of COS-I cells after infection with *L. monocytogenes* delivering EGFP mRNA

Comparison of GFP positive cells after infection shows a pronounced difference between the cells infected with either of the two RNA delivery strains. While the two plasmid encoded system is able to elicit up to 10% of fluorescent cells, the system based on one plasmid yields only a maximum of 2% fluorescent cells. In the timecourse GFP positive cells peak between 50h and 60h p.i. in both systems followed by reduction of fluorescence. Taken together a metabolically more robust bacterial mutant delivering functional mRNAs was established.

6.II.2 shRNA delivery

6.II.2.a Cloning of SMAC/DIABLO shRNA delivery vector

The *L. monocytogenes* RNA delivery system was modified for delivery of shRNAs by introducing a shRNA expression cassette into plasmid pCSBI. The EGFP expression cassette was removed from pCSBI using *Cfr9I* followed by *BamHI* digestion. The vector backbone was eluted after agarose electrophoresis and dephosphorylated before ligation. The shRNA expression cassette silencing *SMAC/DIABLO* was generated by annealing of the purchased oligomers 'Smac shRNA BamHI/XmaI s' and 'Smac shRNA BamHI/XmaI as'. The two oligomer sequences were reverse complementary with additional overhangs mimicking *Cfr9I* and *BamHI* overhangs. The shRNA design for *SMAC/DIABLO* silencing including the loop structure was kindly provided by Krishna Rajalingam as published in (Rajalingam et al., 2007). Annealed oligomers were phosphorylated using T4 polynucleotide kinase and ligated into the pCSBI vector backbone. Bacterial clones were screened by PCR using primers 'T7 EPK s' and 'T7 EPK a' and analyzed using a 2% agarose gel as depicted in figure 6.4. Plasmid DNA isolated from clone 5 and 6 was sequenced for confirmation of pCSB-shSmac.

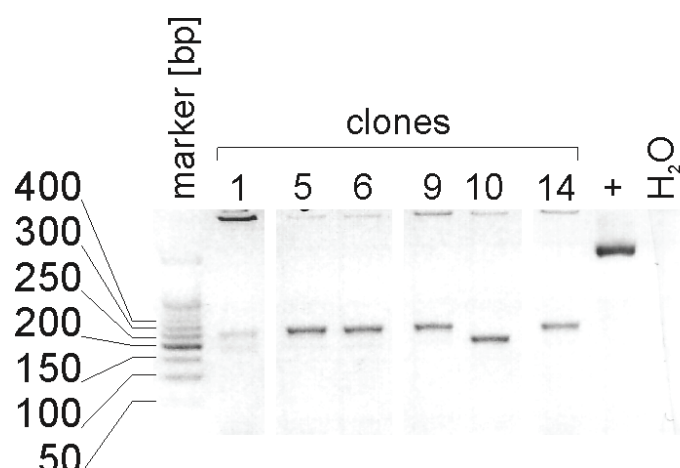


figure 6.4: Agarose gel electrophoresis of PCR products using pCSB-shSmac clones as template

6.II.2.b Purification and analysis of small RNAs

The plasmid pCSB-shSmac was electroporated into *E.coli* BL21/DE3, expressing the T7RNAP under control of the lacUV5 promoter. Detection of shRNAs was attempted by RNA acrylamide gel electrophoresis.

RNA was isolated from bacterial cultures after induction of T7RNAP expression by adding 1mM IPTG during 2h of incubation at 37°C. RNAs were distinguished in small and large RNAs during RNA isolation. The separation of 1 µg of RNA per sample and 0,5µg of RNA marker was performed using TBE acrylamide gel electrophoresis as shown in figure 6.5.

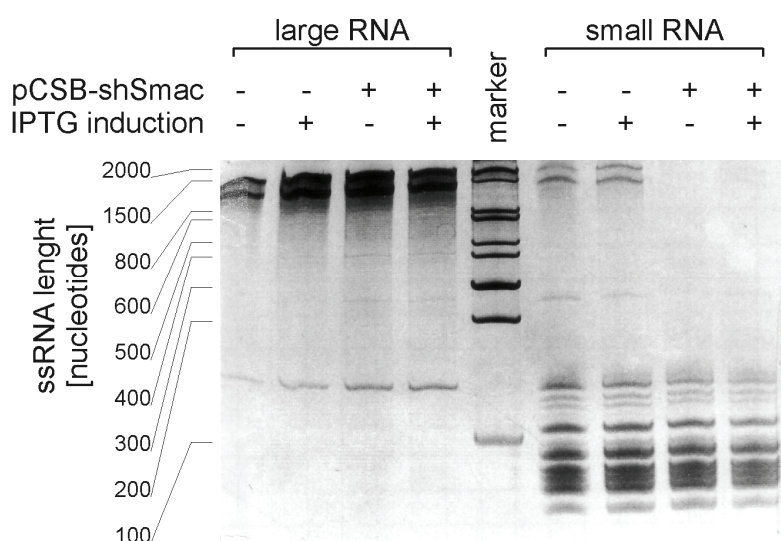


figure 6.5: TBE acrylamide gel electrophoresis of RNA isolated from *E.coli* BL21/DE3 ± pCSB-shSmac after IPTG induction (1 µg RNA per lane)

Separation of bacterial RNAs showed a distinct band pattern depending on the isolation protocol. Boundary value between the two different protocols ranged between 100 and 200 nucleotides of ssRNA, but a partial carryover of ribosomal RNAs into the small RNA fraction was observed in both the samples.

On production of shRNAs by the bacteria, an additional band at approximately 200 nucleotides should appear following IPTG induction in the strain carrying pCSB-shSmac. This additional band would only show up, if the amount of produced shRNA exceeded 0,01 µg. Otherwise the sensitivity of the acrylamide gel would be insufficient. Gel separation showed no additional RNA band in the plasmid transformed strains on IPTG induction. As the sensitivity of acrylamide electrophoresis is limited a qRT-PCR approach with higher detection limit was employed.

The quantification of shRNA amounts by qRT-PCR in *L. monocytogenes* was performed using primers 'shSmac RT (F)' and 'shSmac RT (R)'. Relative RNA amounts were normalized to mRNA levels of the housekeeping gene *rpoB* (analyzed using primers 'RpoB RT (F)' and 'RpoB RT (R)'). *L. monocytogenes* $\Delta trpS$ was transformed with pCSAI and pCSB-shSmac, RNA was isolated from a bacterial culture induced with 1% XAD for 2h at 37°C, reverse transcribed and investigated by qRT-PCR. XAD addition to the growth medium was used to induce the major bacterial virulence regulator *prfA* resulting in increased virulence gene transcription. The T7RNAP in this bacterial mutant was transcribed under control of the *prfA*-dependent *actA* promotor resulting in increased amounts of T7RNAP on induction with XAD.

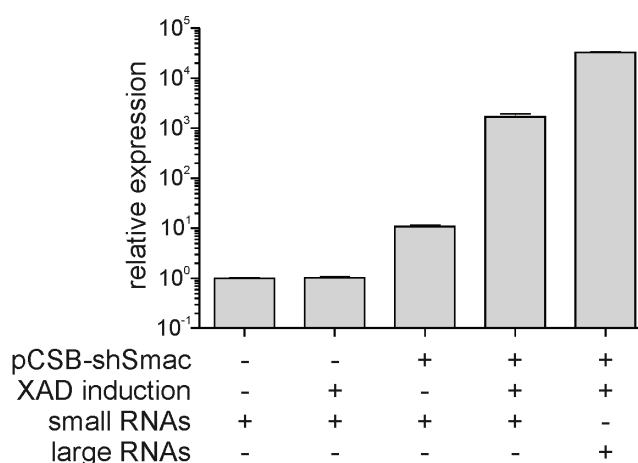


figure 6.6: qRT-PCR analysis of shSmac amount in *L. monocytogenes* $\Delta trpS$ x pCSAI ± pCSB-shSmac after XAD induction

The relative amount of shRNA was arbitrarily set to 1 (10^0) in *L. monocytogenes* $\Delta trpS$ x pCSAI without pCSB-shRNA and the relative amounts in comparison thereof were calculated for the other strains. No increase of shSmac was detected in the control strain on XAD

induction; while the shSmac amount was increased in the plasmid bearing strain 100-fold on induction.

The shRNA expression cassette was approximately 200 nucleotides in size and showed highest abundance in the large RNA fraction of the plasmid bearing strain. In comparison, shSmac was present in the small RNA fraction at a 10-fold lower level indicating that size separation of RNAs during RNA isolation had no clear cutoff value but showed a gradual transition. Increase of the relative shRNA amount on XAD induction indicated a functional expression cassette leading to expression of shSmac on promotor induction.

Functional experiments investigating *SMAC/DIABLO* silencing on shSmac delivery by *L. monocytogenes* were conducted *in vitro* as well. Following infection of HeLa- and COS-I cells, alterations in relative *SMAC/DIABLO* transcript amounts were detected, but showed no reproducible and consistent pattern of regulation (data not shown).

6.III Protein A mediated antibody coating of *L. monocytogenes*

6.III.1 Characterization of bacterial antibody coating

6.III.1.a Quantitation and specificity of antibody binding

Antibody binding specificity of Lm aroA⁺spa⁺ was compared to Lm aroA⁺spa⁻ by western blot analysis. 5×10^8 bacteria were incubated in 100µl PBS containing 1µg of polyclonal antibody directed against native murine serum albumin. 200ng of purified murine serum albumin were added and the coating procedure was performed for 1h at RT under vigorous shaking. Following coating, excess albumin was removed by washing the bacteria. Samples in lane 1 to 4 were washed 5 times using 1 ml PBS, bacteria shown in lane 5 to 6 were washed three times using 0.05% Tween 20 in PBS (PBST) before resuspending and boiling in Laemmli buffer. Samples were analyzed by western blot analysis using polyclonal antibody directed against denatured murine serum albumin (figure 6.7). 10 ng of purified murine serum albumin (69 kDa) was loaded as positive control in lane 7.

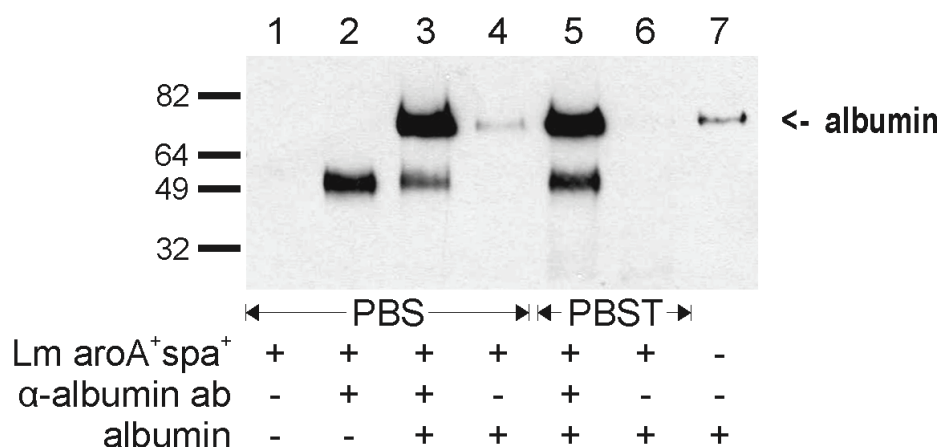


figure 6.7: Western blot analysis detecting the amount of albumin bound to Lm-aroA⁺spa⁺

Incubation of protein A expressing *L. monocytogenes* together with the antibody directed against native albumin resulted in a side band at about 50 kDa (lane 2,3,5). Specific bacterial albumin binding was observed only on addition of antibody and albumin (lane 3, 5). Lm-aroA⁺spa⁺ showed a slight antibody independent serum albumin binding as seen in lane 4. This intrinsic binding capacity was abrogated by washing with buffered detergent solution as shown in lane 6. The amount of antibody-mediated serum albumin binding was not altered after the washing.

In comparison to the distinct amount of albumin in the control lane the size of bacterial bound serum albumin allowed a rough calculation of the amount of attached albumin per bacterial cell. Computer aided band quantitation of the membrane shown in figure 6.8 estimated 70 ng of albumin bound to 5×10^8 bacteria (Rosenman R.). 70 ng of protein with a weight of 69 kDa correspond to 8.7×10^9 molecules of serum albumin bound to the bacteria. By division of the number of molecules by the bacterial count the number of albumin molecules per bacterial cell was calculated. About 120 albumin molecules corresponding to at least 60 molecules of antibody were bound on the surface of each bacterial cell.

Dependence of albumin binding on bacterial protein A expression was examined comparing Lm aroA⁺spa⁺ and Lm aroA⁺spa⁻ simultaneously (figure 6.8). Lanes 1 to 4 show albumin binding of Lm aroA⁺spa⁺, Lm aroA⁺spa⁻ was assessed in lanes 5 to 8. 10 ng of purified murine serum albumin (69 kDa) were loaded as positive control in lane 9.

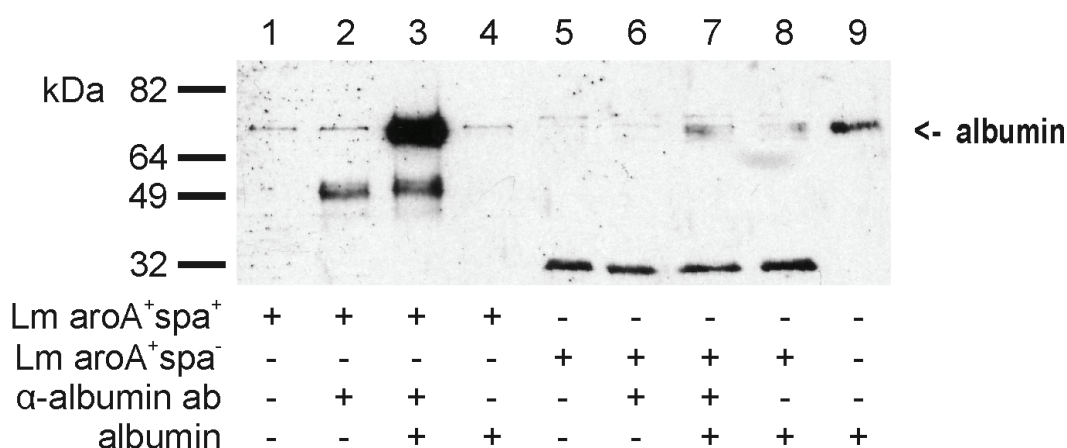


figure 6.8: Western blot analysis detecting the amount of albumin bound to Lm-aroA⁺-spa⁺

The unspecific band at 50 kDa was detected only in samples containing protein A expressing bacteria, protein A deficient bacteria did not show this band. Western blot analysis of Lm aroA⁺spa⁻ using a serum albumin specific antibody detected a side band at approximately 32 kDa.

Protein A expressing bacteria incubated with antibody and albumin show specific albumin binding (lane 3), as expected protein A deficient bacteria are unable to bind albumin (lane 7).

6.III.1.b Kinetics of antibody coating

Kinetics of bacterial antibody coating was investigated by western blot analysis as shown in figure 6.9. As described in 6.III.1.a bacteria were incubated with antibody directed against albumin followed by detection of the bound albumin by western blot analysis. Antibody coating was interrupted after different incubation times ranging from 5 to 60 minutes. After coating, bacteria were washed three times using 0.05% Tween 20 in PBS and analyzed as described in 6.III.1.a. Coating of bacteria analyzed in lane 7 was performed with double amounts of antibody and albumin compared to lanes 2-6 and 8 for investigation of coating saturation. Positive control shown in lane 9 consists of 10 ng of purified albumin.

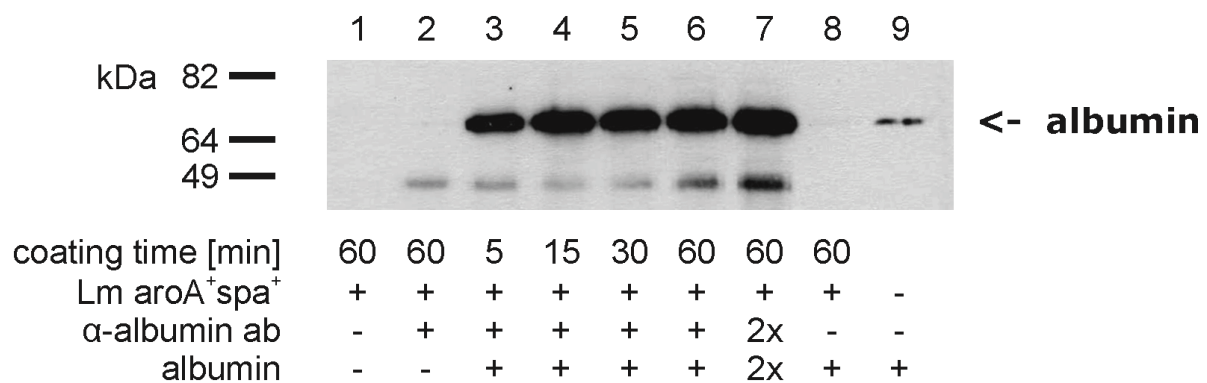


figure 6.9: Western blot analysis showing the kinetics of albumin binding to Lm-aroA⁺-spa⁺

Antibody-mediated albumin binding of Lm-aroA⁺-spa⁺ was saturated already after 15 minutes. Coating for as little as 5 min was sufficient to mediate 80% of final albumin binding (computer aided band quantitation using Rosenman R. (Rosenman R.).

6.III.2 Antibody-mediated internalization of *L. monocytogenes* *in vitro*

Antibody-mediated cell targeting of Lm-aroA⁺-spa⁺ and Lm-spa⁺ has already been shown (Frentzen, 2007). The results revealed a 20-fold increased internalization of protein A expressing *L. monocytogenes* into SKBR3 cells on coating with Trastuzumab. The intracellular behavior of bacteria after antibody-mediated uptake was also analyzed. It was shown that the bacteria, internalized in an antibody-mediated manner and show a similar intracellular behavior like the wildtype with regards to phagosomal escape and replication. Following these initial observations, antibody-mediated targeting was further characterized and optimized in this study as described below.

6.III.2.a Evaluation of optimal antibody concentrations for antibody-mediated internalization

Influence of antibody concentrations on the efficiency of Lm-spa⁺ to internalize into SK-BR-3 and SK-OV-3 cells was evaluated in *in vitro* infection experiments. SK-BR-3 is a human breast cancer cell line overexpressing EGFR and HER2/neu receptors. The SK-OV-3 cell line was isolated from human ovarian carcinoma and overexpressed both receptors likewise (Heisig, data not shown; Warnberg et al., 2006).

The bacteria were coated with antibodies using different antibody concentrations during the coating reaction. Antibody coated bacteria were employed in *in vitro* infections determining

the number of intracellular bacteria following infection and gentamicin assay. Relative internalization rates of the differentially treated bacteria in comparison to untreated bacteria (-ab) are shown in figure 6.10.

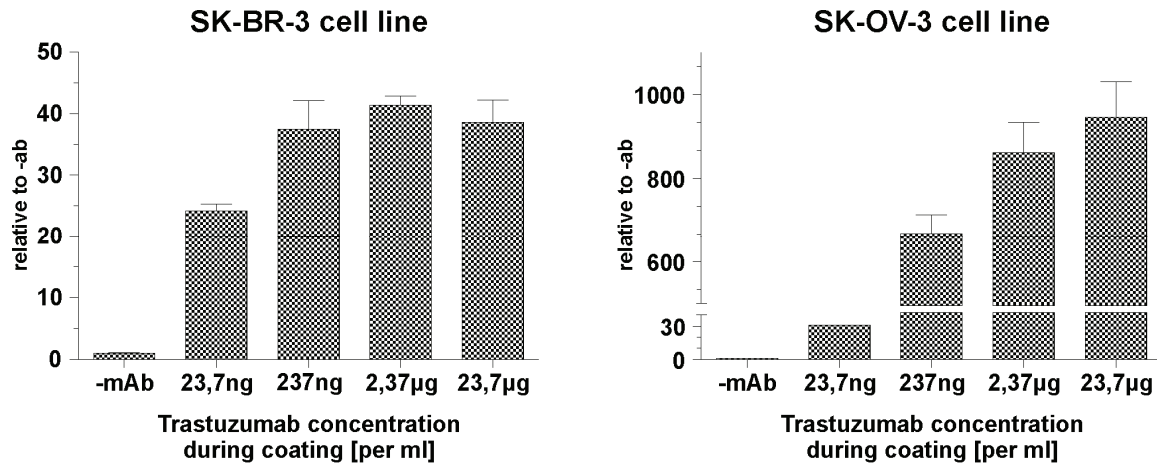


figure 6.10: *In vitro* infection of cell lines investigating the optimal antibody concentrations for bacterial internalization

With increasing amounts of antibody addition the number of intracellular bacteria also increased until reaching a maximal value. In SK-BR-3 cells, coating with 237 ng/ml antibody was sufficient for maximal bacterial internalization rate. In contrast, internalization into SK-OV-3 cells requires about 100-fold more antibody for maximal internalization. The overall internalization rate differs in between the two cell lines by approximately 20-fold. This difference is presumably caused by different amounts of HER2/neu receptor on the surface of the two cell lines (Heisig, data not shown; Warnberg et al., 2006).

In subsequent experiments 1µl Herceptin (equaling 2,37µg antibody) was used for coating of $1 \cdot 10^8$ CFU bacteria.

6.III.2.b Comparison of bacterial internalization into isogenic cell lines

Specificity of antibody-mediated bacterial internalization was examined in two isogenic cell lines. 4T1 mouse mammary gland cells and HER2/neu transduced 4T1-HER2 cells were infected with antibody coated Lm-spa⁻ and Lm-spa⁺ (Kershaw et al., 2004). Infection was performed for 1h using an MOI of 100 bacteria per cell followed by gentamicin treatment of 1h. The raw number of CFUs is depicted in the left diagram, while internalization rate of antibody coated bacteria divided by the number of uncoated bacteria from the identical experiment is shown on the right. In figure 6.11, the results of infection using antibody coated Lm-spa⁻ are shown.

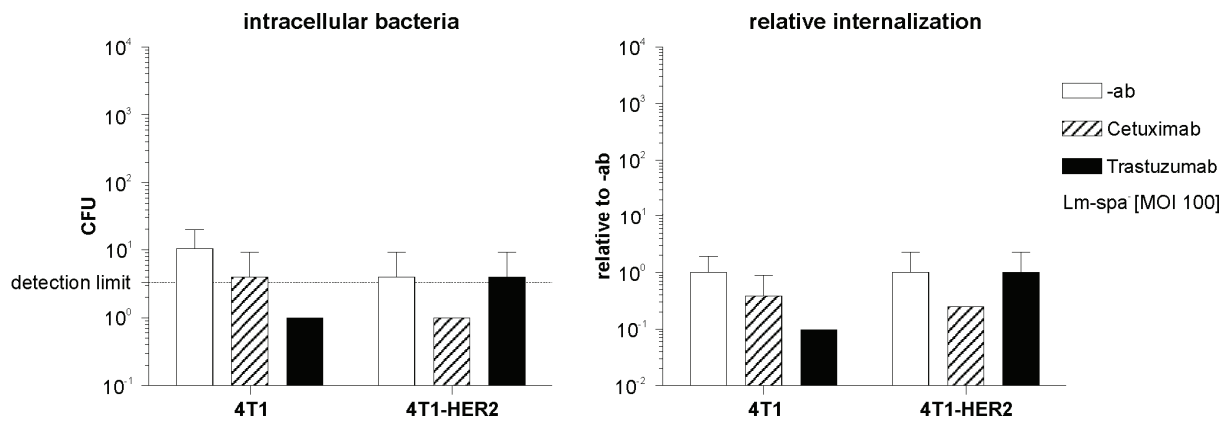


figure 6.11: *In vitro* infection of 4T1 and 4T1-HER2 cells using antibody coated Lm-spa⁻

The amounts of intracellular Lm-spa⁻ are close to the detection limit, indicating a very low intrinsic invasion property of *inlA* and *inlB* deficient *Listeria monocytogenes* into both cell lines. In 4T1- as well as 4T1-HER2 cells nearly no intracellular bacteria were detected. Despite of the low overall bacterial count, no antibody-mediated effects on bacterial internalization were observed. Coating the bacteria with the chimeric mouse-human antibody Cetuximab (® Erbitux) directed against the EGF-receptor was used as negative control in this experiment, as neither 4T1 nor 4T1-HER2 cells overexpress the EGFR.

Results of antibody coated Lm-spa⁺ on infection of these cell lines are shown in figure 6.12.

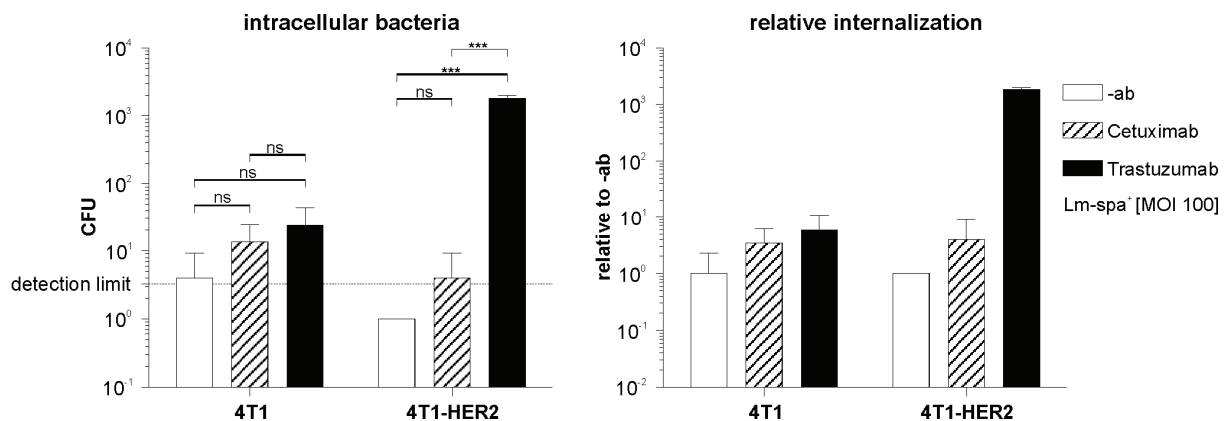


figure 6.12: *In vitro* infection of 4T1 and 4T1-HER2 cells using antibody coated Lm-spa⁺

Internalization of Lm-spa⁺ into 4T1 cells showed no antibody-dependent alterations in the number of intracellular bacteria. In contrast, a major increase was detected on infection of 4T1-HER2 cells using Trastuzumab coated Lm-spa⁺. Comparing uncoated and Trastuzumab coated bacteria, the number of intracellular bacteria is increased approximately 1000-fold as shown in the right graph of figure 6.12.

Combining the results of figure 6.11 and figure 6.12, antibody-dependent internalization is strictly dependent on presence of protein A on the bacterial surface, receptor expression on

the eukaryotic target cells and coating with the appropriate antibody. Only combination of these three properties permits antibody-mediated bacterial internalization.

6.III.2.c Influence of cell density and bacterial MOI during infection on antibody-mediated internalization

The influence of cell density on antibody-mediated internalization *in vitro* was determined by infection of 4T1-HER2 cells. Different amounts of cells were seeded into 24 well plates and infected with differentially coated Lm-spa⁺ using 100 bacteria per cell as MOI and 2 h p.i. the intracellular bacterial count was determined. The raw CFU values are shown in the left graph of figure 6.13 and the relative internalization rates of antibody coated bacteria divided by the number of uncoated bacteria are shown on the right side.

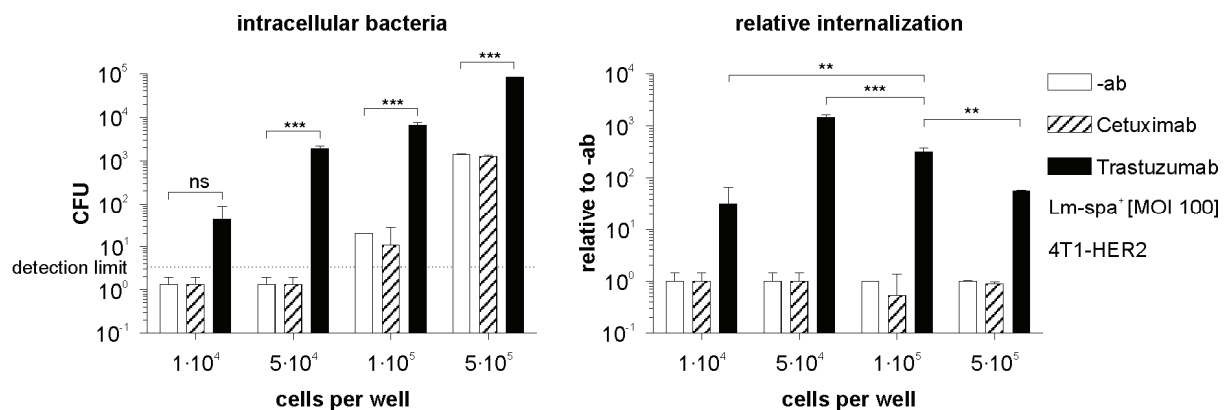


figure 6.13: *In vitro* infection of 4T1-HER2 cells using antibody coated Lm-spa⁺

The number of intracellular bacteria correlated with the amount of infected cells, indicating that antibody-mediated internalization is functional in principal with different cell counts. The internalization rates however differed significantly depending on cellular confluence. The highest internalization rate was observed upon infection of 5·10⁴ cells, but this rate was calculated using CFU values of uncoated bacteria below the detection limit. Infection of 1·10⁵ cells marked the lowest cell number allowing internalization of uncoated bacteria using a MOI of 100. Infecting more than 1·10⁵ cells increased antibody-independent internalization and decreased the internalization ratio.

Influence of bacterial MOI applied during infection on internalization was investigated in 4T1-HER2 cell as shown in figure 6.14.

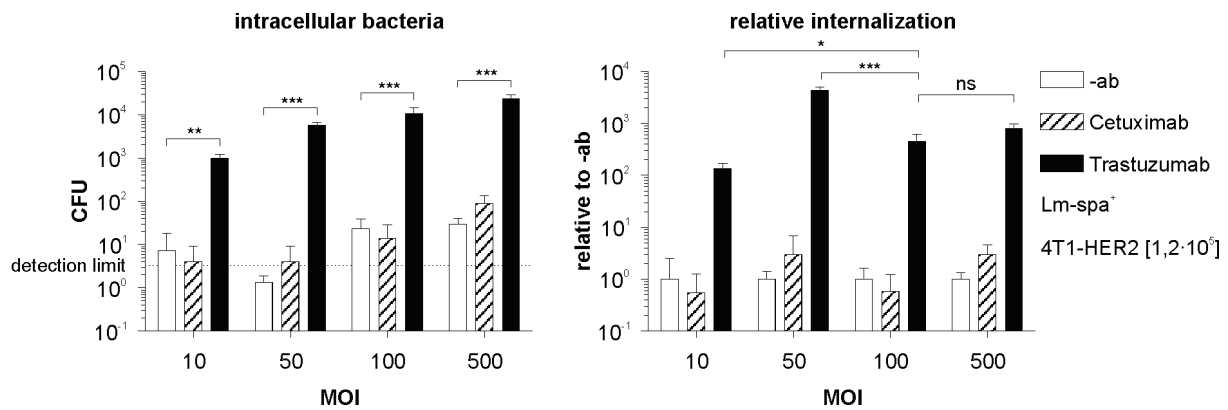


figure 6.14: *In vitro* infection of 4T1-HER2 cells using antibody coated Lm-spa⁺

A total number of $1.2 \cdot 10^5$ 4T1-HER2 cells were infected with differentially coated Lm-spa⁺ using MOI values ranging from MOI 10 to MOI 500. 2 h p.i. the intracellular bacterial count was determined.

In the CFU data, internalization of differentially coated bacteria increased with higher MOI values independent of the antibody coating. The internalization rate was highest on infection using MOI of 50, but this internalization rate was calculated using CFUs below the detection limit. Using a higher MOI of 100 or 500 resulted in a lower infection rate, but was calculated using measured CFU values.

Following the experiments shown above all *in vitro* infection experiments were performed using a MOI of 100 and $1.2 \cdot 10^5$ cells per well.

6.III.2.d Adherence, internalization and replication of protein A expressing *L. monocytogenes*

In addition to antibody-mediated internalization, adhesion / early internalization and replication of protein A expressing *L. monocytogenes* were examined *in vitro*. The internalization process of bacteria coated with polyclonal α -GFP antibody (α -GFP ab) as non-binding control or Trastuzumab was compared to uncoated bacteria. Non-attenuated Lm-aroA⁺spa⁺ and Δ aroA attenuated Lm-spa⁺ were used for infection of 4T1 and 4T1-HER2 cells. The raw bacterial count was determined and the relative values in relation to uncoated bacteria were calculated thereof. The raw bacterial counts are shown on the left side, the calculated relative values on the right side of figure 6.15 and figure 6.16 for Lm-aroA⁺spa⁺ and Lm-spa⁺ respectively. Adhesion / early internalization 1h p.i., internalization 2h p.i. and replication 24h p.i. are shown top down. Experiments shown in figure 6.15 and figure 6.16 were performed once in triplicates.

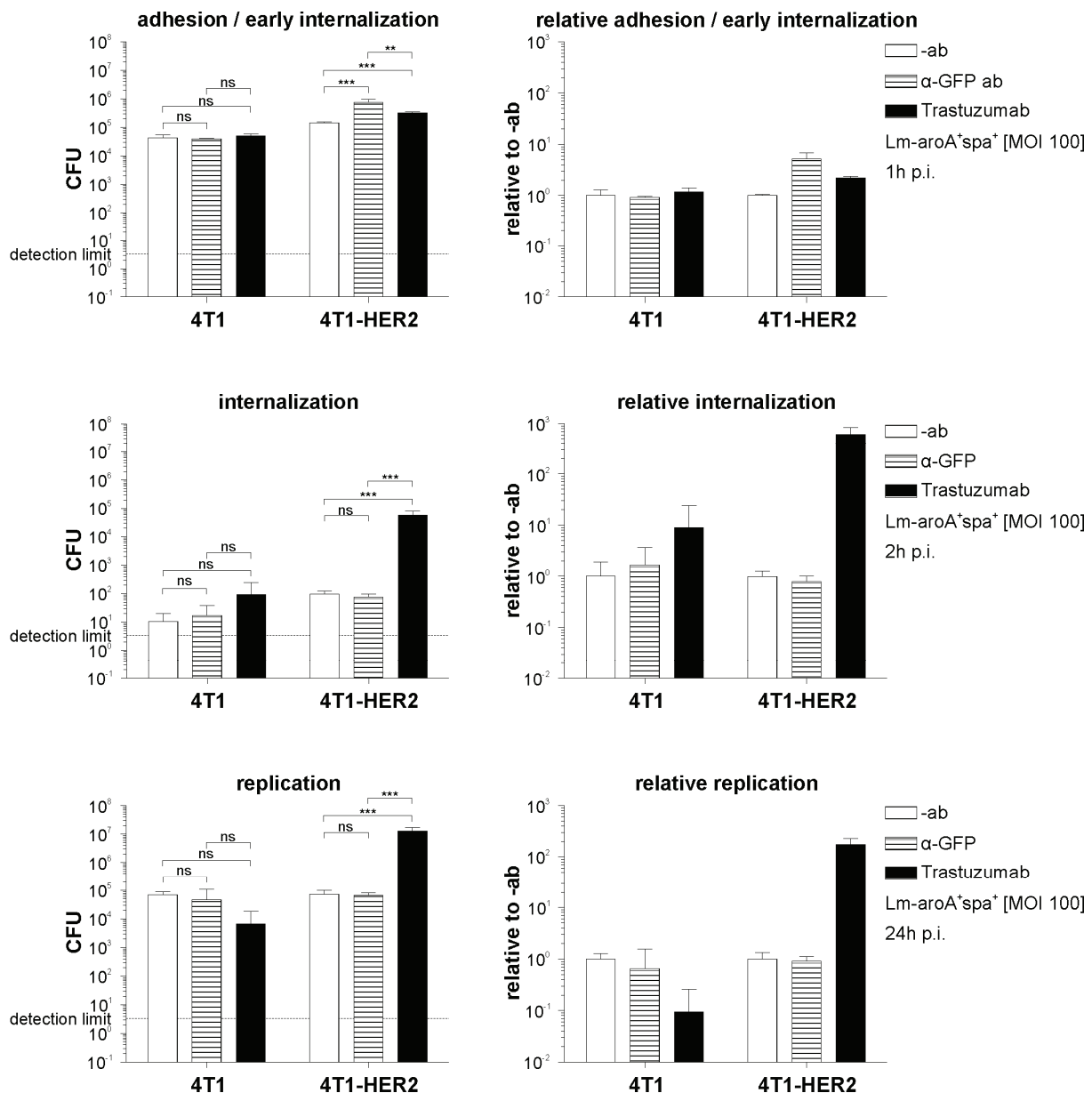


figure 6.15: *In vitro* infection of 4T1 and 4T1-HER2 cells using antibody coated Lm-aroA⁺spa⁺

Adhesion of Lm-aroA⁺spa⁺ to 4T1 cells was independent of bacterial antibody coating. In contrast bacteria loaded with α-GFP antibody or Trastuzumab attached better to 4T1-HER2 cells than uncoated bacteria. While the increase in adhesion after Trastuzumab coating was expected, the 10-fold increase on α-GFP antibody coating was astonishing. 4T1-HER2 cells express GFP, because this protein was used as marker for viral transduction of HER2. Lm-spa⁺ showed no α-GFP antibody-mediated increase in adhesion in the same experiment as shown in figure 6.16.

The overall internalization rate of differentially coated bacteria was comparable to the results shown in figure 6.12. Coating of the bacteria using α-GFP antibody showed a similar internalization rate as coating using Cetuximab shown in figure 6.12. Both coatings caused

no alteration in internalization into 4T1 or 4T1-HER2 cells in comparison to uncoated bacteria. As shown before, bacterial coating using Trastuzumab increased internalization in 4T1-HER2 cells more than 100-fold.

24 h p.i. the absolute intracellular bacterial counts were increased by 3 orders of logarithmic magnitude in comparison to the bacterial counts 2 h p.i., but the relative proportion in between the differentially coated bacteria remained identical. The different antibody coatings thus had no specific effect on intracellular replication of Lm-aroA⁺spa⁺.

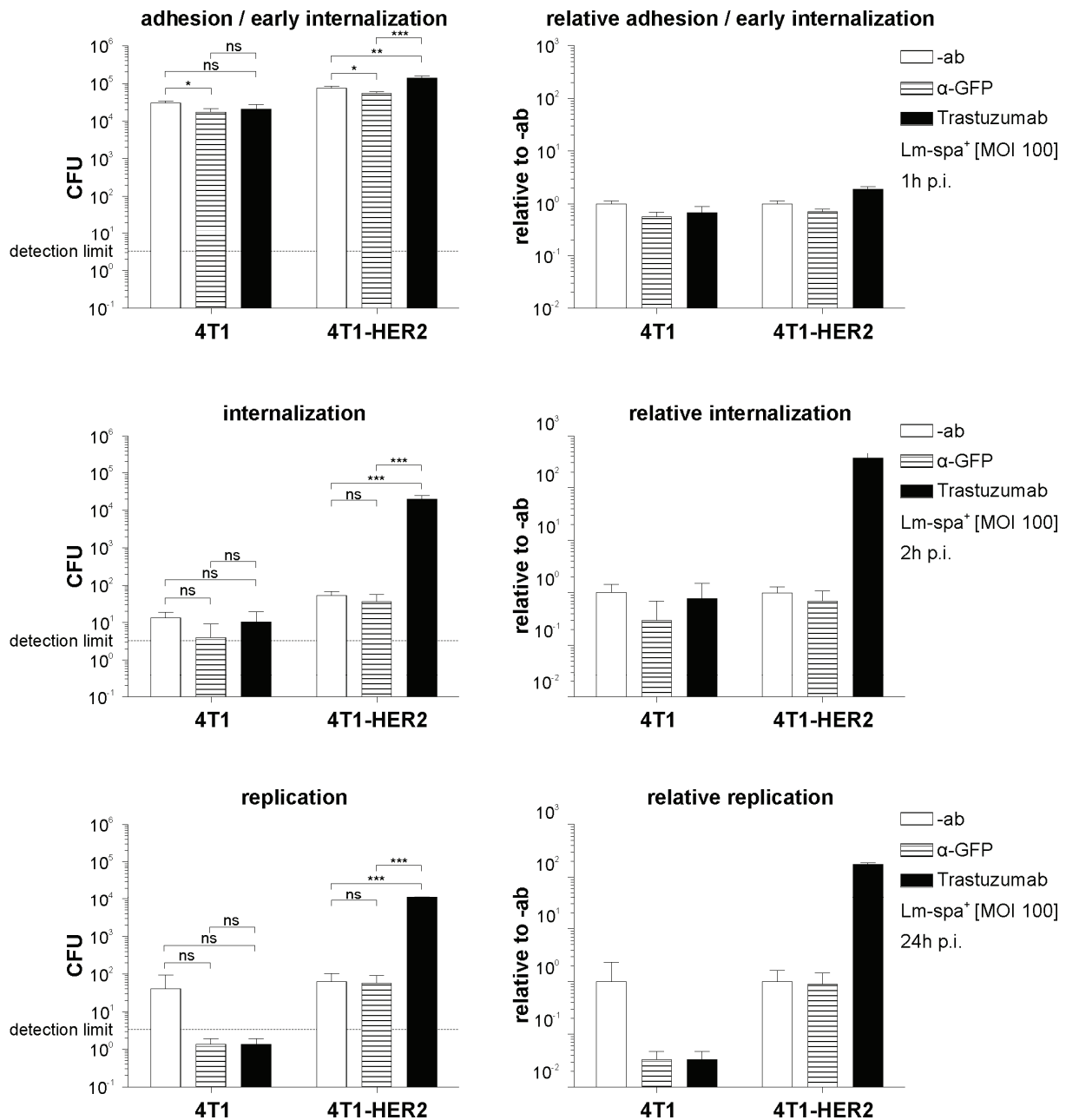


figure 6.16: *In vitro* infection of 4T1 and 4T1-HER2 cells using antibody coated Lm-spa⁺

Results obtained after infection of 4T1 and 4T1-HER2 cells using Lm-spa⁺ as shown in figure 6.16 were similar to the results obtained using Lm-aroA⁺spa⁺ albeit with minor differences.

Adhesion of α -GFP antibody coated Lm-spa⁺ was not significantly increased on infection of 4T1-HER2 cells and replication rate of the carrier strains differed. Because of the attenuation of Lm-spa⁺ the bacterial counts between 2 h p.i. and 24 h p.i. increased only 2-fold, while the unattenuated Lm-aroA⁺spa⁺ showed an increase of approximately 1000-fold in the same time span. Antibody-mediated bacterial internalization was shown in these isogenic cell lines using metabolically attenuated and non-attenuated *L. monocytogenes* mutants.

6.III.2.e Cetuximab-mediated internalization into human cancer cell lines

Antibody-mediated internalization of Lm-spa⁺ into murine cell lines expressing HER2/neu was shown in the experiments above. In this part, of the thesis expansion of targeting was investigated by infection of two human cancer cell lines using the EGF receptor specific antibody Cetuximab (® Erbitux) in addition to Trastuzumab. Infection of both cell lines was performed using Lm-spa⁻ and Lm-spa⁺ coated with Cetuximab or Trastuzumab in comparison to uncoated bacteria. The results are shown in figure 6.17

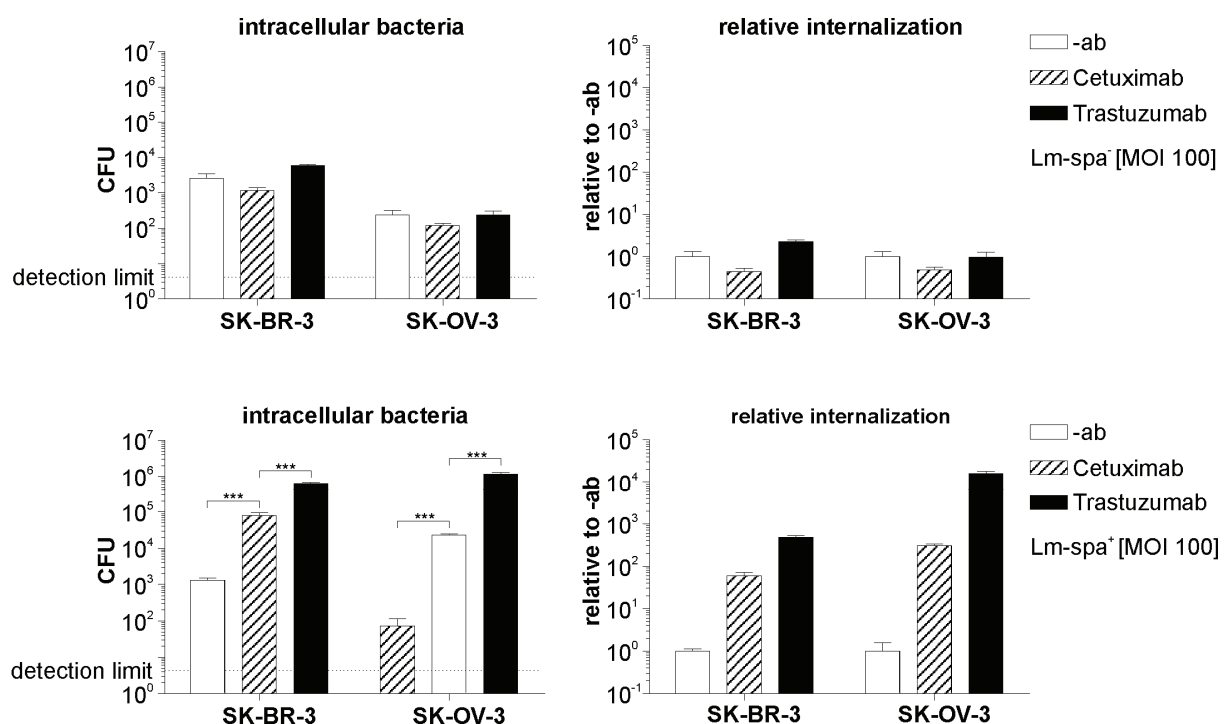


figure 6.17: *In vitro* infection of SK-BR-3 and SK-OV-3 cells using antibody coated Lm-spa⁻ and Lm-spa⁺

Lm-spa⁻ as well as Lm-spa⁺ are able to infect SK-BR-3 and SK-OV-3 cells intrinsically without antibody coating at a low level. Internalization of Lm-spa⁻ into both cell lines is unaffected by additional antibody coating. In contrast, internalization of protein A expressing *L. monocytogenes* is massively increased upon Cetuximab- or Trastuzumab coating. Both

antibodies, directed against members of the EGFR family mediated internalization. Increase of intracellular bacteria is approximately 100- to 10.000-fold, depending on the cell line and antibody coating.

This experiment exemplifies the versatility of antibody-mediated internalization by protein A expressing *L. monocytogenes*, as two different antibody coatings mediate bacterial internalization.

6.III.2.f Antibody-mediated internalization of prodrug-converting *L. monocytogenes*

Utilization of bacterial tumor targeting in therapeutic approaches can be accomplished either by exploitation of intrinsic effects the bacteria exert on the tumor tissue, or by delivery of therapeutic agents. One possible approach is the delivery of prodrug-converting enzymes causing cytotoxicity at site of infection. Prodrug-converting enzymes catalyze non-toxic drug precursors (prodrugs) into potent cytotoxic drugs. Transferring the chimeric yeast enzyme FCU1 catalyzes conversion of 5-Fluorocytosine (5-FC) into the cytotoxic 5-Fluorouracil (5-FU) and further into 5-Fluorouridinemonophosphate (5-FUMP) (Erbs et al., 2000). RNA delivery of FCU1 into eukaryotic cells by *L. monocytogenes* was described by combination of plasmids published in Schoen *et al.*, 2005 and Stritzker *et al.*, 2008 (Heisig, 2005; Schoen et al., 2005; Stritzker et al., 2008). Combination of a plasmid encoding the T7RNAP (pCSA1) and a plasmid harbouring a T7RNAP driven expression cassette of FCU1 (pCSb-FCU1) in *L. monocytogenes* efficiently mediated cytotoxicity on prodrug addition *in vitro* (Heisig, 2005). In this study these plasmids were transformed into Lm-spa⁺ and first infection experiments in 4T1-HER2 cells were performed with the novel strains. Following infection, the medium of half of the samples was supplemented with 1mM 5-FC and eukaryotic cell viability was measured at three timepoints p.i.. The efficiency of prodrug conversion was measured using a cell viability assay and comparing the samples with prodrug addition to the control samples without prodrug addition. If no prodrug is converted, the viability ratio would be around 100%, while lower ratios indicated cytotoxicity.

In figure 6.18 the survival ratio of 4T1-HER2 cells following infection by *L. monocytogenes* mutants delivering FCU1 mRNA and the corresponding control strains are shown. All strains were incubated with Trastuzumab as described in chapter 5.II.11.a. The survival ratio was calculated by division of viable cells with prodrug addition by the number of viable cells without prodrug addition. *L. monocytogenes* strains harbouring pCSA1 and pCSB1 were used as negative controls unable to mediate prodrug conversion.

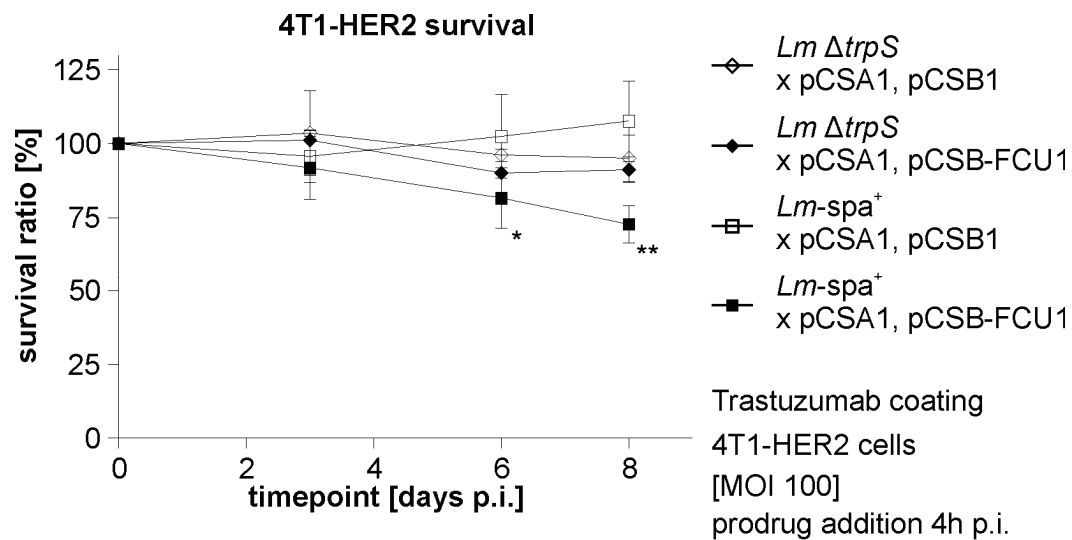


figure 6.18: Eukaryotic cell survival ratio of 4T1-HER2 cells infected with Trastuzumab incubated *L. monocytogenes* with and without prodrug addition

The *L. monocytogenes* $\Delta trpS$ x pCSA1, pCSB-FCU1 mutant was included as control, as this strain showed prodrug conversion in COS-1 cells (Heisig, 2005). In the experiment shown here, this strain exerted no cytotoxic effects in the 4T1-HER2 cells. Trastuzumab coated $Lm-spa^+$ x pCSA1, pCSB-FCU1 (■) exerted a cytotoxic effect on the eukaryotic cells in comparison to the control strain $Lm-spa^+$ x pCSA1, pCSB1 (□). Eight days after infection, about 25% of the $Lm-spa^+$ x pCSA1, pCSB-FCU1 infected cells had died on prodrug treatment. Survival after day 6 and 8 p.i. differed significantly from the control strain as calculated using two-way ANOVA followed by Bonferroni post-test.

Results of this experiment demonstrated the functional application of antibody-mediated bacterial internalization in delivery of prodrug converting enzymes for the first time. Consequently the failure of the intended positive control to mediate cytotoxic effects was investigated further.

An infection experiment using an attenuated *L. monocytogenes* strain harbouring all internalin genes in comparison to $Lm-spa^+$ with and without antibody coating was performed. Bacterial adhesion and the number of intracellular bacteria were investigated following infection at an MOI of 100. Results of the experiment are shown in figure 6.19

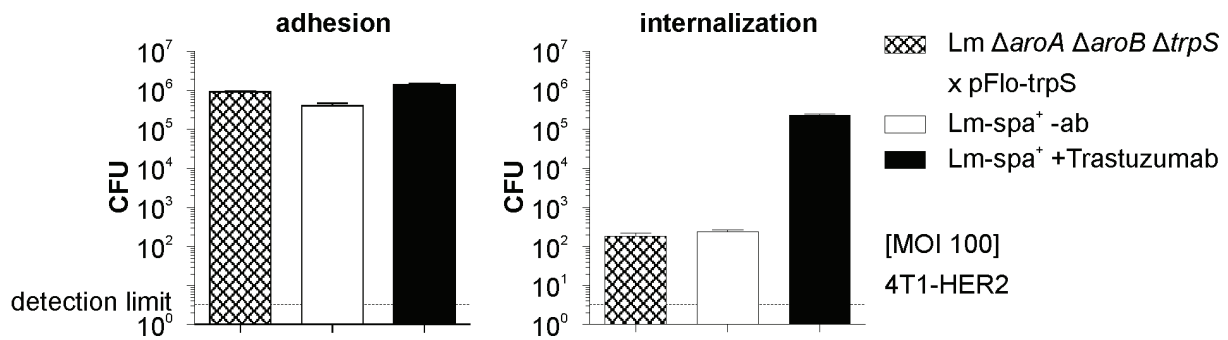


figure 6.19: Adhesion and internalization of *L. monocytogenes* Δ aroA Δ aroB Δ trpS x pFlo-trpS and *Lm*-spa⁺ with and without Trastuzumab coating on infection of 4T1-HER2 cells

While the three bacterial mutants adhered to 4T1-HER2 cells in a similar fashion, the invasion behavior differed drastically. As shown before, uncoated *Lm*-spa⁺ is almost unable to internalize into 4T1-HER2 cells. In contrast, the same mutant coated with Trastuzumab enters the cells efficiently. Surprisingly the metabolically attenuated, but otherwise wildtypic strain showed the same invasion as the uncoated internalin A and B deficient *Lm*-spa⁺. This result explains the lack of cytotoxicity in the control strain as seen in figure 6.18. The strain is unable to efficiently enter into the investigated cell line.

6.III.3 Mechanistic insights into antibody-mediated internalization

6.III.3.a Antibody-mediated internalization of *Lm*-spa⁺ using fluorescent antibodies

In addition to infection experiments investigating intracellular CFU, antibody-mediated bacterial internalization was investigated using immunofluorescence microscopy (figure 6.20).

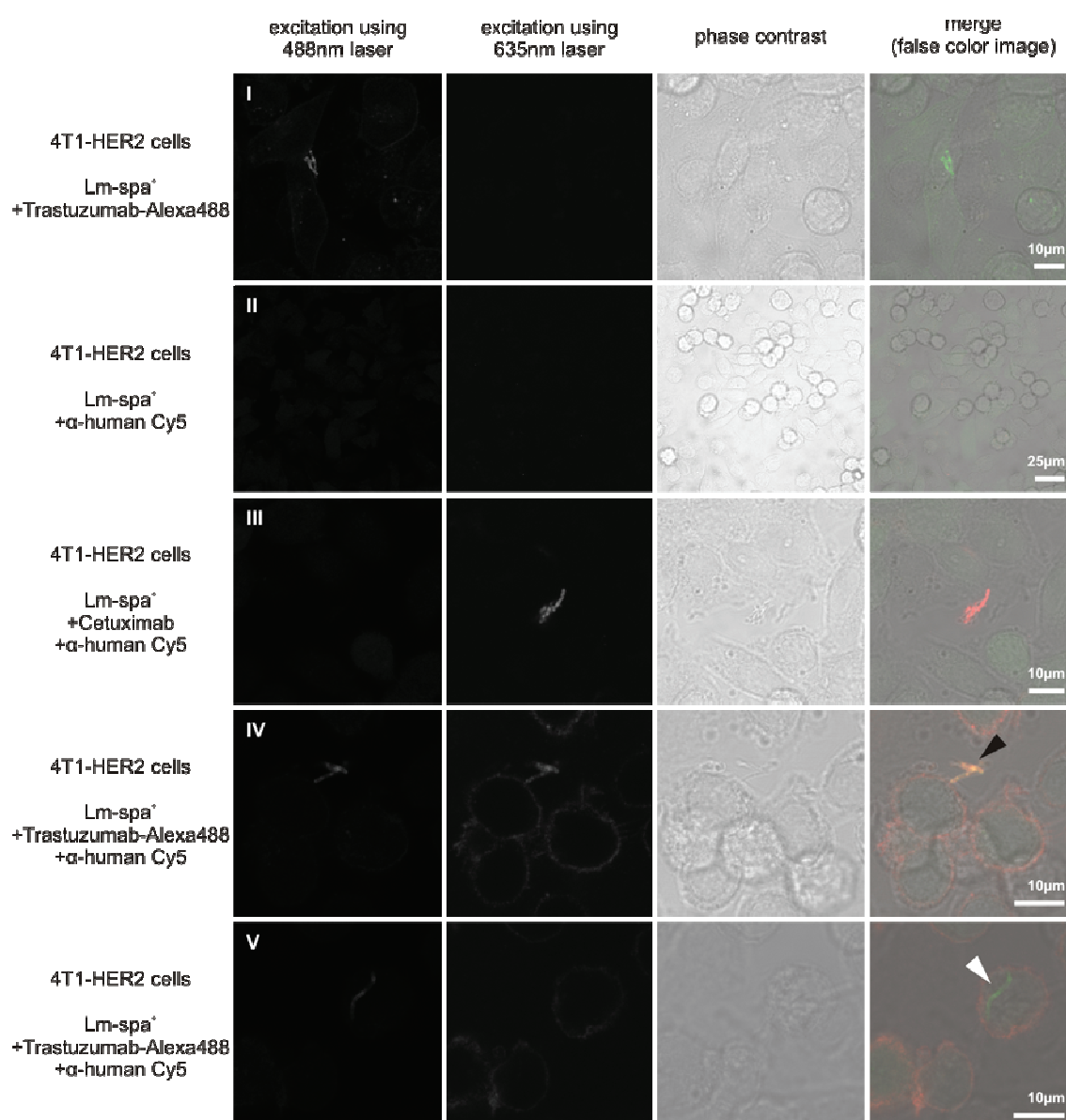


figure 6.20: Infection of 4T1-HER2 cells using Lm-spa⁺ coated with fluorescently labeled antibodies.

Incubation of Lm-spa⁺ with Alexa488-labeled Trastuzumab marks almost 100% of the bacteria with the fluorescent dye (Heisig, data not shown). Using these labeled bacteria for infection of 4T1-HER2 cells, the bacteria were detected by immunofluorescence microscopy (I; figure 6.20). Direct bacterial labeling using a Cy5 labeled goat α-human antibody was impossible as protein A has a low affinity to goat antibodies. (II; figure 6.20). Incubation of the bacteria with non-labeled Cetuximab prior to treatment with Cy5 labeled goat α-human antibody allowed secondary antibody binding (III; figure 6.20).

Infection of 4T1-HER2 cells using bacteria coated with Alexa488-coupled Trastuzumab and incubated after fixation with Cy5 labeled goat α-human antibody revealed bacteria showing both fluorescence signals (▲; IV ; figure 6.20) and bacteria with a single fluorescence signal (Δ; V ; figure 6.20). As the cells were not permeabilized following infection, antibody-

incubation after fixation corresponds to an extracellular staining. Therefore bacteria labeled only with the initial Alexa488 staining are located intracellularly, while double stained bacteria are located extracellularly. This experiment confirmed the internalization of Lm-spa⁺ into 4T1-HER2 cells on Trastuzumab coating as shown in chapter 6.III.2. In addition this experiment proves, that Alexa488 labeled Trastuzumab is able to mediate internalization of Lm-spa⁺ as already shown using unlabeled Trastuzumab.

The experimental settings evaluated in this experiment were used in the following section to assess whether listerial virulence factors are involved in antibody-mediated internalization.

6.III.3.b Coating beads with fluorescent antibodies

Antibody-mediated internalization of Trastuzumab- or Erbitux-coated Lm-spa⁺ was shown already in chapter 6.III.2. Although internalization was characterized regarding several aspects, the mechanism of internalization still remains unknown. As Lm-spa⁺ is deficient in *inlA* and *inlB* the main invasion factors of *L. monocytogenes* can not be involved in antibody-mediated internalization. To rule out the involvement of other bacterial virulence factors in antibody-mediated bacterial internalization, studies with antibody-coated Dynabeads® Protein A (beads) were performed (figure 6.21).

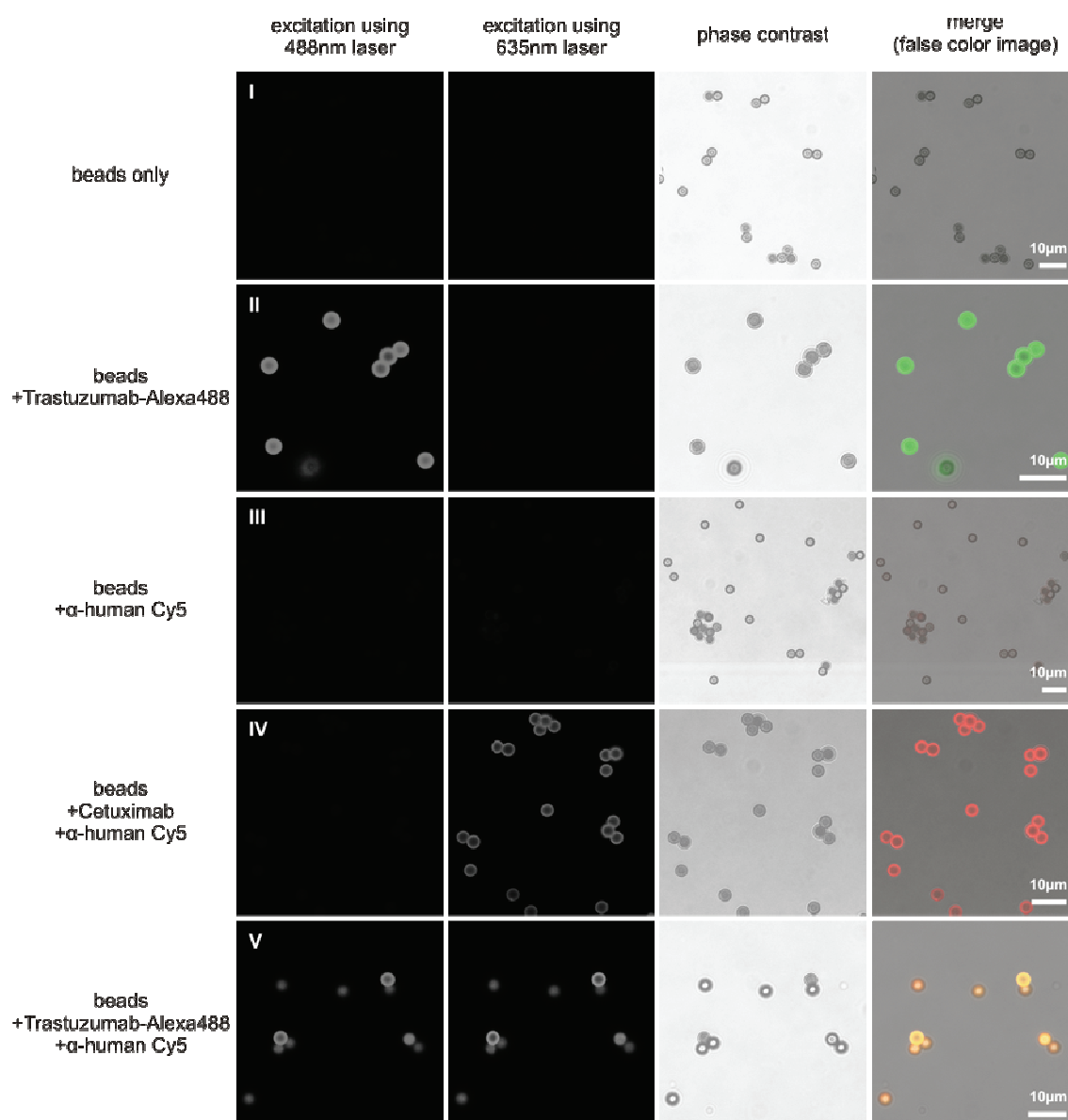


figure 6.21: Coating protein A covered beads using fluorescently labeled and unlabeled Trastuzumab and Erbitux

Bead diameter was specified by the manufacturer to be 2,4µm, but no size range was declared. Investigating beads without antibody treatment revealed a homogenous particle size and almost no intrinsic fluorescence at the investigated wavelength (I; figure 6.21). Bead incubation using Alexa488-coupled Trastuzumab showed a strong fluorescence signal on excitation using a 488nm laser, indicating efficient antibody binding to the bead surface (II; figure 6.21). In contrast the Cy5 labeled goat α-human antibody was unable to bind to the beads, because of the low affinity of protein A to goat antibodies (III; figure 6.21). Incubation using non-labeled Cetuximab prior to incubation with Cy5 labeled goat α-human antibody allowed indirect bead-binding (IV; figure 6.21). Sequential bead-incubation with labeled Trastuzumab and goat α-human antibody showed a clear fluorescence signal in both excitation wavelengths (V; figure 6.21).

6.III.3.c Antibody-mediated internalization of Dynabeads®

By incubation of 4T1-cells with differentially coated beads, the antibody-mediated internalization was investigated independent of bacterial virulence factors. As shown in chapter 6.III.3.a, beads were coated with Trastuzumab and Cetuximab allowing experiments similar to the infection experiments with bacteria (figure 6.22).

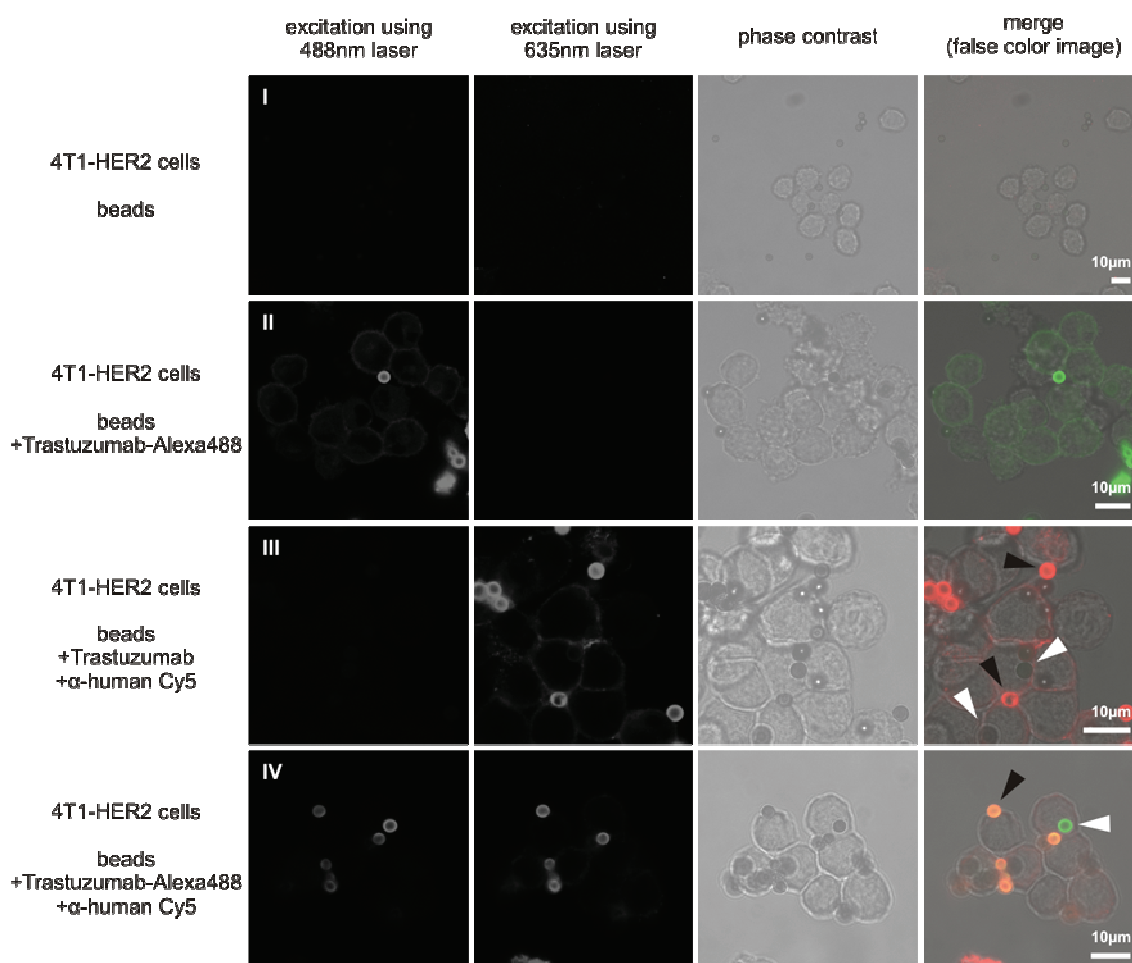


figure 6.22: Treatment of 4T1-HER2 cells with differentially coated beads

To simulate an infection-assay-like experiment, beads were treated with the antibody indicated under the 'bead'-label in figure 6.22 before incubation with the cells. Incubation with the second antibody in picture row III and IV was performed following cell fixation. Here the beads were labeled to 100% with the first antibody, while the second antibody marked extracellular beads only, as the cells were not permeabilized.

Beads labeled with Alexa488-coupled Trastuzumab were clearly visible in the fluorescence image, beads were labeled to 100% as examined by investigating optical layers of the sample (II; figure 6.22; image stack data not shown). Coating the beads with unlabeled

Trastuzumab allowed later binding of goat α -human antibody as already shown for Cetuximab coating in figure 6.21 (III;figure 6.22). Investigating optical layers, several fluorescent (\blacktriangle) and non-fluorescent (\triangle) beads were found (III; figure 6.22; image stack data not shown). Obviously some beads were internalized (\triangle), while most of them remained extracellular (\blacktriangle).

Treating cells with beads labeled with Alexa488-coupled Trastuzumab and incubating them after fixation with Cy5 labeled goat α -human antibody revealed some beads labeled with Alexa488 but not Cy5 (\triangle). Although most beads showed both fluorescence signals (\blacktriangle) some beads with a single fluorescence signal (\triangle) were visible, indicating intracellular positioning. In conclusion, Trastuzumab with or without fluorescent labeling mediated internalization of beads into 4T1-HER2 cells.

6.III.4 Examination of antibody-mediated tumor targeting *in vivo*

6.III.4.a Generation of a xenograft tumor model using cell lines overexpressing HER2/neu

For examination of antibody-mediated tumor targeting *in vivo* several mouse xenograft tumor models were analyzed. The initially used SK-BR-3 cell line was published for tumor generation in nude mice (Hu et al., 2006). In our hands the subcutaneous injection of this ATCC derived cell line into Foxn1 nu/nu mice failed to induce a stable tumor growth as shown in figure 6.23. A total amount of 1×10^6 and 2×10^6 cells were injected subcutaneously into the abdomen and tumor growth was measured using a caliper.

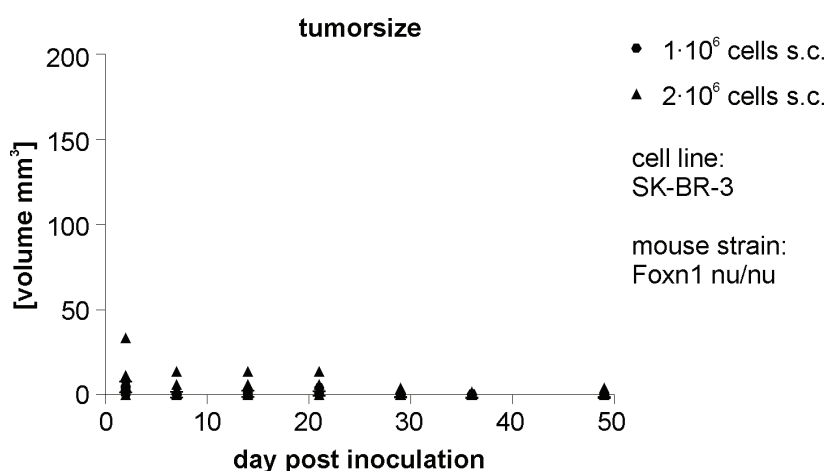


figure 6.23: Growth of SK-BR-3 cell xenografts in Foxn1 nu/nu mice

The available SK-BR-3 cell line failed to induce reproducible tumor growth in nude mice. As an alternative the SK-OV-3 cell line was used for induction of tumor growth. 4×10^6 cells were injected subcutaneously into Foxn1 nu/nu mice and tumor growth was measured using a caliper as shown in figure 6.24.

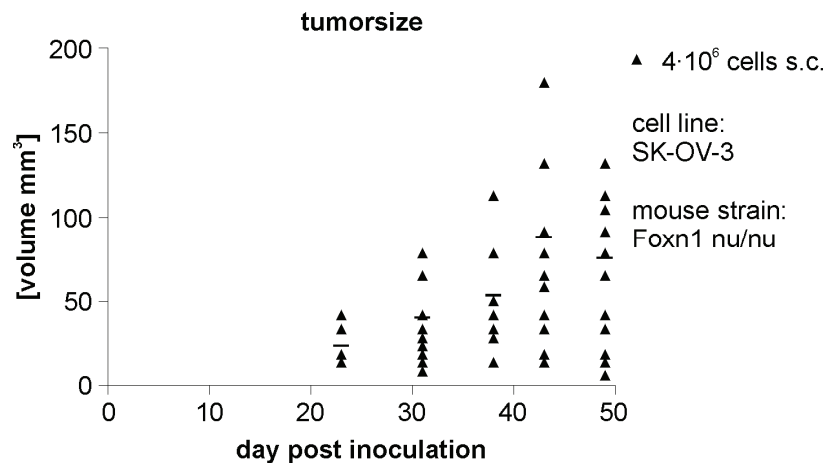


figure 6.24: Growth of SK-OV-3 cell xenografts in Foxn1 nu/nu mice

Although xenograft tumor growth was observed on injection of SK-OV-3 cells in this mouse model, this tumor model comprises strong handling disadvantages during experimental procedure. On the one hand, a huge amount of cells has to be injected for a single tumor induction. On the other hand, tumor growth is very slow, requiring approximately two month until experimentally required tumor sizes of roughly 6-8 mm in diameter are grown.

Tumor induction of the murine breast cancer cell line 4T1-HER2 was examined in Balb/c and Balb/c SCID mice (figure 6.25 and figure 6.26 respectively). A total number of 5×10^4 cells were injected subcutaneously into the abdominal skin of Balb/c and Balb/c SCID mice and tumor growth was measured using a caliper.

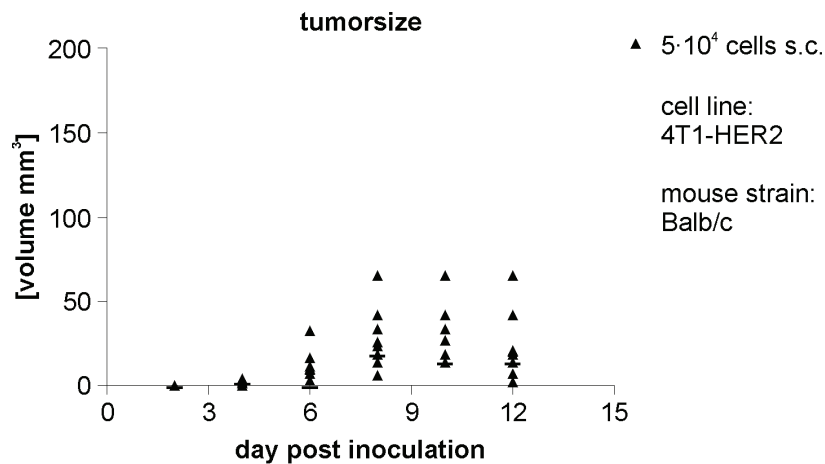


figure 6.25: Growth of 4T1-HER2 cell xenografts in Balb/c mice

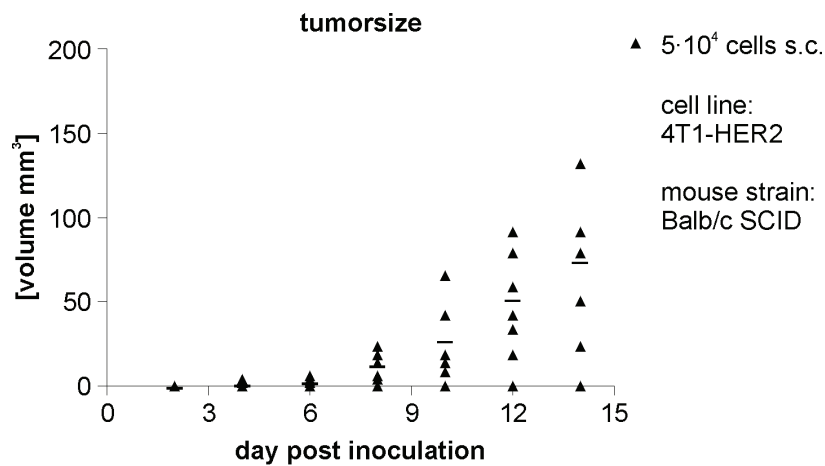


figure 6.26: Growth of 4T1-HER2 cell xenografts in Balb/c SCID mice

In Balb/c mice, no persistent tumor growth was observed on injection of 4T1-HER2 cells. In contrast, 4T1-HER2 xenograft tumor growth was comparable to xenograft growth following injection of the parental cell line 4T1 into Balb/c SCID mice (figure 6.27).

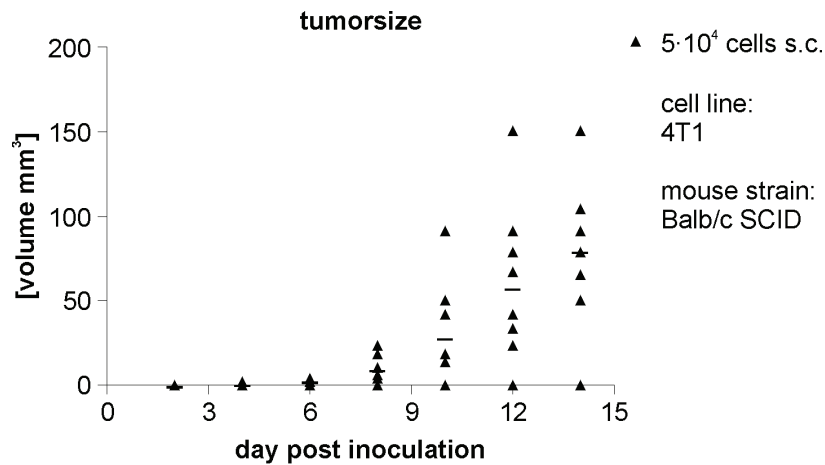


figure 6.27: Growth of 4T1 cell xenografts in Balb/c SCID mice

Subcutaneous injection of 4T1-HER2 cells into Balb/c SCID mice induced persistent xenograft tumor growth. Tumors grew to an appropriate size for bacterial targeting experiments in approximately 2-3 weeks. All subsequent animal experiments investigating antibody-mediated bacterial tumor targeting were conducted in Balb/c SCID mice bearing 4T1 or 4T1-HER2 induced xenograft tumors.

6.III.4.b Antibody-mediated bacterial tumor targeting *in vivo*

Following the successful *in vitro* internalization experiments, antibody-mediated bacterial targeting was investigated *in vivo* in murine xenograft tumors. Tumor growth was induced by s.c. injection of 4×10^4 4T1 cells into the left side- and 4T1-HER2 cells into the right side of the shaven abdominal skin of 4 Balb/c SCID mice per group. 19 days after tumor induction, the mice were injected i.v. with 1×10^8 CFU of Trastuzumab coated Lm-*spa*⁺ and the bacterial count in liver, spleen and tumors was determined 6h and 26h post infection. Later timepoints were also investigated, but as the overall number of colonizing bacteria increases initial antibody-mediated effects might be masked. If Trastuzumab coated bacteria preferentially colonized 4T1-HER2 tumors, this would indicate antibody-mediated bacterial tumor targeting.

In figure 6.28 the CFU per organ divided by the organ weight is shown.

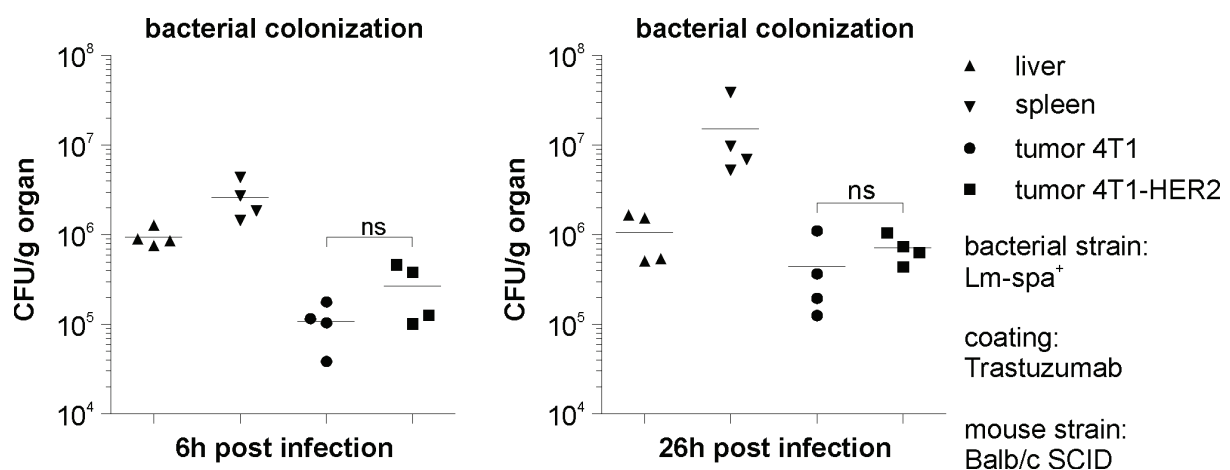


figure 6.28: I.v. infection of 4T1 and 4T1-HER2 xenograft bearing Balb/c SCID mice using 1×10^8 CFU Trastuzumab coated Lm-*spa*⁺

The major share of bacteria was detected in liver and spleen at both time-points. Bacterial counts in the liver remained constant during the first day of infection while bacterial counts in spleen and tumors doubled their counts. Organ colonization by Lm-*spa*⁺ indicated approximately one bacterial replication during the first 26h although overall bacterial counts remained similar.

Although the 4T1-HER2 tumor xenografts contained more bacteria than the 4T1 xenografts, this difference was not statistically significant using two-sided Student's t-test. In contrast to the *in vitro* studies where specific antibody-mediated internalization was shown in a receptor dependent manner, no antibody-mediated bacterial targeting to tumor tissue could be shown *in vivo* in this experiment.

In all subsequent animal experiments investigating antibody-mediated targeting the bacterial counts were determined 24h post infection.

6.III.4.c Investigation of the non-functionality of antibody-mediated targeting *in vivo*

Initial animal experiments revealed the failure of antibody-mediated bacterial tumor targeting in a murine xenograft model. Possible reasons for this observation were examined in different *in vitro* experiments allowing separation into particular potential causes. Infection experiments with additional treatments simulating distinct characteristics of the *in vivo* infection were performed.

4T1-HER2 cells were infected using Trastuzumab-coated Lm-spa⁺ and additional treatments with murine serum, heat inactivated serum, proteinase inhibitors or Cetuximab were performed. Serum treatment reflects the bacterial blood passage following murine i.v. infection. Non-cellular components of the serum like the complement system, proteinases or antibodies might interfere with antibody coating inhibiting the targeting effect *in vivo*. The influence of the complement system on bacterial targeting was investigated by comparing treatments of fresh murine serum with heat inactivated serum. Addition of proteinase inhibitors was used to break down potential influences of serum proteinases by cleavage of the surface bound antibodies. By incubation with an excess of Cetuximab following Trastuzumab coating the exchange of protein A bound antibody by arbitrary antibodies was simulated. As already shown in figure 6.12, Cetuximab does not mediate internalization into 4T1-HER2 cells and was used in this experiment as model for competing antibodies available in murine serum.

In the left graph of figure 6.29 the intracellular CFU after infection is shown, in the right graph relative internalization of Trastuzumab coated Lm-spa⁺ divided by the count of uncoated bacteria is shown.

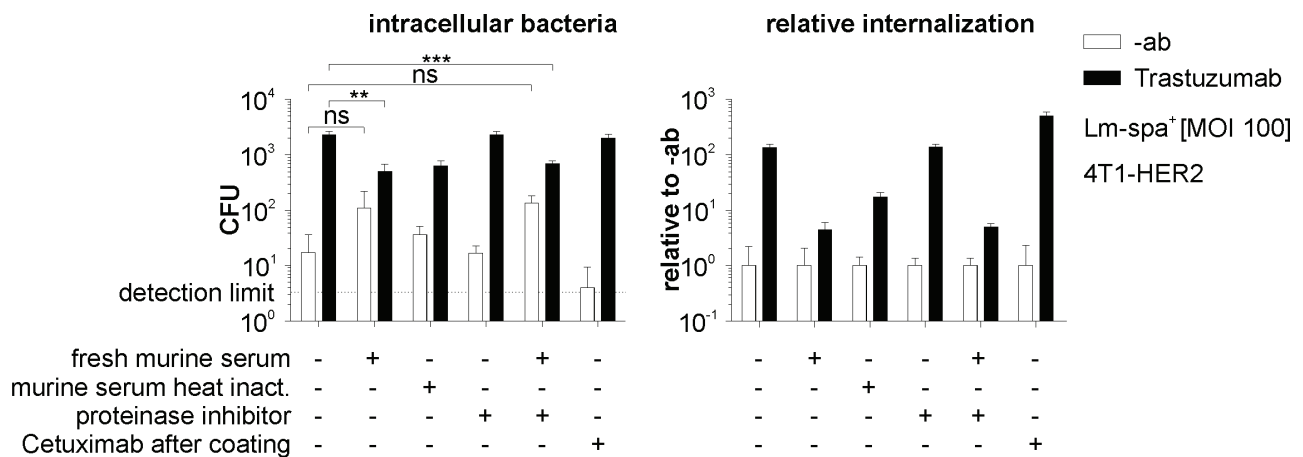


figure 6.29: *In vitro* infection of 4T1-HER2 cells using antibody coated Lm-spa⁺

The first pair of bars depicts the control group showing 100-fold increased internalization of Trastuzumab coated Lm-spa⁺ in comparison to uncoated bacteria. 1h pretreatment of these bacteria in 50% murine serum abrogated the internalization difference between Trastuzumab coated bacteria and uncoated bacteria resulting in a relative internalization rate of almost one. Similar pretreatment using heat inactivated resulted in an intermediate internalization rate.

In the same experiment the influence of proteinase inhibitors on antibody-mediated internalization was analyzed. In between coating and 4T1-HER2 infection, bacteria were incubated for 1h in PBS containing 50µg/ml PMSF, 0,25µg/ml Leupeptin, 0,35µg/ml Pepstatin, 0,5µg/ml Antipain and 10µg/ml Aprotinin or in 50% murine serum containing these inhibitors. After thorough washing, the infection experiment was performed. Proteinase inhibitors showed no influence on internalization regardless of murine serum presence.

The exchange of protein A bound Trastuzumab by antibodies unable to mediate internalization into 4T1-HER2 cells was investigated by additional incubation of coated bacteria for 1h in an excess of Cetuximab. As shown in the two rightmost bars both graphs in figure 6.29 no influence was detected.

Infection experiments *in vitro* revealed a marked effect of fresh murine serum on antibody-mediated bacterial internalization into 4T1-HER2 cells. This might explain the missing functionality of antibody-mediated bacterial tumor targeting *in vivo* following i.v. infection. Though some components of murine serum were investigated, no particular causative agent was found in this study. The experiment shown in figure 6.29 was performed only once, because results shown in the following chapter (6.III.4.d) indicated a main cause for the effect of murine serum.

6.III.4.d Covalent crosslinking of antibodies to protein A on the surface of viable *Lm-spa*⁺

In the experiment shown in figure 6.29 an excess of Cetuximab did not alter the internalization of Trastuzumab-coated *L. monocytogenes* into 4T1-HER2 cells. This clearly indicated that exchange of antibody bound to protein A on the surface of *L. monocytogenes* was not the reason for the effect of murine serum on bacterial internalization. In spite of this the covalent linkage of antibodies to protein A was investigated to tighten the connection between bacterium and antibody. Covalent connection of the antibodies to protein A using a chemical crosslinker would presumably prevent replacement and displacement. To date only Dimethyl pimelinediimide dihydrochloride (DMP) was published to crosslink antibodies in a functional manner to protein A (Harlow and Lane, 1999; Kerrigan and Brooks, 1999; Schneider et al., 1982). The homobifunctional crosslinker DMP reacts at light alkaline pH with primary amines forming amidine bonds. At neutral pH DMP is hydrolyzed. The chemical structure of DMP is shown in figure 6.30.

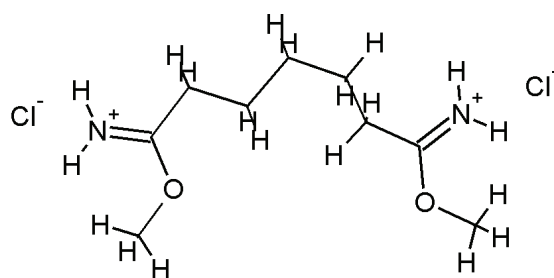


figure 6.30: Chemical structure of Dimethyl pimelinediimide dihydrochloride (DMP)

Crosslinking protocols for connection of protein A sepharose beads to antibodies were available and had to be adapted for application using viable bacteria instead of beads (Schneider et al., 1982). The bacterial viability on treatment with different DMP concentrations and various agents modifying the crosslinking process was investigated in the following (figure 6.31 and figure 6.32).

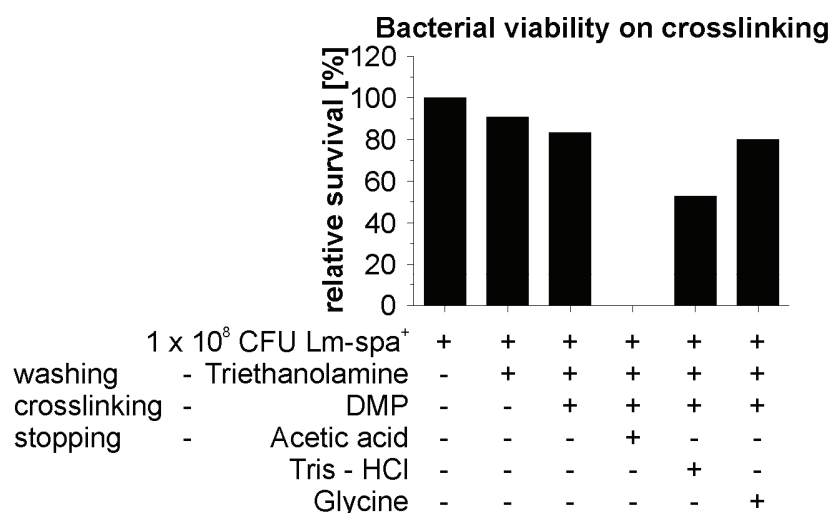


figure 6.31: Influence of Triethanolamine, DMP, Acetic acid, Tris-Cl and Glycine during crosslinking on the viability of Lm-spa⁺

Using available protocols protein A Sepharose-bead crosslinking to approximately 20µg antibody was performed after Triethanolamine (TEA) washing using DMP (20-25 mM) for 45 min and stopped by addition of Acetic acid, Tris-HCl, Glycine or Ethanolamine (Harlow and Lane, 1999; Kerrigan and Brooks, 1999; Schneider et al., 1982).

The initial experiment using viable bacteria was performed using 1 x 10⁸ CFU Lm-spa⁺ coated with 2 µg Trastuzumab. Coated bacteria were washed in TEA 1 ml (TEA; 0.2 M, pH 8.2), incubated for 45 min at RT in 100µl of DMP (250 µM, in 0.2 M TEA, pH 8.2) and the reaction was stopped by addition of 25µl Acetic acid (100%), Tris-HCl(200mM), Glycine(200mM). Relative survival was calculated after plating bacterial aliquots following each incubation step.

The initial TEA washing step buffering the pH for efficient crosslinking lowered the number of viable bacteria slightly, treatment with 250 µM DMP reduced the CFU likewise. Stopping of the crosslinking procedure using Acetic acid killed all remaining bacteria while Glycine had no effect. Tris-HCl treatment and Ethanolamine showed intermediate effects on the viability of the bacteria (Ethanolamine data not shown).

Titration of different DMP concentrations was examined dissolved in PBS (pH 8.2) because TEA as solvent caused an antibacterial effect . DMP titration results are shown in figure 6.32.

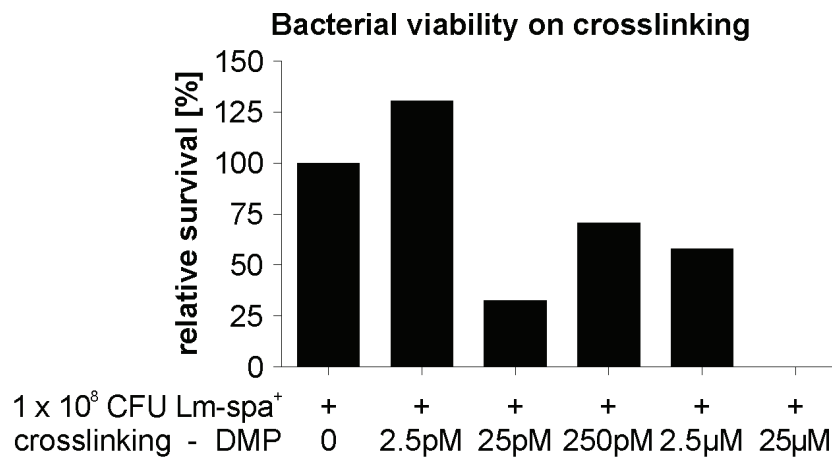


figure 6.32: Influence of different DMP concentrations on the viability of Lm-spa⁺ during crosslinking

Only the lowest DMP concentration of 2,5 pM caused no decrease in bacterial viability and was used for all further crosslinking experiments.

6.III.4.e Crosslinking partially prevents the effect of murine serum on antibody-mediated internalization

Whether antibody crosslinking to Lm-spa⁺ was able to prevent the effect of murine serum on the antibody mediated internalization capacity was examined *in vitro*. Crosslinking of antibody coated bacteria prior to infection was performed either simultaneously with antibody coating of Lm-spa⁺, after coating or at both timepoints. Following antibody coating and crosslinking, the bacteria were incubated for 1h in 50% murine serum. Finally, bacteria were diluted and used for infection of 4T1-HER2 cells at an MOI of 100. The number of intracellular bacteria is shown in the upper graph of figure 6.33 while the lower graph depicts the internalization rate of coated bacteria relative to uncoated bacteria.

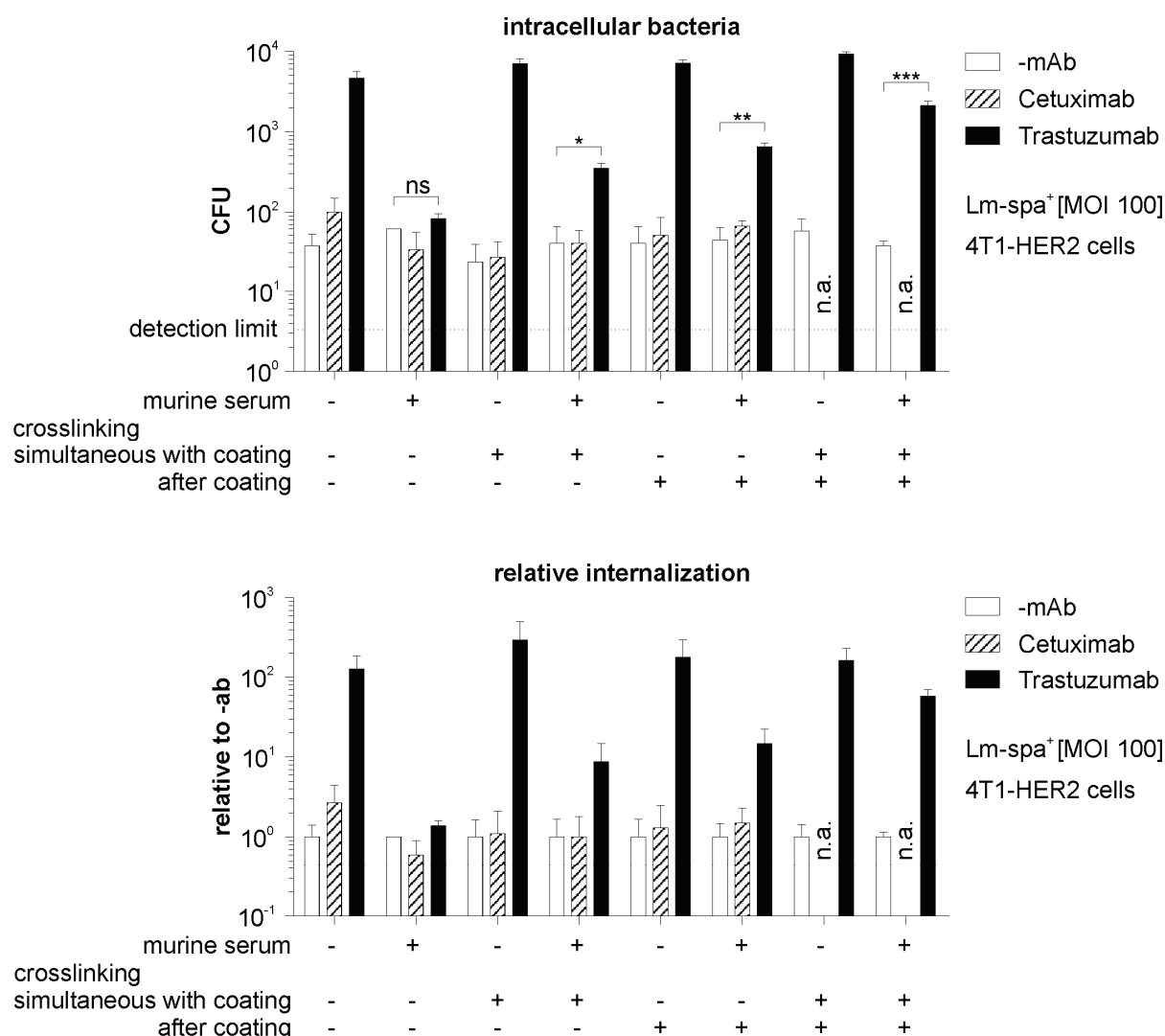


figure 6.33: Influence of murine serum after antibody crosslinking on antibody-mediated bacterial internalization

In the first group of three bars, the internalization of Lm-spa⁺ coated with Cetuximab or Trastuzumab in comparison to uncoated bacteria is shown as positive control. The second group depicts the data after additional incubation in murine serum. Antibody-mediated specific internalization was abrogated completely; the bacteria were unable to enter into the cells independent of their antibody treatment. Crosslinking during or after antibody coating had no effect on antibody-mediated internalization as seen in bar groups three and five. Unspecific internalization of Cetuximab coated or uncoated bacteria was also not altered by chemical crosslinking. However, antibody coated and crosslinked bacteria showed a specific internalization on incubation with murine serum. In contrast antibody-mediated internalization was completely abrogated using bacteria only coated with antibodies prior to serum treatment. Compared to serum treated bacteria, the specific internalization was increased approximately 10-fold upon single Trastuzumab crosslinking. Crosslinking twice, during and

after antibody coating, increased bacterial internalization on Trastuzumab coating and serum treatment more than 50-fold in comparison to uncoated bacteria as shown in the lower graph of figure 6.33 on the right.

Crosslinking antibodies to protein A on the surface of viable bacteria reduced detrimental effects of murine serum on antibody-mediated internalization and allowed efficient bacterial internalization in spite of serum treatment. This newly generated serum stability of the antibody coating was investigated in a murine tumor model.

6.III.4.f Tumor targeting of Lm-spa⁺ crosslinked to antibodies

Targeting bacteria in an antibody-mediated fashion to tumors in a mouse xenograft model was shown to be unsuccessful in 6.III.4.b. *In vitro*, it was shown that antibody coating was not serum stable, but crosslinking of antibodies almost abolished the serum susceptibility of the antibody coating.

In Balb/c SCID mice (n=7 per group) bearing 4T1-HER2 xenografts, tumor targeting of Lm-spa⁺ crosslinked to antibodies was examined. Organ colonization of bacteria coated and crosslinked with Trastuzumab or Cetuximab was compared to uncoated but DMP treated bacteria following i.v. infection using 1×10^8 CFU. One day p.i. mice were sacrificed and bacterial counts in liver, spleen and tumors were determined. Bacterial colonization of livers and spleens was analyzed directly, while tumors were analyzed in four differentially treated fractions. Tumors were separated into single cell suspensions and were not treated, gentamicin treated, gentamicin treated and macrophage enriched as well as gentamicin treated and macrophage depleted. Macrophages were analysed differentially in this experiment to exclude active phagocytosis of the bacteria and assess predominantly antibody-mediated bacterial internalization. Subsequently, separated tumor cells were plated in serial dilutions. Bacterial tumor colonization was calculated relative to the amount of plated eukaryotic cells while CFU in liver and spleen was calculated per gram of organ mass. Tumor colonization data are shown in figure 6.35 and figure 6.36, liver and spleen data are depicted in figure 6.34.

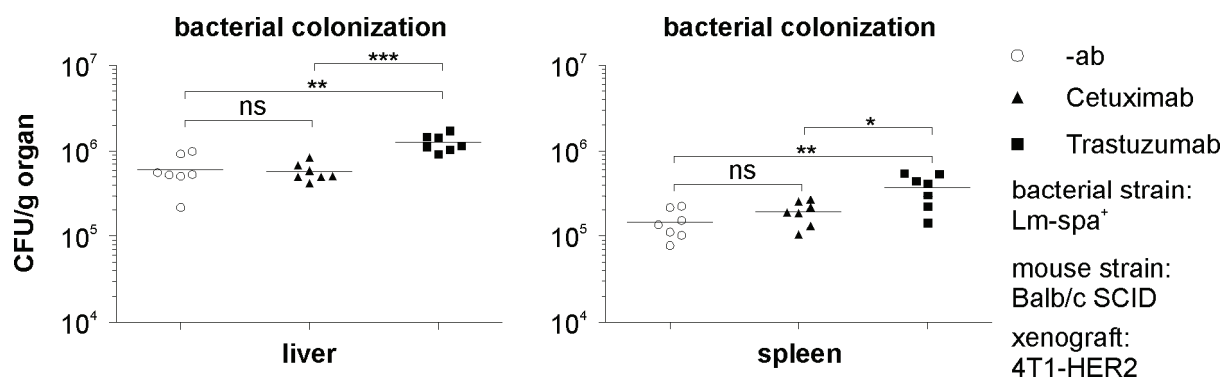


figure 6.34: Bacterial colonization of livers and spleens 24h p.i. using 1×10^8 CFU antibody crosslinked Lm-spa⁺

Compared to uncoated or Cetuximab crosslinked bacteria twice the amount of Trastuzumab crosslinked Lm-spa⁺ was found in livers and spleens. Although small, the colonization difference was highly significant.

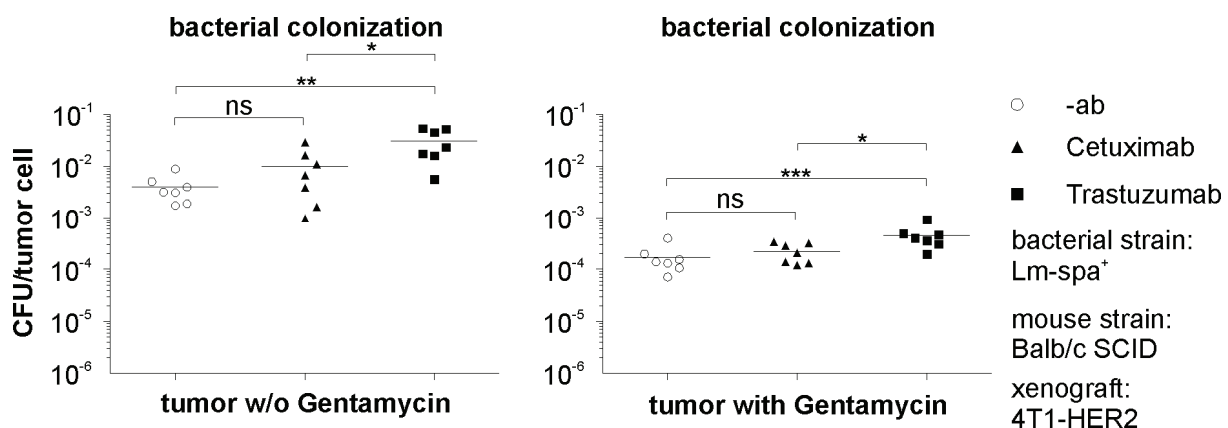


figure 6.35: Overall tumor colonization 24h p.i. using 1×10^8 CFU antibody crosslinked Lm-spa⁺

In tumor tissue Lm-spa⁺ crosslinked with Trastuzumab showed a significantly higher CFU/cell ratio than the control groups. Overall bacterial counts in tumors, shown in the left graph of figure 6.35, were increased 8-fold on specific antibody crosslinking, while intracellular counts were increased only 3-fold as shown in the right graph. Comparison of gentamicin treated versus untreated tumor cells indicated an almost complete extracellular localization of the bacteria in the tumor tissue. The ratio of intracellular to extracellular bacteria was not altered in an antibody-dependent manner (data not shown).

The tumor cell population comprising the intracellular bacteria was more precisely analyzed by MACS separation into macrophage enriched and macrophage depleted cells as shown in figure 6.36.

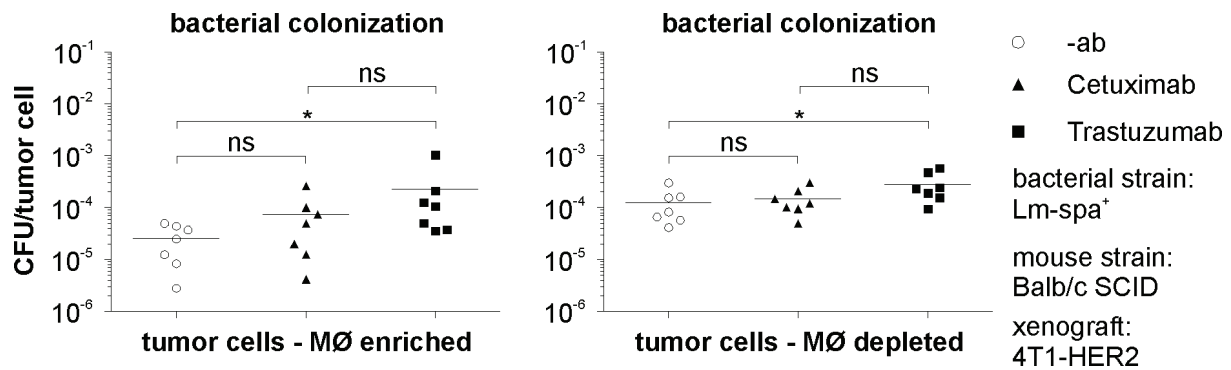


figure 6.36: Bacterial colonization of enriched or depleted tumor macrophages 24h p.i. using 1 x 10⁸ CFU antibody crosslinked Lm-spa⁺

Intracellular bacteria preferentially resided in the macrophage depleted cell fraction of tumor tissue as seen on comparison of the two graphs in figure 6.36. In both fractions Trastuzumab crosslinked Lm-spa⁺ were significantly enriched compared to uncoated bacteria, although the difference was more pronounced in the macrophage enriched fraction.

Infection of 4T1-HER2 xenograft tumor mice using Lm-spa⁺ crosslinked to Cetuximab or Trastuzumab in comparison to bacteria untreated with antibodies showed for the first time antibody-mediated bacterial tumor targeting of *L. monocytogenes*. Trastuzumab crosslinked bacteria showed increased bacterial counts in all examined organs including liver and spleen compared to control groups. The colonization behavior of bacteria crosslinked with Cetuximab was indistinguishable from uncoated bacteria in the examined organs.

6.IV Bacterial colonization of murine organs after infection using different *L. monocytogenes* mutants

6.IV.1 Colonization pattern of *L. monocytogenes* Δhpt mutants in a murine tumor model

The intrinsic capacity of bacteria to accumulate in tumor tissue was investigated for *L. monocytogenes* Δhpt and $\Delta inIGHE$ mutants in comparison to wildtype strains. The Δhpt mutant, published in 2002 by Chico-Calero *et al.*, carries a deletion in Imo0838 encoding a hexose phosphate transporter (Chico-Calero *et al.*, 2002). This mutant was published to show reduced virulence on i.v. infection of ICR mice because of lowered liver colonization and earlier bacterial clearance in the spleen caused by the bacterial inability to take up phosphorylated hexoses (Chico-Calero *et al.*, 2002). Lowered bacterial counts in liver and spleen would be beneficial for bacterial application in tumor therapy as a higher colonization rate of tumor to other organs would be advantageous for prevention of side effects.

6.IV.1.a The Δhpt mutant in a xenograft mouse tumor model

The Δhpt mutant, which was generated in *L. monocytogenes* serovar 4b, strain P14 was compared to *L. monocytogenes* EGD wildtype (serovar 1/2b) in a tumor mouse model. Three B78-D14 xenograft C57BL/6 mice per group were infected i.v. using 5×10^3 CFU. Four- and nine days p.i. the mice were sacrificed and the bacterial count in liver and spleen was determined. In figure 6.37 the results for the WT and Δhpt mutant are shown, data for infection using *L. monocytogenes* $\Delta inlGHE$, performed simultaneous in the same experiment, are shown in figure 6.39.

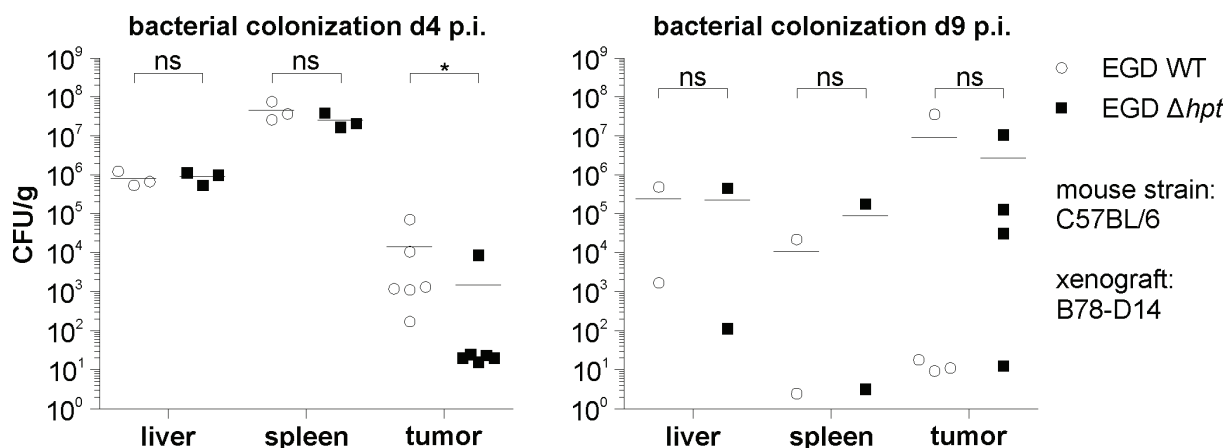


figure 6.37: Bacterial colonization of liver, spleen and tumors four and nine days p.i. using 5×10^3 CFU *L. monocytogenes* WT and *L. monocytogenes* Δhpt

On the left, the organ colonization 4 days p.i. is shown for three mice (bearing two tumors each) per group. Colonization 9 days p.i. was examined similarly, but one mouse per group died before CFU determination, due to bacterial pathogenicity.

In spite of the distinct serotypic background, 4d p.i. liver and spleen showed no differential colonization in between the two strains. In comparison to the data published by Chico-Calero *et al.* the Δhpt mutant exhibited an at least 100-fold higher bacterial titer in this mouse model in both organs at both investigated timepoints (Chico-Calero *et al.*, 2002). In tumor tissue, the Δhpt mutant was detected to a lower extent than the EGD wt strain. Because of the high bacterial virulence the mice exhibited a severe infection and partially succumbed to the infection. The right diagram comprising the colonization of the remaining animals 9 days p.i. shows a very broad distribution of colonization values in between the animals without evident trends.

This first experiment using the Δhpt mutant for investigation of tumor colonization produced no clear answer whether this mutant was suited for tumor therapeutic approaches. To allow higher infection doses without increasing the burden on the animals the Δhpt mutant was attenuated by $\Delta aroA$ deletion.

6.IV.1.b Attenuation of *L. monocytogenes* Δhpt

L. monocytogenes Δhpt was attenuated by deletion of *aroA* as published in Stritzker *et al.* (Stritzker and Goebel, 2004). Briefly, the gene was removed by double crossover of the listerial genome with a plasmid bearing only the flanking regions of the *aroA* gene. The required deletion plasmid pLSV-*aroA* was provided by Jochen Stritzker. Strain attenuation was verified by sequencing the corresponding genomic area using primers *aroA* check -1 and *aroA* check -4.

6.IV.1.c The $\Delta aroA$ Δhpt mutant in a xenograft mouse tumor model

The newly generated attenuated $\Delta aroA/hpt$ mutant was used for infection of tumor mice as described in 6.IV.1.a but using an infection dose of 1×10^8 CFU. The colonization of $\Delta aroA$ Δhpt was investigated together with *L. monocytogenes* $\Delta aroA$ (serovar 1/2b) and *L. monocytogenes* $\Delta aroA$ $\Delta inlGHE$ (serovar 1/2b) three and seven days p.i. Experimental results for $\Delta aroA$ and $\Delta aroA$ Δhpt are shown in figure 6.38, results for $\Delta aroA$ $\Delta inlGHE$ in figure 6.40.

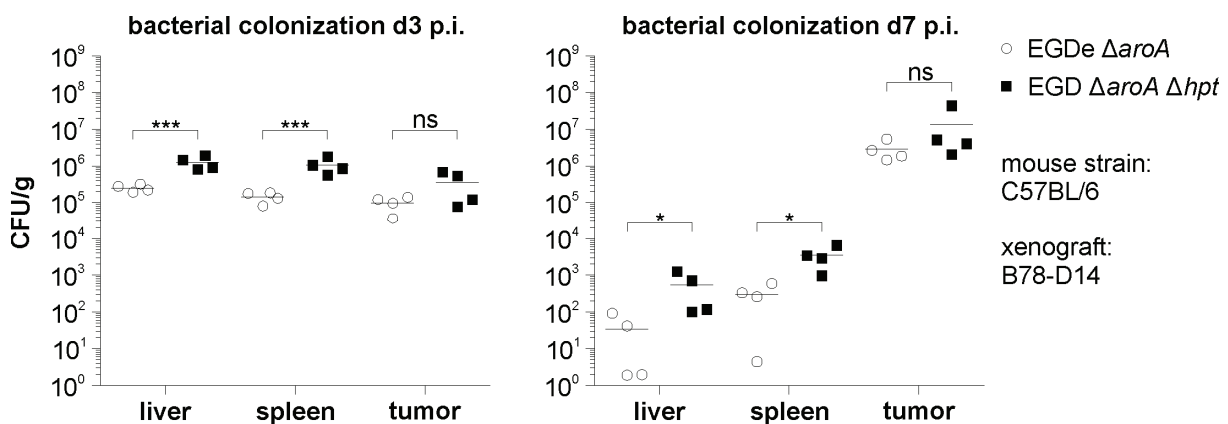


figure 6.38: Bacterial colonization of liver, spleen and tumor three and seven days p.i. using 1×10^8 CFU *L. monocytogenes* $\Delta aroA$ and *L. monocytogenes* $\Delta aroA \Delta hpt$

Compared to the control strain, the $\Delta aroA$ Δhpt mutant revealed an increased colonization in liver and spleen on both investigated time-points. In tumor tissue, no distinct colonization difference was observed.

Using the attenuated *hpt* mutant the colonization pattern in a xenograft mouse tumor model was resolved. It was shown that this mutant is less suited for tumor therapeutic approaches than the control strain because of lower bacterial titers in tumor tissue.

6.IV.2 Colonization pattern of *L. monocytogenes* Δ inIGHE mutants in a murine tumor model

The *L. monocytogenes* mutant lacking internalins G,H and E was generated and initially analyzed by Raffelsbauer *et al.* (Raffelsbauer *et al.*, 1998). Bergmann *et al.* performed further analyses discovering the hyper invasive phenotype of the Δ inIGHE mutant *in vitro* in different cell lines including endothelial and epithelial cell lines (Bergmann *et al.*, 2002). Additional information was also gathered illustrating increased invasion of the mutant into a melanoma- and a fibroblast cell line (Duechs, 2007).

6.IV.2.a The Δ inIGHE mutant in a xenograft mouse tumor model

The high infection rate of *L. monocytogenes* Δ inIGHE into (tumor) cell lines poses a promising property for delivery of functional DNA and RNA. Efficient invasion is one of the major prerequisites triggering a potent transcription and translation of the delivered nucleic acids.

In C57BL/6 mice bearing B78-D14 xenografts the bacterial organ colonization was examined. Three mice per group were infected i.v. with 5×10^3 CFU *L. monocytogenes* Δ inIGHE and four and nine days p.i. the mice were sacrificed and the bacterial count was determined as shown in figure 6.39. Shown results were generated in one experiment with the data shown in figure 6.37.

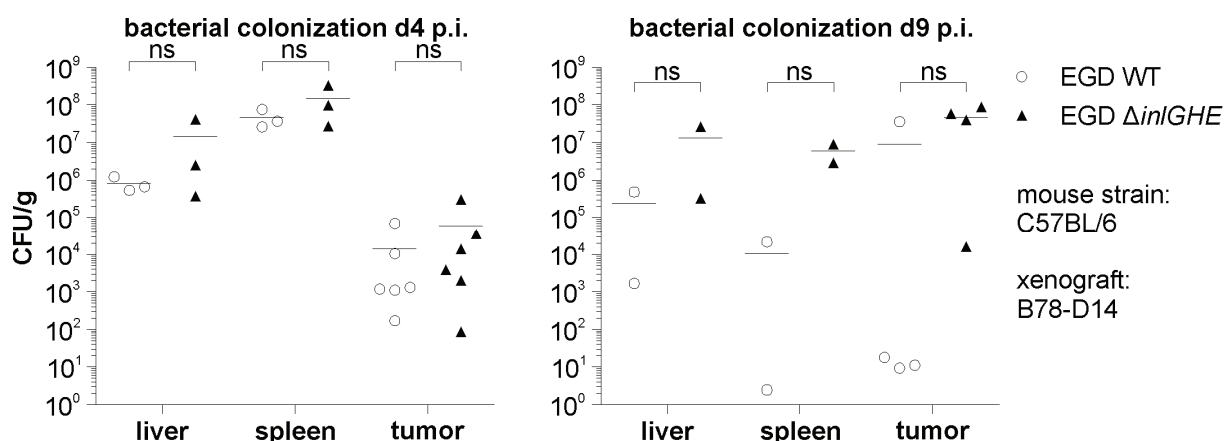


figure 6.39: Bacterial colonization of liver, spleen and tumors four and nine days p.i. using 5×10^3 CFU *L. monocytogenes* WT and *L. monocytogenes* Δ inIGHE

Although the Δ inIGHE mutant showed higher bacterial loads in all examined organs at both timepoints, no significant differences were observed. Nine days p.i. one mouse of each group had succumbed to the bacterial infection indicating high bacterial virulence.

To allow higher infection doses without increasing the burden on the animals, the $\Delta inlGHE$ mutant was attenuated by $aroA$ deletion as described for the Δhpt mutant in 6.IV.1.b.

6.IV.2.b The $\Delta aroA \Delta inlGHE$ mutant in a xenograft mouse tumor model

The $\Delta aroA \Delta inlGHE$ mutant was used for infection of B78-D14 tumor bearing C57BL/6 mice using 1×10^8 CFU for i.v. infection. Three and seven days p.i. the bacterial counts in liver, spleen and tumors were determined. Tumors of each mouse were pooled. The calculated CFU per gram of organ is depicted in figure 6.40.

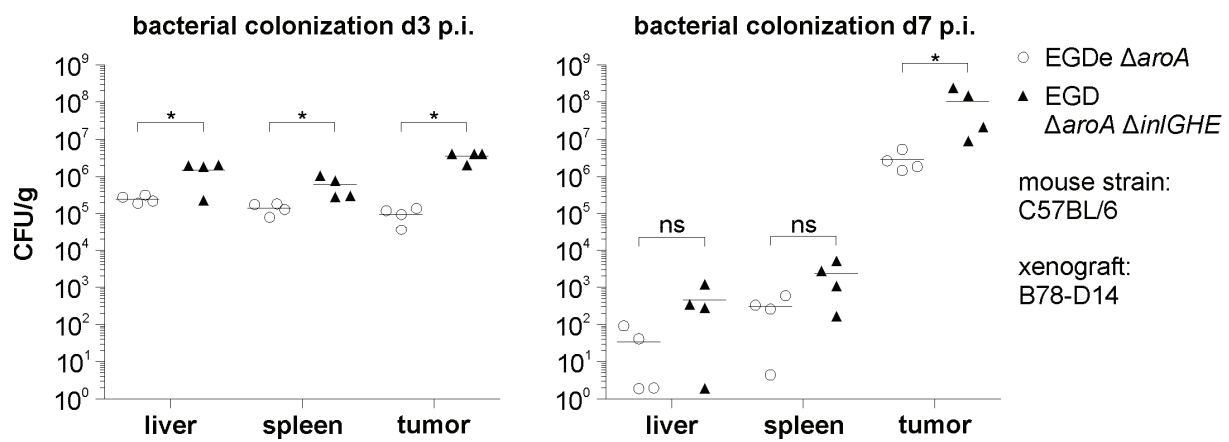


figure 6.40: Bacterial colonization of liver, spleen and tumors three and seven days p.i. using 1×10^8 CFU *L. monocytogenes* $\Delta aroA$ and *L. monocytogenes* $\Delta aroA \Delta inlGHE$

Three days p.i. the $\Delta aroA \Delta inlGHE$ mutant showed an increased colonization in all organs in comparison to *L. monocytogenes* $\Delta aroA$ (EGDe). While bacterial titers of the control strain were rather equal in all examined organs, the $\Delta aroA \Delta inlGHE$ mutant colonized the tumors best. Seven days p.i. bacterial colonization in liver and spleen showed no difference between the strains. In contrast, bacterial counts in tumor tissue were elevated 40-fold compared to the control strain. A mean of 10^8 CFU per gram were detected in tumor tissue, an *in vivo* titer of *L. monocytogenes* never obtained in former experiments. The ratio of bacteria in tumor tissue to bacteria in liver and spleen exceeds $10^5:1$, indicating efficient tumor accumulation. Although absolute values are promising, direct comparison of *L. monocytogenes* $\Delta aroA$ and *L. monocytogenes* $\Delta aroA \Delta inlGHE$ is not fully appropriate as the control strain is in the EGDe background and the double mutant was generated in the EGD serotype.

7 Discussion

7.1 Influence of InIC on apical cell junctions and cell-to-cell spread by *L. monocytogenes*

In this part the molecular mode of action of InIC during the infection process of *L. monocytogenes* was examined. In the first experiments the interaction of InIC with Tuba was characterized biochemically while in the following the functional aspects during infection were examined.

The importance of *inIC* for pathogenicity and virulence of *L. monocytogenes* was already demonstrated in the initial publication by Engelbrecht *et al.* (Engelbrecht *et al.*, 1996). Upregulation of *inIC* two hours p.i. was shown, indicating a function in the late stages during the infection process. Comparing replication of the *inIC* deletion mutant and the corresponding wildtype strain in macrophage- and epithelial cell lines showed no significant differences. Although the replication rate was similar in both strains, their virulence in mice differed markedly. The LD₅₀ of the *inIC* deletion mutant on i.v. infection was 50-fold increased in mice, demonstrating the importance for bacterial virulence (Engelbrecht *et al.*, 1996). These results are in accord with the data described in chapter 6.I. Interaction of InIC enables the bacteria to manipulate their host cell environment to enhance cell-to-cell spreading. This contributes to bacterial virulence without altering invasion or intracellular replication.

Tuba seems to be involved in regulation of apical cell membrane tension of by linking proteins involved in endocytosis, actin polymerization and cell junction morphology (Cestra *et al.*, 2005; Otani *et al.*, 2006; Qualmann and Kessels, 2002; Salazar *et al.*, 2003). As scaffold protein Tuba is interacting with dynamin and several actin regulatory proteins like N-WASP (Salazar *et al.*, 2003). Downregulation of Tuba or N-WASP using RNAi leads to reduced membrane tension resulting in curved apical membranes measured by a elevated membrane linearity index (Otani *et al.*, 2006). On infection of epithelial cell *L. monocytogenes* wildtype caused the same cellular phenotype, while *inIC* deletion mutants or the *inIC.K173A* mutant failed to do so (Rajabian *et al.*, 2009). By displacing N-WASP from Tuba InIC interferes with a crucial protein-protein interaction resulting in reduction of membrane tension. This reduction allows *L. monocytogenes* a higher spreading efficiency by simplifying the generation of membrane protrusions. This report is the first description of a bacterial virulence factor altering host cell membrane tension to enhance bacterial tissue distribution on infection.

While the interaction of InIC with Tuba resolved the *L. monocytogenes* phenotype observed already by Engelbrecht *et al.*, the mechanism of membrane tension control by Tuba remains

to be investigated. It will be fascinating to examine other bacteria like *Shigella* or *Rickettsia*, which maintain an intracytosolic lifestyle and are capable of cell-to-cell spread, whether these bacteria express proteins with similar functions.

7.II RNA delivery into eukaryotic cells by *L. monocytogenes*

In this project a previously established *L. monocytogenes*-based mRNA delivery system was reengineered in several aspects. Reduction of the initially two-plasmid based RNA delivery system to one-plasmid expression was performed. In an associated project the delivery of shRNA using this RNA delivery system was examined. The first experiments comprised the construction of the carrier strains while in the following the constructed mutants were examined regarding their particular delivery behavior.

In the past, two strategies were developed utilizing *L. monocytogenes* as carrier for delivery of nucleic acids into the cytosol of eukaryotic cells. The first delivery system transferred plasmid encoded eukaryotic expression constructs into macrophage cell lines (Dietrich G. et al., 1998). While showing for the first time DNA delivery using *L. monocytogenes* as carrier, the delivery of DNA comprised disadvantages for use in therapeutic settings. Plasmid-based transfer of eukaryotic expression constructs into the host cell cytosol requires translocation of the plasmid into the nucleus for transcription. This process is not well understood and rather inefficient in non-dividing cells limiting the overall delivery performance (Munkonge et al., 2003). One of the major risks on application of this bacterial DNA delivery is integration of plasmid DNA into the host cell genome as observed in Dietrich et al. (Dietrich G. et al., 1998). Construction of the *L. monocytogenes* RNA delivery system circumvented these problems and decreased the time interval between bacterial infection and delivery effects (Schoen et al., 2005). Following phagosomal escape the autolysing bacteria release mRNA, directly translated by the eukaryotic translation system. The described RNA delivery system resulted in protein expression as early as 4h p.i. *in vitro*.

One of the major drawbacks regarding the RNA delivery system was the impossibility to attenuate the carrier strains for *in vivo* applications. While application of non-attenuated RNA delivery strains delivering heterologous antigens has shown promising results, tumor targeted therapies require much higher infective doses (Loeffler et al., 2006; Stritzker et al., 2007). As described in chapter 6.II.1 of this thesis, the RNA delivery system was altered to a single-plasmid based system for reduction of the growth retardation caused in the carrier by the delivery system. The mutant with integrated T7RNAP showed comparable growth kinetics in BHI medium as the corresponding *L. monocytogenes* $\Delta trpS$ x pFlo-*trpS* wildtype strain as shown in figure 6.2. By reduction of the the T7RNAP copy number the growth rate

efficiency was enhanced although no T7RNAP driven expression cassette was present. These results encouraged the metabolic attenuation of this trimmed RNA delivery system. The generation of the attenuated strain per se additionally indicated the metabolic downsizing of the system, as attenuation was not feasible using the published (2 plasmid) RNA delivery system (Pilgrim, personal communication; Schoen et al., 2005). The attenuated RNA delivery strain unfortunately did not fulfill the expectations because of pronounced growth retardation in BHI medium. As shown in figure 6.2. the attenuated strain needed more than 24h to reach an optical density (at 600nm) of 1.0, while the corresponding wildtype strain grew to this density in a third of the time.

Comparison of RNA delivery efficiency between the two-plasmid system and the novel one-plasmid system was performed by FACS analysis. The time course of GFP positive cells following infection with the two non-attenuated RNA delivery strains in figure 6.3 shows the pronounced performance difference. While infection using the published carrier resulted in up to 10% of fluorescent cells, the novel carrier peaked at a maximum of 2% positive cells. As the RNA delivery plasmids are high copy plasmids an efficiency reduction by an estimated factor between 50 and 100 would be expected if the copy number reduction would be the only factor influencing delivery efficiency. But the delivery decrease was only about five-fold, indicating the improved tolerance of the one-plasmid RNA by the carrier strain. Although the delivery carrier was trimmed for application *in vivo*, in the end this goal was not achieved. Even the downsized delivery system resulted in a pronounced growth retardation of the carrier strain that an *in vivo* use is not possible using the actual strains. The bilateral balance between safety (attenuation) and function (delivery efficiency) was shifted into the safety direction decreasing the applicability because of over-attenuation. As published in many other approaches using bacteria or viruses the optimal balance is crucial for overall performance (Hoft, 2008; Linde et al., 1991; Tijhaar et al., 1994). In case of the attenuation by *aroA* deletion the metabolic limitations can be abrogated by growing the bacteria in complete medium supplemented with menaquinone as described in Stritzker et al. (Stritzker et al., 2004). Interestingly supplementation of the attenuated novel RNA delivery strain using 50µg/ml menaquinone was not sufficient to abrogate or even reduce growth retardation (data not shown). As an Δ *aroA* attenuated *L. monocytogenes* strain was not restored completely to wildtype growth behavior in the same experiment, the menaquinone might have been partially degraded resulting in application of too low concentrations. If the growth behavior of the attenuated novel RNA delivery strain could be restored, the strain might be saturated with menaquinone during *in vitro* cultivation prior to *in vivo* infection. This might allow aerobic energy generation during the first cycles of replication following *in vivo* infection and thereby enable experimental assessment in animal model systems.

Expansion of the RNA delivery system for transfer of shRNAs was examined in chapter 6.II.2. As described earlier the targeted delivery of RNAs mediating gene silencing remains one of the main challenges in therapeutic *in vivo* applications (Carthew and Sontheimer, 2009; Kurreck, 2009; Takeshita and Ochiya, 2006). Current clinical trials administering siRNAs in lung and eye diseases depend on topical application of the nucleic acids. Only two studies in phase one rely on a systemic siRNA application (reviewed in Pushparaj et al., 2008; Whitehead et al., 2009). At present no targeted delivery systems are sufficiently advanced for examination in clinical studies but some approaches are currently evaluated preclinically. Non-viral siRNA targeting based on aptamers or antibodies is investigated in this context (reviewed in Aigner, 2008; Cerchia et al., 2009).

L. monocytogenes as a facultative intracellular bacterium residing in the cytosol poses an interesting alternative carrier to the currently used systems. To evaluate the feasibility of modifying the published *L. monocytogenes* RNA delivery system for delivery of siRNAs a published shRNA sequence was inserted into the T7RNAP expression cassette. The shRNA sequence including the loop structure was provided by Krishna Rajalingam and was previously shown to efficiently silence the proapoptotic SMAC/DIABLO (Rajalingam et al., 2007). Following construction of the required delivery plasmid the detection of shRNAs was performed in *E. coli* (data not shown) and *L. monocytogenes*. Using RNA-acrylamide gel electrophoresis shRNAs were not detected, presumably because the assay sensitivity was too low. A more sensitive approach using qRT-PCR was performed revealing a pronounced shRNA production in *L. monocytogenes*. Promotor induction by XAD addition increased shRNA levels approximately 100-fold in comparison to the control strain. Although the shRNA expression cassette has a length of slightly less than 200 nucleotides the largest amount of specific shRNA was detected in the large RNA fraction (figure 6.6). Isolation of shRNA containing sequences from the large RNA fraction was initially surprising, but in other systems employing T7RNAP based transcription leakiness of a T7RNAP terminator was also observed to a high extent (Magee et al., 2007). Hence, the presence of RNAs containing the shRNA sequence was shown in this experimental setup though additional nucleotides were presumably attached to the shRNA. The question whether these sequences can assemble the dsRNA hairpin structure required for DICER cleavage remains to be answered. Initial infection experiments using the α -SMAC shRNA delivery strains showed no reproducible silencing pattern (data not shown). Several parameters of the experiment would have to be standardized and supported with the proper controls to finally answer the question of functionality. Silencing of SMAC/DIABLO was found out to be a complex task, as the proapoptotic function of the SMAC protein adds additional parameters to the investigation. Conclusively the shRNA delivery system was modified for delivery of shRNAs directed against the LDH subunit A and B which can be functionally detected by enzymatic assays

(data not shown). The strains have been constructed in this study but functional characterization remains to be examined.

7.III Protein A mediated antibody coating of *L. monocytogenes*

In this part of the study the impact of protein A mediated antibody coating on bacterial internalization and tumor targeting was investigated. Following the initial experiments antibody mediated bacterial internalization was improved and expanded *in vitro* in this study (Frentzen, 2008). Experiments performed in tumor bearing mice were used to assess the improvement of antibody-mediated tumor targeting *in vivo*.

The experiments described in chapter 6.III.1, further characterized antibody binding by protein A expressing *L. monocytogenes*. Interaction of the bacteria with the antibodies was strictly dependent on bacterial protein A expression and was accomplished in a fast process. Already 5 to 15 min after antibody addition, the amount of bound antibody reached the maximal level. An average of at least 60 antibody molecules were bound per bacterial cell. Antibody binding kinetics of protein A expressing *L. monocytogenes* were comparable to established protocols of biochemical antibody binding to protein A sepharose *in vitro* (Schneider et al., 1982). The high speed of antibody binding is caused by the high affinity of protein A to IgG antibodies in general and rabbit, guinea pig and human antibodies in particular (Richman et al., 1982). During the coating experiments, the bacteria showed the same characteristics expected from sepharose beads. No influence of replication or other bacterial factors except the virulence regulator *prfA* was observed. Upon upregulation of *prfA* by XAD addition, the expression of protein A increased because of regulation via the *hly* promoter (Heisig, data not shown).

Following biochemical characterization the antibody-mediated bacterial internalization was examined *in vitro*. The antibody amount applied during the bacterial coating process was investigated after infection of SK-BR-3 and SK-OV-3 cells. Using at least 2 µg of antibody per 10⁸ CFU bacteria was sufficient for maximal bacterial internalization. Optimal antibody amounts used for bacterial coating resulted in 40 up to 900-fold increased internalization rates compared to uncoated bacteria. Specificity of antibody-receptor interaction and dependence of internalization on this interaction was examined by infection of isogenic cell lines thereof one overexpressing HER2/neu. Bacterial internalization was increased by 2-3 orders of logarithmic magnitude due to coating with the HER2/neu specific Trastuzumab. The internalization increase mediated by specific antibody coating ranged in similar magnitudes as described for viral targeting relying on protein A expression. Protein A mediated infection of Adenovirus and Vesicular stomatitis virus was enhanced by specific antibody binding

about 100-fold in susceptible cell lines (Bergman et al., 2003; Volpers et al., 2003). Currently, there is no comparable report published investigating bacterial cell targeting or internalization mediated by protein A bound antibodies.

In comparison to the antibody-mediated bacterial internalization investigated earlier the internalization rate following coating optimization as shown in this thesis was significantly increased (Frentzen, 2008). Internalization in comparison to the results of the previous study was improved by factor 10 to 50 depending on the investigated cell line (Frentzen, 2008). Further increase was even possible on artificial *prfA* activation by XAD addition. Adding 1% XAD to the bacterial growth medium increased the amount of antibody bound to Lm-spa⁺ approximately threefold (Heisig, data not shown). In a preliminary *in vitro* experiment XAD incubated Lm-spa⁺ coated with Trastuzumab displayed tenfold higher internalization into 4T1-HER2 cells than the otherwise equally treated control strain (Heisig, data not shown). Ongoing experiments currently investigate whether the internalization increase by XAD addition can be fully added on top of the antibody-mediated targeting system as presented in this study. Performed experiments have to be repeated and the specificity of internalization has to be investigated to proof existing data.

Bacterial coating using the EGFR specific Cetuximab did not alter internalization into cells lacking EGFR overexpression. Cells overexpressing EGFR and HER2/neu like the SK-BR-3- and SK-OV-3 cell line showed efficient bacterial internalization on coating with either antibody. Hence, in addition to the already mentioned requirement of protein A expression, bacterial internalization was thereby shown to be strictly dependent on coating with an antibody directed against an epitope overexpressed by the target cells. Antibodies recognizing epitopes absent on target cells were unable to mediate bacterial internalization. Similarly, these antibodies had no influence on bacterial adhesion whereas antibodies mediating internalization increased bacterial adhesion to receptor-overexpressing eukaryotic cells.

While antibody-mediated internalization was considerably enhanced as shown in this study, only recently insights regarding the mechanism of the internalization process were gained. The coating of magnetic beads with Trastuzumab led to internalization of these beads into 4T1-HER2 cells, while the coating with Cetuximab did not (Heisig, data not shown). Antibody-mediated internalization of beads indicates the independence of the internalization on bacterial virulence factors. Ligand binding to EGFR as well as Trastuzumab binding to HER2/neu was published to increase receptor endocytosis (Ceresa and Schmid, 2000; Opresko et al., 1995; Yarden, 2001). The bacteria might be taken up by receptor-mediated endocytosis and thereby enter target cells. Preliminary results using inhibitors of clathrin mediated endocytosis on infection of Trastuzumab coated Lm-spa⁺ into 4T1-HER2 cells

showed a distinct decrease of internalization (Heisig, data not shown). Currently, all experimental evidence indicates uptake of antibody-coated bacteria by receptor-mediated endocytosis. Further experiments are needed to clarify this internalization mechanism in detail. Coating the bacteria using an antibody directed against a region of HER2/neu which does not increase receptor dimerisation / endocytosis should not increase bacterial internalization. Pertuzumab (® Omnitarg) might be used for Lm-spa⁺ coating on infection of HER2/neu overexpressing cells as Pertuzumab does not induce receptor endocytosis like Trastuzumab. Additional hints regarding the internalization mechanism might be gained by using receptor-tyrosine-kinase (RTK) specific inhibitors like GW2974 or Lapatinib (® Tykerb) during infection (Burris, 2004; Rusnak et al., 2001). These experiments would reveal whether bacterial internalization is depending on RTK phosphorylation.

Antibody-mediated bacterial cell targeting and internalization as described above were developed as tools for efficient and specific therapeutic delivery by bacterial carrier strains. First experiments using antibody mediated bacterial internalization in an *in vitro* therapeutic application were shown in chapter 6.III.2.f. Antibody-targeted *L. monocytogenes* were equipped with plasmids encoding prodrug-converting enzymes and used for infection of 4T1-HER2 cells. Following infection using Trastuzumab-coated bacteria delivering the converting enzyme eukaryotic cell viability decreased following prodrug addition. Although only 25% of the cells were killed the proof of concept for functional delivery enabled by antibody-mediated bacterial internalization was shown. Future improvements have to elevate the bacterial killing rate to allow *in vivo* therapeutic applications. Infection experiments investigating RNA delivery of prodrug-converting enzymes by *L. monocytogenes* have previously achieved almost 90% killing rate in COS-1 cells, though without antibody-mediated internalization (Heisig, 2005). The results cannot be directly compared to the ones shown here because of the complete dissimilarity of cell lines and experimental protocols. Nevertheless confirmation of the possibility of high killing rates encourages further improvement of antibody-mediated delivery.

In addition to the mentioned proof of the concept an interesting observation was made in the described experiment. The intended positive control for prodrug-conversion was unable to elicit any cytotoxic effects in 4T1-HER2 cells on prodrug addition. During further investigations, the almost complete inability of this strain for infection of 4T1-HER2 cells was revealed. While adhesion to this cell line by *L. monocytogenes* Δ aroA Δ aroB Δ trpS x pFlo-trpS and Lm-spa⁺ with and without Trastuzumab coating was similar, only the Trastuzumab coated Lm-spa⁺ was able to internalize into the cells (shown in figure 6.19). The amount of intracellular bacteria in both uncoated strains was close to the detection limit, despite one of

them possessing all internalins. As described in the introduction, *L. monocytogenes* is able to invade almost every cell line using the endogenous invasion proteins *inlA* and *inlB*. To date no reports of cell lines resistant to *L. monocytogenes* infection have been published. In contrast, in experimental settings every investigated cell line including epithelial-, endothelial- and neuronal cells but also fibroblasts and hepatocytes was actively infected so far (Drams et al., 1998; Drevets et al., 1995; Gaillard et al., 1987; Guzman et al., 1995; Kuhn et al., 1988; Wood et al., 1993). The parental cell line 4T1 is readily infected by *L. monocytogenes* wt bacteria consequently the HER2 overexpression remains as sole cause for prevention of infection in 4T1-HER2 cells (Fensterle, personal communication; Lütkenhaus, 2005). As the 4T1 cell line was isolated from a murine mammary cancer, *inlA* cannot be involved in the invasion process. The receptor of *inlA*, E-cadherin is mutated in mice at one critical aminoacid residue preventing *inlA* mediated infection of murine cells by *L. monocytogenes* (Lecuit et al., 1999).

With *inlA* not being involved, the invasion has to be caused by *inlB*, the second major invasion factor in *L. monocytogenes*. As described above, *InlB* interacts with MET or gC1qR and either of them is sufficient to induce uptake in distinct cell lines (reviewed in Braun and Cossart, 2000). In transformed tissues, MET is overexpressed frequently and high MET levels correlate with bad prognosis in breast cancer patients (Lengyel et al., 2005). No reports of MET downregulation in neoplastic lesions are published so far. However, *in vitro* experiments using CaCo cells proved receptor translocation to the nucleus in cells growing at low density while densely growing cells showed membrane bound MET (Pozner-Moulis et al., 2006). The authors speculate that nuclear MET might represent a more mesenchymal or germinal cell phenotype, while the membrane bound receptor is found only in fully differentiated cells (Pozner-Moulis et al., 2006). Indeed, the 4T1-HER2 cells showed a distinct cell morphology different from the parental cell line in microscopic analysis. While the 4T1 cells grew to a epithelial monolayer in cell culture, the 4T1-HER2 cells showed fibroblast-like cell shapes and grew on top of each other (Heisig, data not shown).

HER2 transduction during generation of the 4T1-HER2 cell line might have induced a transition to less-differentiated cell type causing nuclear translocation of MET and thereby inhibiting infection by *L. monocytogenes* wt bacteria. This hypothesis might be proven by measuring the MET abundance and localization via qRT-PCR and western blot analysis, as well as histological studies.

Tumor targeting of Lm-spa⁺ in xenografted tumor mice was investigated starting with chapter 6.III.3.

Finding a murine tumor model that can be easily induced by subcutaneous cell injection of a cell line overexpressing HER2/neu proved to be more difficult than initially estimated. Tumor

xenografts of SK-BR-3 cells and SK-OV-3 cells comprise disadvantages in several aspects. Tumor growth following SK-BR-3 cell injection was observed only in a small percentage of injected animals and penetrance remained low. Subcutaneous injection of SK-OV-3 cells resulted in tumor growth in all injected animals, but huge deviations were observed in between the individuals. As 4×10^6 cells had to be injected per tumor xenograft, the cell suspension had a high viscosity clogging the syringe needle. Additionally, the huge amount of required cells, cell cultivation for xenograft induction was laborious.

caused large efforts in the cell culture for cell cultivation prior to xenograft induction. Using 4T1-HER2 cells for xenograft induction in Balb/c SCID mice, disposed these disadvantages and resulted in faster and more reproducible tumor induction.

First experiments investigating antibody-mediated bacterial tumor targeting in 4T1-HER2 tumor-bearing mice failed completely. Although the amount of Trastuzumab-coated Lm-spa⁺ was slightly increased in tumors expressing HER2/neu, the difference was statistically not significant. Several *in vitro* experiments were performed mimicking the *in vivo* environment affecting antibody-coated bacteria after intravenous injection. Explanation for missing antibody-mediated targeting functionality was narrowed down to the influence of murine serum on the coated bacteria (shown in figure 6.29). Incubation of coated bacteria in murine serum completely abolished specific targeting effects in 4T1-HER2 cells. Some components of murine serum were investigated in more detail but no correlation was found in these experiments. Neither the complement system nor serum proteinases showed an influence on antibody-mediated internalization.

The final hint explaining the targeting inhibition by murine serum was given on covalent coupling of Trastuzumab to protein A. Chemical crosslinking of the antibody to protein A prior to serum incubation partially prevented the serum effect on antibody coated bacteria. The serum effect therefore had to be caused at least partially by antibodies contained in the serum. These serum antibodies compete for the bacterial protein A molecules and lead to dilution of internalization-mediating antibodies on the bacterial surface. Incubation of the antibody-coated bacteria with the chemical crosslinker covalently linked the coated antibodies to protein A and largely prevented antibody exchange during serum incubation. Protocols for crosslinking of viable bacteria had to be established and optimized to yield maximal crosslinking efficiency inherent with bacterial viability. Results shown in chapters 6.III.4.d and 6.III.4.e show the progress of protocol development regarding crosslinker solvent, crosslinker concentrations, termination of the crosslinking process and finally timing of the crosslinking process. The optimization process finally resulted in maintenance of approximately 50% of the antibody-mediated bacterial internalization rate on crosslinking prior to serum incubation. Crosslinking could not prevent the effect of murine serum on antibody-coated bacteria completely leading to the conclusion that either antibody

crosslinking is incomplete or that other serum components influence targeting, too. Only about 10^{-6} of the crosslinker concentrations published in protocols for antibody binding to protein A sepharose beads could be used due to cytotoxic effects on the bacterial carrier. Therefore, an incomplete crosslinking penetrance is likely, but this does not rule out the influence of other serum components.

Results contrasting the explanation of antibody exchange on the bacterial surface are depicted in the last treatment group of the experiment shown in figure 6.29. Trastuzumab-coated bacteria incubated with an excess of Cetuximab internalize into 4T1-HER2 cells like bacteria coated only with Trastuzumab. As Cetuximab does not mediate internalization into this cell line potential exchanges of bound antibodies against serum antibodies were simulated in this experiment. The clear result shows no influence of Cetuximab incubation on specific internalization. Antibody crosslinking prior to serum incubation in contrast prevents antibody exchange in serum and clearly has an effect as discussed above. Addition of a homogenous solution of purified antibody like Cetuximab might not mirror the complex mixture of serum antibodies encountered by the coated bacteria on i.v. infection properly. Consequently, serum antibodies might be isolated by protein A sepharose and used in the same experimental protocol like Cetuximab. An explanation for the experimental discrepancy might be that coated antibodies are not directly displaced by other antibodies but the bond is weakened at first by antibodies recognizing protein A. On lateral binding to protein A the strong interaction with the bound antibody might be relaxed allowing antibody exchange. This might explain the stabilizing effect of antibody crosslinking, as lateral antibody binding should not weaken a covalent bond.

Finally, antibody coated and crosslinked Lm-spa⁺ were used *in vivo* investigating antibody-mediated tumor targeting in xenografted tumor mice. Following i.v. infection using antibody crosslinked Lm-spa⁺ the bacterial load in liver, spleen and tumors was examined. Colonization in all examined organs was significantly increased upon coating and crosslinking of the bacteria using Trastuzumab in comparison to Cetuximab- or uncoated bacteria. Though the differences in bacterial titers of liver and spleen were as low as twofold, statistical analysis showed high significance. The Trastuzumab specific increase of bacteria in the liver tissue might be caused by micrometastases spread from the primary tumor following tumor induction. A report investigating the metastatic potential of the 4T1 cell line in Balb/c mice showed a metastatic penetrance in 80 to 90% of the mice 30 days after subcutaneous tumor induction (Pulaski and Ostrand-Rosenberg, 1998). The number of micrometastases in the published study exhibited a broad range of up to 3700 metastases per liver. Transduction of HER2/neu into the 4T1 cell line presumably increased the metastatic potential even further, as HER2/neu overexpression correlates with increased

angiogenesis simplifying metastatic spreading (Kumar and Yarmand-Bagheri, 2001). The metastatic potential of the 4T1-HER2 cell line was not compared directly with the parental cell line, but in murine model system the HER2/neu transduced cell line induced massive amounts of micrometastases (Kershaw et al., 2004). As the 4T1 cell line is 6-Thioguanine resistant the absolute number of micrometastases in liver and spleen might be assessed in the 4T1-HER2 cell line, too. Histological HER2/neu stainings of liver and spleen tissue might give further hints why Trastuzumab crosslinked bacteria show an increased liver and spleen colonization.

Extracellular bacterial titers in tumor tissue were elevated approximately 8-fold when using Trastuzumab-crosslinked Lm-spa⁺ while the intracellular increase was approximately 2-3 fold. Although this colonization increase indicated the proof of principle for antibody-mediated bacterial tumor targeting, the sole targeting efficiency was rather low. The *in vivo* observed antibody-mediated internalization rate was astonishingly small, in comparison to the high efficiency in cell culture systems. But the environment encountered by the bacterial delivery strains *in vivo* is completely different from the standardized *in vitro* situation.

In order to differentiate antibody-mediated effects from intrinsic bacterial infection the major bacterial internalins had been deleted in Lm-spa⁺. After the successful proof of principle the antibody-mediated tumor targeting might be investigated in combination with other bacterial tumor targeting mutants like the ones described in the following. Employing the antibody-mediated targeting on top of other bacterial tumor targeting strains might add to the overall colonization efficiency because boosting an already functional system 8-fold, might make therapeutic approaches possible.

Only one report is currently published investigating the improvement of bacterial tumor targeting in an scFv-mediated manner. In contrast to the approach described in this thesis, the published experiments were performed using *S. enterica* serovar *typhimurium* VNP20009 expressing a single chain antibody directed against CEA (Bereta et al., 2007). The authors claim that 3000 to 4000 bacteria found per gram of CEA overexpressing tumor tissue 7 days p.i. completely block tumor growth. However, they fail to compare bacteria expressing the scFv against CEA with bacteria that do not express the scFv in the investigated therapeutic setting. In addition, bacterial colonization data showing the CEA expressing cell line in comparison to the corresponding cell line lacking CEA expression is absent. Therefore, the comparison of data presented in this thesis to the limited data regarding specificity and efficiency of scFv-mediated bacterial tumor targeting shown in the mentioned publication is difficult. The overall targeting efficiency as scales by raw bacterial titers in the tumor tissue seems to be superior on protein A mediated antibody coupling. Kinetics of bacterial tumor accumulation as well as the achieved targeting ratio shown in this thesis exceeded the published scFv based approach. But in contrast to the published data currently no functional

therapeutic information is available for the antibody-mediated targeting presented in this thesis. In comparison to the scFv based approach protein A based antibody coating is a highly versatile approach. It requires no genetic strain modification to switch the TAA, only another antibody has to be coated on the bacterial carrier strain.

If the hypothesis of passive internalization by receptor-mediated endocytosis is valid, not all antibodies might allow bacterial internalization. Using intrinsically invasive bacterial mutants, antibody-mediated targeting would not be required to provoke internalization but rather be responsible for initial enrichment of the bacteria in the tumor vicinity.

The antibody-mediated tumor targeting system as shown in this thesis improves tumor targeting by *L. monocytogenes*. Though the sole targeting is too small to allow direct therapeutic use, the system might be applicable to improve existing bacterial tumor targeting mutants. Connecting the targeting system with functional units like prodrug-converting enzymes would allow improved delivery of cytotoxic drugs to the site of disease. Targeted transport of functional shRNAs would even enlarge the range of possible applications towards gene therapy. In comparison to tumor targeting based on viral carriers the bacterial approach presented here is closer to basic research than to therapeutic applications. But the current perspectives look rather promising that future research might further improve the *L. monocytogenes* based delivery systems.

7.IV Bacterial colonization of murine organs after infection using different *L. monocytogenes* mutants

In the last part of this study two *L. monocytogenes* mutants were examined regarding their tumor colonization behavior in xenografted tumor mice. As described already the Δhpt mutant was analyzed because of the published reduction in liver colonization, while the $\Delta inlGHE$ mutant was investigated because of the hyper invasive phenotype in melanoma cell lines (Chico-Calero et al., 2002; Duechs, 2007). While the Δhpt mutant completely failed to show the published liver colonization phenotype in tumor mice, the $\Delta inlGHE$ mutant outranged all prior speculations. Following metabolic attenuation the internalin mutant reached 10^8 CFU/g of tumor mass 7 days p.i. whereas being almost absent in liver and spleen. Though comparison to the used control strain is not completely appropriate, the absolute *L. monocytogenes* titers in the tumor tissue are much higher than all bacterial tumor titers obtained before (Fensterle, personal communication). The ratio of colonization in tumor- to healthy tissue exceeds $10^5:1$ and is thereby similar to the maximal accumulation ratios ever published for facultative anaerobe bacteria. Only studies applying *S. choleraesuis* were able to report specific accumulation ratios in the same magnitude, reports investigating

other species of *Salmonella* or *Vibrio* showed lower tumor to liver ratios (Lee et al., 2004; Lee et al., 2005; Pawelek et al., 1997). The attenuated *L. monocytogenes* mutants replicated in the tumor tissue about once a day thereby doubling the overall bacterial count. Future experiments will investigate whether the maximal bacterial colonization is already reached 7 days p.i., or whether the bacterial replication continues further. Histological tumor sections will elucidate where the bacteria reside in the tumor tissue and whether they spread to adjacent tissues. The results have to be consolidated in other tumor models to prevent concentration on one model system.

Finally, tumor targeting might even further be enhanced by combination with the antibody-mediated uptake system described above. Integration of functional entities like the delivery systems published for *L. monocytogenes* might allow therapeutic use of this bacterial mutant.

8 References

Aigner, A. (2008). Cellular delivery in vivo of siRNA-based therapeutics. *Curr Pharm Des* 14, 3603-3619.

Ambion DNA-free http://www.ambion.com/techlib/prot/bp_1906.pdf.

Andrade, A.A., Silva, P.N., Pereira, A.C., De Sousa, L.P., Ferreira, P.C., Gazzinelli, R.T., Kroon, E.G., Ropert, C., and Bonjardim, C.A. (2004). The vaccinia virus-stimulated mitogen-activated protein kinase (MAPK) pathway is required for virus multiplication. *Biochem J* 381, 437-446.

Angelakopoulos, H., Loock, K., Sisul, D.M., Jensen, E.R., Miller, J.F., and Hohmann, E.L. (2002). Safety and shedding of an attenuated strain of *Listeria monocytogenes* with a deletion of *actA/plcB* in adult volunteers: a dose escalation study of oral inoculation. *Infect Immun* 70, 3592-3601.

Barbacid, M. (1987). *ras* genes. *Annu Rev Biochem* 56, 779-827.

Beauregard, K.E., Lee, K.D., Collier, R.J., and Swanson, J.A. (1997). pH-dependent perforation of macrophage phagosomes by listeriolysin O from *Listeria monocytogenes*. *J Exp Med* 186, 1159-1163.

Belkowsky, L.S., and Sen, G.C. (1987). Inhibition of vesicular stomatitis viral mRNA synthesis by interferons. *J Virol* 61, 653-660.

Bereta, M., Hayhurst, A., Gajda, M., Chorobik, P., Targosz, M., Marcinkiewicz, J., and Kaufman, H.L. (2007). Improving tumor targeting and therapeutic potential of *Salmonella* VNP20009 by displaying cell surface CEA-specific antibodies. *Vaccine* 25, 4183-4192.

Bergman, I., Whitaker-Dowling, P., Gao, Y., Griffin, J.A., and Watkins, S.C. (2003). Vesicular stomatitis virus expressing a chimeric Sindbis glycoprotein containing an Fc antibody binding domain targets to Her2/neu overexpressing breast cancer cells. *Virology* 316, 337-347.

Bergmann, B., Raffelsbauer, D., Kuhn, M., Goetz, M., Hom, S., and Goebel, W. (2002). InlA- but not InlB-mediated internalization of *Listeria monocytogenes* by non-phagocytic mammalian cells needs the support of other internalins. *Molecular Microbiology* 43, 557-570.

Bischoff, J.R., Kirn, D.H., Williams, A., Heise, C., Horn, S., Muna, M., Ng, L., Nye, J.A., Sampson-Johannes, A., Fattaey, A., *et al.* (1996). An Adenovirus Mutant That Replicates Selectively in p53- Deficient Human Tumor Cells. *Science* 274, 373-376.

Brantner, H., and Schwager, J. (1979). [Enzymatic mechanisms of the oncolysis by *Clostridium oncolyticum* M 55 ATCC 13.732 (author's transl)]. *Zentralbl Bakteriol [Orig A]* 243, 113-118.

Brantner, H., and Schwager, J. (1980). A theoretical models of oncolysis by *Clostridium oncolyticum* M 55 ATCC 13,732. *Arch Geschwulstforsch* 50, 601-612.

Braun, L., and Cossart, P. (2000). Interactions between *Listeria monocytogenes* and host mammalian cells. *Microbes Infect* 2, 803-811.

Braun, L., Ghebrehiwet, B., and Cossart, P. (2000). gC1q-R/p32, a C1q-binding protein, is a receptor for the InlB invasion protein of *Listeria monocytogenes*. *Embo J* 19, 1458-1466.

- Brockstedt, D.G., Giedlin, M.A., Leong, M.L., Bahjat, K.S., Gao, Y., Lockett, W., Liu, W., Cook, D.N., Portnoy, D.A., and Dubensky, T.W., Jr. (2004). Listeria-based cancer vaccines that segregate immunogenicity from toxicity. *Proc Natl Acad Sci U S A* *101*, 13832-13837.
- Brown, J.M. (1999). The Hypoxic Cell: A Target for Selective Cancer Therapy--Eighteenth Bruce F. Cain Memorial Award Lecture. *Cancer Res* *59*, 5863-5870.
- Brown, J.M., and Giaccia, A.J. (1998). The unique physiology of solid tumors: opportunities (and problems) for cancer therapy. *Cancer Res* *58*, 1408-1416.
- Burris, H.A., 3rd (2004). Dual kinase inhibition in the treatment of breast cancer: initial experience with the EGFR/ErbB-2 inhibitor lapatinib. *Oncologist* *9 Suppl 3*, 10-15.
- Busch, W. (1866). Einfluß von Erysipel. *Berliner Klin Wschr* *3*, 245-246.
- Carey, R.W., Holland, J.F., Whang, H.Y., Neter, E., and Bryant, B. (1965). Clostridial oncolysis in man. *European Journal of Cancer* *3*, 37-42.
- Carthew, R.W., and Sontheimer, E.J. (2009). Origins and Mechanisms of miRNAs and siRNAs. *Cell* *136*, 642-655.
- Cerchia, L., Giangrande, P.H., McNamara, J.O., and de Franciscis, V. (2009). Cell-specific aptamers for targeted therapies. *Methods Mol Biol* *535*, 59-78.
- Ceresa, B.P., and Schmid, S.L. (2000). Regulation of signal transduction by endocytosis. *Curr Opin Cell Biol* *12*, 204-210.
- Cestra, G., Kwiatkowski, A., Salazar, M., Gertler, F., and De Camilli, P. (2005). Tuba, a GEF for CDC42, links dynamin to actin regulatory proteins. *Methods Enzymol* *404*, 537-545.
- Chakrabarty, A.M. (2003). Microorganisms and cancer: quest for a therapy. *J Bacteriol* *185*, 2683-2686.
- Chico-Calero, I., Suarez, M., Gonzalez-Zorn, B., Scortti, M., Slaghuis, J., Goebel, W., and Vazquez-Boland, J.A. (2002). Hpt, a bacterial homolog of the microsomal glucose- 6-phosphate translocase, mediates rapid intracellular proliferation in Listeria. *Proc Natl Acad Sci U S A* *99*, 431-436.
- Chomczynski, P., and Rymaszewski, M. (2006). Alkaline polyethylene glycol-based method for direct PCR from bacteria, eukaryotic tissue samples, and whole blood. *Biotechniques* *40*, 454, 456, 458.
- Coffey, M.C., Strong, J.E., Forsyth, P.A., and Lee, P.W. (1998). Reovirus therapy of tumors with activated Ras pathway. *Science* *282*, 1332-1334.
- Coley, W. (1896). The therapeutic value of the mixed toxins of the streptococcus of erysipelas and bacillus prodigiosus in the treatment of inoperable malignant tumors. With a report of 160 cases. *Am J Med Sci* *112*, 251-281.
- Coley, W.B. (1991). The treatment of malignant tumors by repeated inoculations of erysipelas. With a report of ten original cases. 1893. *Clin Orthop Relat Res*, 3-11.
- Cossart, P. (2002). Molecular and cellular basis of the infection by Listeria monocytogenes: an overview. *Int J Med Microbiol* *291*, 401-409.
- Cossart, P., and Lecuit, M. (1998). Interactions of Listeria monocytogenes with mammalian cells during entry and actin-based movement: bacterial factors, cellular ligands and signaling.

Embo J 17, 3797-3806.

Cunningham, C., and Nemunaitis, J. (2001). A phase I trial of genetically modified *Salmonella typhimurium* expressing cytosine deaminase (TAPET-CD, VNP20029) administered by intratumoral injection in combination with 5-fluorocytosine for patients with advanced or metastatic cancer. Protocol no: CL-017. Version: April 9, 2001. Hum Gene Ther 12, 1594-1596.

Dang, L.H., Bettegowda, C., Huso, D.L., Kinzler, K.W., and Vogelstein, B. (2001). Combination bacteriolytic therapy for the treatment of experimental tumors. Proc Natl Acad Sci U S A 98, 15155-15160.

de Magalhaes, J.C., Andrade, A.A., Silva, P.N., Sousa, L.P., Ropert, C., Ferreira, P.C., Kroon, E.G., Gazzinelli, R.T., and Bonjardim, C.A. (2001). A mitogenic signal triggered at an early stage of vaccinia virus infection: implication of MEK/ERK and protein kinase A in virus multiplication. J Biol Chem 276, 38353-38360.

de Pace, N. (1912). Sulla scomparsa di un enorme cancro vegetante del collo dell'utero senza cura chirurgica. Ginecologia 9, 82-89.

Di Nicolantonio, F., Mercer, S.J., Knight, L.A., Gabriel, F.G., Whitehouse, P.A., Sharma, S., Fernando, A., Glaysher, S., Di Palma, S., Johnson, P., *et al.* (2005). Cancer cell adaptation to chemotherapy. BMC Cancer 5, 78.

Dietrich G., Bubert A., Gentschev I., Sokolovic Z., Simm A., Catic A., Kaufmann S. H., Hess J., Szalay A. A., and W., G. (1998). Delivery of antigen-encoding plasmid DNA into the cytosol of macrophages by attenuated suicide *Listeria monocytogenes*. Nat Biotechnol 16, 181-185.

Domann, E., Wehland, J., Rohde, M., Pistor, S., Hartl, M., Goebel, W., Leimeister-Wachter, M., Wuenscher, M., and Chakraborty, T. (1992). A novel bacterial virulence gene in *Listeria monocytogenes* required for host cell microfilament interaction with homology to the proline-rich region of vinculin. Embo J 11, 1981-1990.

Dougan, G., Hormaeche, C.E., and Maskell, D.J. (1987). Live oral *Salmonella* vaccines: potential use of attenuated strains as carriers of heterologous antigens to the immune system. Parasite Immunol 9, 151-160.

Drams, S., Levi, S., Triller, A., and Cossart, P. (1998). Entry of *Listeria monocytogenes* into neurons occurs by cell-to-cell spread: an in vitro study. Infect Immun 66, 4461-4468.

Drevets, D.A., Sawyer, R.T., Potter, T.A., and Campbell, P.A. (1995). *Listeria monocytogenes* infects human endothelial cells by two distinct mechanisms. Infect Immun 63, 4268-4276.

Duechs, M. (2007). Construction and evaluation of *L. monocytogenes* strains as novel bacterial tumor targeting vectors. Diplom Biologe.

Ebe, Y., Hasegawa, G., Takatsuka, H., Umezu, H., Mitsuyama, M., Arakawa, M., Mukaida, N., and Naito, M. (1999). The role of Kupffer cells and regulation of neutrophil migration into the liver by macrophage inflammatory protein-2 in primary listeriosis in mice. Pathol Int 49, 519-532.

Ellermann, V., and Bang, O. (1908). Experimentelle leukämie bei hühnern. Zentralbl Bakt Abt I (Orig) 46, 595-609.

Engelbrecht, F., Chun, S.K., Ochs, C., Hess, J., Lottspeich, F., Goebel, W., and Sokolovic, Z. (1996). A new PrfA-regulated gene of *Listeria monocytogenes* encoding a small, secreted protein which belongs to the family of internalins. *Mol Microbiol* 21, 823-837.

Erbs, P., Regulier, E., Kintz, J., Leroy, P., Poitevin, Y., Exinger, F., Jund, R., and Mehtali, M. (2000). In vivo cancer gene therapy by adenovirus-mediated transfer of a bifunctional yeast cytosine deaminase/uracil phosphoribosyltransferase fusion gene. *Cancer Res* 60, 3813-3822.

Espey, M.G. (2006). Tumor macrophage redox and effector mechanisms associated with hypoxia. *Free Radic Biol Med* 41, 1621-1628.

Fattal, E., and Bochot, A. (2006). Ocular delivery of nucleic acids: antisense oligonucleotides, aptamers and siRNA. *Adv Drug Deliv Rev* 58, 1203-1223.

Fehleisen, V. (1882). Über die Züchtung von Erysipelkokken auf künstlichem Nährboden und Ihre Übertragbarkeit auf den Menschen. *Dtsch Med Wochenschr* 8, 533-554.

Fensterle, J. (personal communication).

Fensterle, J., Bergmann, B., Yone, C.L., Hotz, C., Meyer, S.R., Spreng, S., Goebel, W., Rapp, U.R., and Gentschev, I. (2008). Cancer immunotherapy based on recombinant *Salmonella enterica* serovar Typhimurium aroA strains secreting prostate-specific antigen and cholera toxin subunit B. *Cancer Gene Ther* 15, 85-93.

Fermentas first strand cDNA synthesis kit
http://www.fermentas.com/profiles/kits/pdf/coa_k1612.pdf.

Fermentas restriction digestion <http://www.fermentas.com/catalog/re/index.html>.

Ferreira, A.C., Isomoto, H., Moriyama, M., Fujioka, T., Machado, J.C., and Yamaoka, Y. (2008). *Helicobacter* and gastric malignancies. *Helicobacter* 13 Suppl 1, 28-34.

Finnzymes DyNAmo™ HS SYBR® Green qPCR Kit
http://www.finnzymes.com/pdf/dynamo_hs_sybrgreenqpcr_f410_1_9.pdf.

Fire, A., Xu, S., Montgomery, M.K., Kostas, S.A., Driver, S.E., and Mello, C.C. (1998). Potent and specific genetic interference by double-stranded RNA in *Caenorhabditis elegans*. *Nature* 391, 806-811.

Fischer, G., Brantner, H., and Platzer, P. (1975). The kininase activity of Ehrlich's ascites solid tumor after treatment with oncolytic clostridia. *Z Krebsforsch Klin Onkol Cancer Res Clin Oncol* 84, 203-206.

Forbes, N.S., Munn, L.L., Fukumura, D., and Jain, R.K. (2003). Sparse initial entrapment of systemically injected *Salmonella typhimurium* leads to heterogeneous accumulation within tumors. *Cancer Res* 63, 5188-5193.

Frentzen, A. (2007). Posttranskriptionale Regulation der Internalinexpression und alternative Internalin-unabhängige Aufnahme von *Listeria monocytogenes* in Animalzellen.

Frentzen, A. (2008). Posttranskriptionale Regulation der Internalinexpression und alternative Internalin-unabhängige Aufnahme von *Listeria monocytogenes* in Animalzellen.

Friedlos, F., Lehouritis, P., Ogilvie, L., Hedley, D., Davies, L., Bermudes, D., King, I., Martin, J., Marais, R., and Springer, C.J. (2008). Attenuated *Salmonella* targets prodrug activating enzyme carboxypeptidase G2 to mouse melanoma and human breast and colon carcinomas

for effective suicide gene therapy. *Clin Cancer Res* 14, 4259-4266.

Fujimori, M. (2006). Genetically engineered bifidobacterium as a drug delivery system for systemic therapy of metastatic breast cancer patients. *Breast Cancer* 13, 27-31.

Fujimori, M., Amano, J., and Taniguchi, S. (2002). The genus *Bifidobacterium* for cancer gene therapy. *Curr Opin Drug Discov Devel* 5, 200-203.

Fukumura, D., and Jain, R.K. (2007). Tumor microvasculature and microenvironment: targets for anti-angiogenesis and normalization. *Microvasc Res* 74, 72-84.

Gaillard, J.L., Berche, P., Mounier, J., Richard, S., and Sansonetti, P. (1987). In vitro model of penetration and intracellular growth of *Listeria monocytogenes* in the human enterocyte-like cell line Caco-2. *Infect Immun* 55, 2822-2829.

Gentschev, I., Dietrich, G., Spreng, S., Kolb-Mäurer, A., Daniels, J., Hess, J., Kaufmann, S.H.E., and Goebel, W. (2000). Delivery of protein antigens and DNA by virulence-attenuated strains of *Salmonella typhimurium* and *Listeria monocytogenes*. *Journal of Biotechnology* 83, 19-26.

Gregory, S.H., and Liu, C.C. (2000). CD8+ T-cell-mediated response to *Listeria monocytogenes* taken up in the liver and replicating within hepatocytes. *Immunol Rev* 174, 112-122.

Guinn, B.A., Kasahara, N., Farzaneh, F., Habib, N.A., Norris, J.S., and Deisseroth, A.B. (2007). Recent advances and current challenges in tumor immunology and immunotherapy. *Mol Ther* 15, 1065-1071.

Guzman, C.A., Rohde, M., Chakraborty, T., Domann, E., Hudel, M., Wehland, J., and Timmis, K.N. (1995). Interaction of *Listeria monocytogenes* with mouse dendritic cells. *Infect Immun* 63, 3665-3673.

Haller, E.M., and Brantner, H. (1979). [Enzymological examinations on *Clostridium oncolyticum* M 55 ATCC 13,732 (author's transl)]. *Zentralbl Bakteriell [Orig A]* 243, 522-527.

Hamon, M., Bierne, H., and Cossart, P. (2006). *Listeria monocytogenes*: a multifaceted model. *Nat Rev Microbiol* 4, 423-434.

Hanahan, D., and Weinberg, R.A. (2000). The hallmarks of cancer. *Cell* 100, 57-70.

Harlow, E., and Lane, D. (1999). Using Antibodies - Immunoaffinity Purification (Chapter 9), Vol Chapter 9 (Cold Spring Harbor, NY, USA, Cold Spring Harbor Laboratory Press).

Harty, J.T., Schreiber, R.D., and Bevan, M.J. (1992). CD8 T cells can protect against an intracellular bacterium in an interferon gamma-independent fashion. *Proc Natl Acad Sci U S A* 89, 11612-11616.

Heise, C., Hermiston, T., Johnson, L., Brooks, G., Sampson-Johannes, A., Williams, A., Hawkins, L., and Kirn, D. (2000). An adenovirus E1A mutant that demonstrates potent and selective systemic anti-tumoral efficacy. *Nat Med* 6, 1134-1139.

Heisig (data not shown).

Heisig, M. (2005). Übertragung von therapeutischer RNA in Tumorzellen durch *Listeria monocytogenes*. Diplom-Biologe. Institut für Mikrobiologie

Heisig, M. (unpublished data).

- Hof, H. (2003). History and epidemiology of listeriosis. *FEMS Immunol Med Microbiol* 35, 199-202.
- Hoft, D.F. (2008). Tuberculosis vaccine development: goals, immunological design, and evaluation. *Lancet* 372, 164-175.
- Hu, X., Su, F., Qin, L., Jia, W., Gong, C., Yu, F., Guo, J., and Song, E. (2006). Stable RNA interference of ErbB-2 gene synergistic with epirubicin suppresses breast cancer growth in vitro and in vivo. *Biochem Biophys Res Commun* 346, 778-785.
- Huang, B., Zhao, J., Shen, S., Li, H., He, K.L., Shen, G.X., Mayer, L., Unkeless, J., Li, D., Yuan, Y., *et al.* (2007). *Listeria monocytogenes* promotes tumor growth via tumor cell toll-like receptor 2 signaling. *Cancer Res* 67, 4346-4352.
- Huang, R.S., and Ratain, M.J. (2009). Pharmacogenetics and pharmacogenomics of anticancer agents. *CA Cancer J Clin* 59, 42-55.
- Hudis, C.A. (2007). Trastuzumab--mechanism of action and use in clinical practice. *N Engl J Med* 357, 39-51.
- Huebner, R.J., Rowe, W.P., Schatten, W.E., Smith, R.R., and Thomas, L.B. (1956). Studies on the use of viruses in the treatment of carcinoma of the cervix. *Cancer* 9, 1211-1218.
- Javier, R.T., and Butel, J.S. (2008). The history of tumor virology. *Cancer Res* 68, 7693-7706.
- Jemal, A., Siegel, R., Ward, E., Hao, Y., Xu, J., and Thun, M.J. (2009). Cancer statistics, 2009. *CA Cancer J Clin* 59, 225-249.
- Jemal, A., Siegel, R., Ward, E., Murray, T., Xu, J., and Thun, M.J. (2007). Cancer statistics, 2007. *CA Cancer J Clin* 57, 43-66.
- Jonquieres, R., Pizarro-Cerda, J., and Cossart, P. (2001). Synergy between the N- and C-terminal domains of InlB for efficient invasion of non-phagocytic cells by *Listeria monocytogenes*. *Mol Microbiol* 42, 955-965.
- Joseph, B., and Goebel, W. (2007). Life of *Listeria monocytogenes* in the host cells' cytosol. *Microbes and Infection* 9, 1188-1195.
- Joseph, B., Przybilla, K., Stuhler, C., Schauer, K., Slaghuys, J., Fuchs, T.M., and Goebel, W. (2006). Identification of *Listeria monocytogenes* genes contributing to intracellular replication by expression profiling and mutant screening. *J Bacteriol* 188, 556-568.
- Kasinskas, R.W., and Forbes, N.S. (2006). *Salmonella typhimurium* specifically chemotax and proliferate in heterogeneous tumor tissue in vitro. *Biotechnol Bioeng* 94, 710-721.
- Kasinskas, R.W., and Forbes, N.S. (2007). *Salmonella typhimurium* Lacking Ribose Chemoreceptors Localize in Tumor Quiescence and Induce Apoptosis. *Cancer Res* 67, 3201-3209.
- Kaufmann, S.H. (1993). Immunity to intracellular bacteria. *Annu Rev Immunol* 11, 129-163.
- Kerrigan, S., and Brooks, D.E. (1999). Immunochemical extraction and detection of LSD in whole blood. *J Immunol Methods* 224, 11-18.
- Kershaw, M.H., Jackson, J.T., Haynes, N.M., Teng, M.W.L., Moeller, M., Hayakawa, Y., Street, S.E., Cameron, R., Tanner, J.E., Trapani, J.A., *et al.* (2004). Gene-Engineered T

Cells as a Superior Adjuvant Therapy for Metastatic Cancer. *J Immunol* 173, 2143-2150.

Khelef, N., Lecuit, M., Bierne, H., and Cossart, P. (2006). Species specificity of the *Listeria monocytogenes* InlB protein. *Cell Microbiol* 8, 457-470.

Kim, S.H., Castro, F., Paterson, Y., and Gravekamp, C. (2009). High efficacy of a *Listeria*-based vaccine against metastatic breast cancer reveals a dual mode of action. *Cancer Res* 69, 5860-5866.

Kimura, N.T., Taniguchi, S., Aoki, K., and Baba, T. (1980). Selective localization and growth of *Bifidobacterium bifidum* in mouse tumors following intravenous administration. *Cancer Res* 40, 2061-2068.

kindly provided by Thilo Fuchs.

Klausner, R.D. (1999). Cancer, genomics, and the National Cancer Institute. *J Clin Invest* 104 Suppl, S15-17.

Kleef, R., and Hager, D. (2006). Fever, Pyrogens and Cancer (Landes Bioscience).

Klein, E.A., and Silverman, R. (2008). Inflammation, infection, and prostate cancer. *Curr Opin Urol* 18, 315-319.

Kocks, C., Gouin, E., Tabouret, M., Berche, P., Ohayon, H., and Cossart, P. (1992). *L. monocytogenes*-induced actin assembly requires the actA gene product, a surface protein. *Cell* 68, 521-531.

Kuhn, M., Kathariou, S., and Goebel, W. (1988). Hemolysin supports survival but not entry of the intracellular bacterium *Listeria monocytogenes*. *Infect Immun* 56, 79-82.

Kumar, R., and Yarmand-Bagheri, R. (2001). The role of HER2 in angiogenesis. *Semin Oncol* 28, 27-32.

Kurreck, J. (2009). RNA interference: from basic research to therapeutic applications. *Angew Chem Int Ed Engl* 48, 1378-1398.

Laemmli, U.K. (1970). Cleavage of Structural Proteins during the Assembly of the Head of Bacteriophage T4. *Nature* 227, 680-685.

Lambin, P., Theys, J., Landuyt, W., Rijken, P., van der Kogel, A., van der Schueren, E., Hodgkiss, R., Fowler, J., Nuyts, S., de Bruijn, E., *et al.* (1998). Colonisation of *Clostridium* in the body is restricted to hypoxic and necrotic areas of tumours. *Anaerobe* 4, 183-188.

Lecuit, M., Dramsi, S., Gottardi, C., Fedor-Chaiken, M., Gumbiner, B., and Cossart, P. (1999). A single amino acid in E-cadherin responsible for host specificity towards the human pathogen *Listeria monocytogenes*. *Embo J* 18, 3956-3963.

Lee, C.H., Wu, C.L., and Shiau, A.L. (2004). Endostatin gene therapy delivered by *Salmonella choleraesuis* in murine tumor models. *J Gene Med* 6, 1382-1393.

Lee, C.H., Wu, C.L., Tai, Y.S., and Shiau, A.L. (2005). Systemic administration of attenuated *Salmonella choleraesuis* in combination with cisplatin for cancer therapy. *Mol Ther* 11, 707-716.

Lengyel, E., Prectel, D., Resau, J.H., Gauger, K., Welk, A., Lindemann, K., Salanti, G., Richter, T., Knudsen, B., Vande Woude, G.F., *et al.* (2005). C-Met overexpression in node-positive breast cancer identifies patients with poor clinical outcome independent of Her2/neu.

Int J Cancer 113, 678-682.

Lewis, J.D., Reilly, B.D., and Bright, R.K. (2003). Tumor-associated antigens: from discovery to immunity. *Int Rev Immunol* 22, 81-112.

Li, X., Fu, G.-F., Fan, Y.-R., Liu, W.-H., Liu, X.-J., Wang, J.-J., and Xu, G.-X. (2003). *Bifidobacterium adolescentis* as a delivery system of endostatin for cancer gene therapy: Selective inhibitor of angiogenesis and hypoxic tumor growth. *Cancer Gene Ther* 10, 105-111.

Linde, K., Abraham, A.A., and Beer, J. (1991). Stable *Listeria monocytogenes* live vaccine candidate strains with graded attenuation on the mouse model. *Vaccine* 9, 101-105.

Lockyer, C.R., and Gillatt, D.A. (2001). BCG immunotherapy for superficial bladder cancer. *J R Soc Med* 94, 119-123.

Loeffler, D.I.M., Schoen, C.U., Goebel, W., and Pilgrim, S. (2006). Comparison of Different Live Vaccine Strategies In Vivo for Delivery of Protein Antigen or Antigen-Encoding DNA and mRNA by Virulence-Attenuated *Listeria monocytogenes*. *Infect Immun* 74, 3946-3957.

Loeffler, M., Le'Negrate, G., Krajewska, M., and Reed, J.C. (2008). Inhibition of tumor growth using salmonella expressing Fas ligand. *J Natl Cancer Inst* 100, 1113-1116.

Loessner, M.J., Inman, R.B., Lauer, P., and Calendar, R. (2000). Complete nucleotide sequence, molecular analysis and genome structure of bacteriophage A118 of *Listeria monocytogenes*: implications for phage evolution. *Mol Microbiol* 35, 324-340.

Low, K.B., Ittensohn, M., Le, T., Platt, J., Sodi, S., Amoss, M., Ash, O., Carmichael, E., Chakraborty, A., Fischer, J., *et al.* (1999). Lipid A mutant *Salmonella* with suppressed virulence and TNF α induction retain tumor-targeting in vivo. *Nat Biotechnol* 17, 37-41.

Lütkenhaus, K. (2005). Bakterielle Tumorthherapie im Melanommodell. Diploma thesis.

Mackaness, G.B. (1962). Cellular resistance to infection. *J Exp Med* 116, 381-406.

Magee, A.M., MacLean, D., Gray, J.C., and Kavanagh, T.A. (2007). Disruption of essential plastid gene expression caused by T7 RNA polymerase-mediated transcription of plastid transgenes during early seedling development. *Transgenic Res* 16, 415-428.

Malmgren, R.A., and Flanigan, C.C. (1955). Localization of the vegetative form of *Clostridium tetani* in mouse tumours following intravenous spore administration. *Cancer Res* 15, 473-478.

Marco, A.J., Prats, N., Ramos, J.A., Briones, V., Blanco, M., Dominguez, L., and Domingo, M. (1992). A microbiological, histopathological and immunohistological study of the intragastric inoculation of *Listeria monocytogenes* in mice. *J Comp Pathol* 107, 1-9.

McCann, A.H., Dervan, P.A., O'Regan, M., Codd, M.B., Gullick, W.J., Tobin, B.M., and Carney, D.N. (1991). Prognostic significance of c-erbB-2 and estrogen receptor status in human breast cancer. *Cancer Res* 51, 3296-3303.

McCormick, F. (2003). Cancer-specific viruses and the development of ONYX-015. *Cancer Biol Ther* 2, S157-160.

Mengaud, J., Ohayon, H., Gounon, P., Mège, R.-M., and Cossart, P. (1996). E-Cadherin Is the Receptor for Internalin, a Surface Protein Required for Entry of *L. monocytogenes* into Epithelial Cells. *Cell* 84, 923-932.

- Mielke, M.E., Ehlers, S., and Hahn, H. (1988). T-cell subsets in delayed-type hypersensitivity, protection, and granuloma formation in primary and secondary *Listeria* infection in mice: superior role of Lyt-2+ cells in acquired immunity. *Infect Immun* 56, 1920-1925.
- Mineta, T., Rabkin, S.D., and Martuza, R.L. (1994). Treatment of malignant gliomas using ganciclovir-hypersensitive, ribonucleotide reductase-deficient herpes simplex viral mutant. *Cancer Res* 54, 3963-3966.
- Mineta, T., Rabkin, S.D., Yazaki, T., Hunter, W.D., and Martuza, R.L. (1995). Attenuated multi-mutated herpes simplex virus-1 for the treatment of malignant gliomas. *Nat Med* 1, 938-943.
- Minton, N.P. (2003). Clostridia in cancer therapy. *Nature reviews - Microbiology* 1, 237-242.
- Morales, A., Eiding, D., and Bruce, A.W. (1976). Intracavitary bacillus calmette-guerin in the treatment of superficial bladder tumors. *The Journal of Urology* 116, 180-183.
- Mose, J.R., Fischer, G., and Mobascherie, T.B. (1972). [Bacterial kinases and their physiological importance. I. Studies on Clostridia strains]. *Zentralbl Bakteriol [Orig A]* 219, 530-541.
- Munkonge, F.M., Dean, D.A., Hillery, E., Griesenbach, U., and Alton, E.W. (2003). Emerging significance of plasmid DNA nuclear import in gene therapy. *Adv Drug Deliv Rev* 55, 749-760.
- Neller, M.A., Lopez, J.A., and Schmidt, C.W. (2008). Antigens for cancer immunotherapy. *Semin Immunol* 20, 286-295.
- Nemunaitis, J., Cunningham, C., Senzer, N., Kuhn, J., Cramm, J., Litz, C., Cavagnolo, R., Cahill, A., Clairmont, C., and Szol, M. (2003). Pilot trial of genetically modified, attenuated *Salmonella* expressing the *E. coli* cytosine deaminase gene in refractory cancer patients. *Cancer Gene Ther* 10, 737-744.
- Nishikawa, H., Sato, E., Briones, G., Chen, L.M., Matsuo, M., Nagata, Y., Ritter, G., Jager, E., Nomura, H., Kondo, S., *et al.* (2006). In vivo antigen delivery by a *Salmonella typhimurium* type III secretion system for therapeutic cancer vaccines. *J Clin Invest* 116, 1946-1954.
- Nuyts, S., Van Mellaert, L., Theys, J., Landuyt, W., Lambin, P., and Anne, J. (2002). Clostridium spores for tumor-specific drug delivery. *Anticancer Drugs* 13, 115-125.
- Ohno, K., Sawai, K., Iijima, Y., Levin, B., and Meruelo, D. (1997). Cell-specific targeting of Sindbis virus vectors displaying IgG-binding domains of protein A. *Nat Biotechnol* 15, 763-767.
- Opresko, L.K., Chang, C.P., Will, B.H., Burke, P.M., Gill, G.N., and Wiley, H.S. (1995). Endocytosis and lysosomal targeting of epidermal growth factor receptors are mediated by distinct sequences independent of the tyrosine kinase domain. *J Biol Chem* 270, 4325-4333.
- Otani, T., Ichii, T., Aono, S., and Takeichi, M. (2006). Cdc42 GEF Tuba regulates the junctional configuration of simple epithelial cells. *J Cell Biol* 175, 135-146.
- Paglia, P., Medina, E., Arioli, I., Guzman, C.A., and Colombo, M.P. (1998). Gene transfer in dendritic cells, induced by oral DNA vaccination with *Salmonella typhimurium*, results in protective immunity against a murine fibrosarcoma. *Blood* 92, 3172-3176.
- Paredes, C.J., Alsaker, K.V., and Papoutsakis, E.T. (2005). A comparative genomic view of

clostridial sporulation and physiology. *Nat Rev Microbiol* 3, 969-978.

Parker R. C., Plumber H. C., Siebenmann C. O., and Chapman, M.G. (1947). Effect of histolytic infection and toxin on transplantable mouse tumours. *Proc Soc Exp Biol* 66, 461–465.

Parkin, D.M. (2006). The global health burden of infection-associated cancers in the year 2002. *Int J Cancer* 118, 3030-3044.

Paterson, Y., and Maciag, P.C. (2005). *Listeria*-based vaccines for cancer treatment. *Curr Opin Mol Ther* 7, 454-460.

Pawelek, J.M., Low, K.B., and Bermudes, D. (1997). Tumor-targeted *Salmonella* as a Novel Anticancer Vector. *Cancer Res* 57, 4537-4544.

Pentecost, M., Otto, G., Theriot, J.A., and Amieva, M.R. (2006). *Listeria monocytogenes* invades the epithelial junctions at sites of cell extrusion. *PLoS Pathog* 2, e3.

Pilgrim, S. (personal communication).

Pilgrim, S., Stritzker, J., Schoen, C., Kolb-Maurer, A., Geginat, G., Loessner, M.J., Gentschev, I., and Goebel, W. (2003). Bactofection of mammalian cells by *Listeria monocytogenes*: improvement and mechanism of DNA delivery. *Gene Ther* 10, 2036-2045.

Pozner-Moulis, S., Pappas, D.J., and Rimm, D.L. (2006). Met, the hepatocyte growth factor receptor, localizes to the nucleus in cells at low density. *Cancer Res* 66, 7976-7982.

Pron, B., Boumaila, C., Jaubert, F., Sarnacki, S., Monnet, J.P., Berche, P., and Gaillard, J.L. (1998). Comprehensive study of the intestinal stage of listeriosis in a rat ligated ileal loop system. *Infect Immun* 66, 747-755.

Pulaski, B.A., and Ostrand-Rosenberg, S. (1998). Reduction of Established Spontaneous Mammary Carcinoma Metastases following Immunotherapy with Major Histocompatibility Complex Class II and B7.1 Cell-based Tumor Vaccines. *Cancer Res* 58, 1486-1493.

Pushparaj, P.N., Aarthi, J.J., Manikandan, J., and Kumar, S.D. (2008). siRNA, miRNA, and shRNA: in vivo applications. *J Dent Res* 87, 992-1003.

QIAGEN DNeasy Blood & Tissue Kit
http://www1.qiagen.com/HB/DNeasyBloodTissueKit_EN.

QIAGEN Plasmid Kit http://www1.qiagen.com/HB/QIAGENPlasmidPurification_EN.

QIAGEN RNAeasy Mini Kit http://www1.qiagen.com/HB/RNeasyMiniKit_EN.

QIAGEN RNase-free DNase Set http://www1.qiagen.com/HB/RNaseFreeDNaseSet_EN.

QIAquick PCR Purification Kit http://www1.qiagen.com/HB/QIAquickGelExtractionKit_EN.

Qualmann, B., and Kessels, M.M. (2002). Endocytosis and the cytoskeleton. *Int Rev Cytol* 220, 93-144.

Raffelsbauer, D., Bubert, A., Engelbrecht, F., Scheinpflug, J., Simm, A., Hess, J., Kaufmann, S.H., and Goebel, W. (1998). The gene cluster *inlC2DE* of *Listeria monocytogenes* contains additional new internalin genes and is important for virulence in mice. *Mol Gen Genet* 260, 144-158.

- Rajabian, T., Gavicherla, B., Heisig, M., Muller-Altrock, S., Goebel, W., Gray-Owen, S.D., and Ireton, K. (2009). The bacterial virulence factor InlC perturbs apical cell junctions and promotes cell-to-cell spread of *Listeria*. *Nat Cell Biol*.
- Rajalingam, K., Oswald, M., Gottschalk, K., and Rudel, T. (2007). Smac/DIABLO is required for effector caspase activation during apoptosis in human cells. *Apoptosis* 12, 1503-1510.
- Ratain, M.J., and Relling, M.V. (2001). Gazing into a crystal ball-cancer therapy in the post-genomic era. *Nat Med* 7, 283-285.
- Reichert, J.M., Rosensweig, C.J., Faden, L.B., and Dewitz, M.C. (2005). Monoclonal antibody successes in the clinic. *Nat Biotechnol* 23, 1073-1078.
- Richman, D.D., Cleveland, P.H., Oxman, M.N., and Johnson, K.M. (1982). The binding of staphylococcal protein A by the sera of different animal species. *J Immunol* 128, 2300-2305.
- Richter, P. (1896). Leukemia and Erysipel. *Charite-annalens* 21, 299-309.
- Rogers, H.W., and Unanue, E.R. (1993). Neutrophils are involved in acute, nonspecific resistance to *Listeria monocytogenes* in mice. *Infect Immun* 61, 5090-5096.
- Rosenberg, S.A. (2001). Progress in human tumour immunology and immunotherapy. *Nature* 411, 380-384.
- Rosenman R. Pixel Quantification - <http://www.richardrosenman.com/software/downloads/>.
- Rous, P. (1910). A TRANSMISSIBLE AVIAN NEOPLASM. (SARCOMA OF THE COMMON FOWL.). *J Exp Med* 12, 696-705.
- Rous, P. (1911). A SARCOMA OF THE FOWL TRANSMISSIBLE BY AN AGENT SEPARABLE FROM THE TUMOR CELLS. *J Exp Med* 13, 397-411.
- Rusnak, D.W., Affleck, K., Cockerill, S.G., Stubberfield, C., Harris, R., Page, M., Smith, K.J., Guntrip, S.B., Carter, M.C., Shaw, R.J., *et al.* (2001). The characterization of novel, dual ErbB-2/EGFR, tyrosine kinase inhibitors: potential therapy for cancer. *Cancer Res* 61, 7196-7203.
- Ryan, R.M., Green, J., and Lewis, C.E. (2006). Use of bacteria in anti-cancer therapies. *Bioessays* 28, 84-94.
- Salazar, M.A., Kwiatkowski, A.V., Pellegrini, L., Cestra, G., Butler, M.H., Rossman, K.L., Serna, D.M., Sondek, J., Gertler, F.B., and De Camilli, P. (2003). Tuba, a novel protein containing bin/amphiphysin/Rvs and Dbl homology domains, links dynamin to regulation of the actin cytoskeleton. *J Biol Chem* 278, 49031-49043.
- Sasaki, T., Fujimori, M., Hamaji, Y., Hama, Y., Ito, K., Amano, J., and Taniguchi, S. (2006). Genetically engineered *Bifidobacterium longum* for tumor-targeting enzyme-prodrug therapy of autochthonous mammary tumors in rats. *Cancer Sci* 97, 649-657.
- Schafer, R., Portnoy, D.A., Brassell, S.A., and Paterson, Y. (1992). Induction of a cellular immune response to a foreign antigen by a recombinant *Listeria monocytogenes* vaccine. *J Immunol* 149, 53-59.
- Schietinger, A., Philip, M., and Schreiber, H. (2008). Specificity in cancer immunotherapy. *Semin Immunol* 20, 276-285.
- Schmidt, W., Fabricius, E.M., and Schneeweiss, U. (2006). The tumour-Clostridium

phenomenon: 50 years of developmental research (Review). *Int J Oncol* 29, 1479-1492.

Schneider, C., Newman, R.A., Sutherland, D.R., Asser, U., and Greaves, M.F. (1982). A one-step purification of membrane proteins using a high efficiency immunomatrix. *J Biol Chem* 257, 10766-10769.

Schoen, C., Kolb-Maurer, A., Geginat, G., Löffler, D., Bergmann, B., Stritzker, J., Szalay, A.A., Pilgrim, S., and Goebel, W. (2005). Bacterial delivery of functional messenger RNA to mammalian cells. *Cell Microbiol* 7, 709-724.

Schrama, D., Reisfeld, R.A., and Becker, J.C. (2006). Antibody targeted drugs as cancer therapeutics. *Nat Rev Drug Discov* 5, 147-159.

Schuchat, A., Swaminathan, B., and Broome, C.V. (1991). Epidemiology of human listeriosis. *Clin Microbiol Rev* 4, 169-183.

Sears, R.C., and Nevins, J.R. (2002). Signaling networks that link cell proliferation and cell fate. *J Biol Chem* 277, 11617-11620.

Seeliger, H.P., Winkhaus-Schindl, I., Andries, L., and Viebahn, A. (1965). [The isolation of *Listeria monocytogenes* from fecal, sewage sludge and soil samples (with reference to the epidemiology of listeriosis)]. *Pathol Microbiol (Basel)* 28, 590-601.

Selvaraj, P., Yerra, A., Tien, L., and Shashidharamurthy, R. (2008). Custom designing therapeutic cancer vaccines: delivery of immunostimulatory molecule adjuvants by protein transfer. *Hum Vaccin* 4, 384-388.

Shen, Y., Naujokas, M., Park, M., and Ireton, K. (2000). InlB-dependent internalization of *Listeria* is mediated by the Met receptor tyrosine kinase. *Cell* 103, 501-510.

Southam, C.M., and Moore, A.E. (1952). Clinical studies of viruses as antineoplastic agents with particular reference to Egypt 101 virus. *Cancer* 5, 1025-1034.

St Jean, A.T., Zhang, M., and Forbes, N.S. (2008). Bacterial therapies: completing the cancer treatment toolbox. *Curr Opin Biotechnol* 19, 511-517.

Stark, G.R., Kerr, I.M., Williams, B.R., Silverman, R.H., and Schreiber, R.D. (1998). How cells respond to interferons. *Annu Rev Biochem* 67, 227-264.

Stojdl, D.F., Lichty, B., Knowles, S., Marius, R., Atkins, H., Sonenberg, N., and Bell, J.C. (2000). Exploiting tumor-specific defects in the interferon pathway with a previously unknown oncolytic virus. *Nat Med* 6, 821-825.

Stritzker, J., and Goebel, W. (2004). *Listeria monocytogenes* infection-dependent transfer of exogenously added DNA to fibroblast COS-1 cells. *Mol Genet Genomics* 272, 497-503.

Stritzker, J., Janda, J., Schoen, C., Taupp, M., Pilgrim, S., Gentschev, I., Schreier, P., Geginat, G., and Goebel, W. (2004). Growth, Virulence, and Immunogenicity of *Listeria monocytogenes* aro Mutants. *Infect Immun* 72, 5622-5629.

Stritzker, J., Pilgrim, S., Szalay, A.A., and Goebel, W. (2008). Prodrug converting enzyme gene delivery by *L. monocytogenes*. *BMC Cancer* 8, 94.

Stritzker, J., Weibel, S., Hill, P.J., Oelschlaeger, T.A., Goebel, W., and Szalay, A.A. (2007). Tumor-specific colonization, tissue distribution, and gene induction by probiotic *Escherichia coli* Nissle 1917 in live mice. *International Journal of Medical Microbiology* 297, 151-162.

- Takeshita, F., and Ochiya, T. (2006). Therapeutic potential of RNA interference against cancer. *Cancer Sci* 97, 689-696.
- Tang, Z., Zhou, H., Zhao, G., Chai, L., Zhou, M., Lu, J., Liu, K., Havas, H., and Nauts, H. (1991). Preliminary result of mixed bacterial vaccine as adjuvant treatment of hepatocellular carcinoma. *Medical Oncology* 8, 23-28.
- Thomas, M., Lu, J.J., Chen, J., and Klibanov, A.M. (2007). Non-viral siRNA delivery to the lung. *Adv Drug Deliv Rev* 59, 124-133.
- Thompson, R.J., Bouwer, H.G., Portnoy, D.A., and Frankel, F.R. (1998). Pathogenicity and immunogenicity of a *Listeria monocytogenes* strain that requires D-alanine for growth. *Infect Immun* 66, 3552-3561.
- Thor, A.D., Schwartz, L.H., Koerner, F.C., Edgerton, S.M., Skates, S.J., Yin, S., McKenzie, S.J., Panicali, D.L., Marks, P.J., Fingert, H.J., *et al.* (1989). Analysis of c-erbB-2 expression in breast carcinomas with clinical follow-up. *Cancer Res* 49, 7147-7152.
- Tijhaar, E.J., Zheng-Xin, Y., Karlas, J.A., Meyer, T.F., Stukart, M.J., Osterhaus, A.D., and Mooi, F.R. (1994). Construction and evaluation of an expression vector allowing the stable expression of foreign antigens in a *Salmonella typhimurium* vaccine strain. *Vaccine* 12, 1004-1011.
- Tiu, R.V., Mountantonakis, S.E., Dunbar, A.J., and Schreiber, M.J., Jr. (2007). Tumor lysis syndrome. *Semin Thromb Hemost* 33, 397-407.
- Toso, J.F., Gill, V.J., Hwu, P., Marincola, F.M., Restifo, N.P., Schwartzentruber, D.J., Sherry, R.M., Topalian, S.L., Yang, J.C., Stock, F., *et al.* (2002). Phase I study of the intravenous administration of attenuated *Salmonella typhimurium* to patients with metastatic melanoma. *J Clin Oncol* 20, 142-152.
- Vassaux, G., Nitchau, J., Jezzard, S., and Lemoine, N.R. (2006). Bacterial gene therapy strategies. *J Pathol* 208, 290-298.
- Vazquez-Boland, J.A., Kuhn, M., Berche, P., Chakraborty, T., Dominguez-Bernal, G., Goebel, W., Gonzalez-Zorn, B., Wehland, J., and Kreft, J. (2001). *Listeria* pathogenesis and molecular virulence determinants. *Clin Microbiol Rev* 14, 584-640.
- Venter, D.J., Tuzi, N.L., Kumar, S., and Gullick, W.J. (1987). Overexpression of the c-erbB-2 oncoprotein in human breast carcinomas: immunohistological assessment correlates with gene amplification. *Lancet* 2, 69-72.
- Volpers, C., Thirion, C., Biermann, V., Hussmann, S., Kewes, H., Dunant, P., von der Mark, H., Herrmann, A., Kochanek, S., and Lochmuller, H. (2003). Antibody-mediated targeting of an adenovirus vector modified to contain a synthetic immunoglobulin g-binding domain in the capsid. *J Virol* 77, 2093-2104.
- Wallecha, A., Maciag, P.C., Rivera, S., Paterson, Y., and Shahabi, V. (2009). Construction and characterization of an attenuated *Listeria monocytogenes* strain for clinical use in cancer immunotherapy. *Clin Vaccine Immunol* 16, 96-103.
- Wang, F., Ma, Y., Barrett, J.W., Gao, X., Loh, J., Barton, E., Virgin, H.W., and McFadden, G. (2004). Disruption of Erk-dependent type I interferon induction breaks the myxoma virus species barrier. *Nat Immunol* 5, 1266-1274.
- Wang, L., Pan, L., Shi, L., Sun, Y., Zhang, Y., and Zhou, D. (1999). [Roles of bifidobacterium

on prevention of experimental colorectal carcinoma and induction of apoptosis]. *Zhonghua Yu Fang Yi Xue Za Zhi* 33, 337-339.

Wang, R.F., and Rosenberg, S.A. (1999). Human tumor antigens for cancer vaccine development. *Immunol Rev* 170, 85-100.

Warnberg, F., White, D., Anderson, E., Knox, F., Clarke, R.B., Morris, J., and Bundred, N.J. (2006). Effect of a farnesyl transferase inhibitor (R115777) on ductal carcinoma in situ of the breast in a human xenograft model and on breast and ovarian cancer cell growth in vitro and in vivo. *Breast Cancer Res* 8, R21.

Webb, H.E., Wetherley-Mein, G., Smith, C.E., and McMahon, D. (1966). Leukaemia and neoplastic processes treated with Langat and Kyasanur Forest disease viruses: a clinical and laboratory study of 28 patients. *Br Med J* 1, 258-266.

Wei, M.Q., Mengesha, A., Good, D., and Anne, J. (2008a). Bacterial targeted tumour therapy-dawn of a new era. *Cancer Lett* 259, 16-27.

Wei, M.Q., Ren, R., Good, D., and Anne, J. (2008b). Clostridial spores as live 'Trojan horse' vectors for cancer gene therapy: comparison with viral delivery systems. *Genet Vaccines Ther* 6, 8.

Weinberg, R.A. (2006). *The Biology of Cancer*.

Whitehead, K.A., Langer, R., and Anderson, D.G. (2009). Knocking down barriers: advances in siRNA delivery. *Nat Rev Drug Discov* 8, 129-138.

WHO (2008). *World health statistics (WHO)*, pp. 112.

Wood, S., Maroushek, N., and Czuprynski, C.J. (1993). Multiplication of *Listeria monocytogenes* in a murine hepatocyte cell line. *Infect Immun* 61, 3068-3072.

Wuenschel, M.D., Kohler, S., Goebel, W., and Chakraborty, T. (1991). Gene disruption by plasmid integration in *Listeria monocytogenes*: insertional inactivation of the listeriolysin determinant *lisA*. *Mol Gen Genet* 228, 177-182.

Xu, Y.F., Zhu, L.P., Hu, B., Fu, G.F., Zhang, H.Y., Wang, J.J., and Xu, G.X. (2006). A new expression plasmid in *Bifidobacterium longum* as a delivery system of endostatin for cancer gene therapy. *Cancer Gene Ther* 14, 151-157.

Yarden, Y. (2001). Biology of HER2 and Its Importance in Breast Cancer. *Oncology* 61, 1-13.

Yazawa, K., Fujimori, M., Nakamura, T., Sasaki, T., Amano, J., Kano, Y., and Taniguchi, S. (2001). *Bifidobacterium longum* as a delivery system for gene therapy of chemically induced rat mammary tumors. *Breast Cancer Res Treat* 66, 165-170.

Yu, Y.A., Shabahang, S., Timiryasova, T.M., Zhang, Q., Beltz, R., Gentschev, I., Goebel, W., and Szalay, A.A. (2004). Visualization of tumors and metastases in live animals with bacteria and vaccinia virus encoding light-emitting proteins. *Nat Biotechnol* 22, 313-320.

Zhao, M., Yang, M., Li, X.M., Jiang, P., Baranov, E., Li, S., Xu, M., Penman, S., and Hoffman, R.M. (2005). Tumor-targeting bacterial therapy with amino acid auxotrophs of GFP-expressing *Salmonella typhimurium*. *Proc Natl Acad Sci U S A* 102, 755-760.

Zhao, M., Yang, M., Ma, H., Li, X., Tan, X., Li, S., Yang, Z., and Hoffman, R.M. (2006). Targeted therapy with a *Salmonella typhimurium* leucine-arginine auxotroph cures orthotopic human breast tumors in nude mice. *Cancer Res* 66, 7647-7652.

9 Appendix

9.1 Abbreviations

5-FC	5-Fluorocytosine
5-FU	5-Fluorouracil
5-FUMP	5-Fluorouridinemonophosphate
aa	amino-acid
<i>actA</i>	actin-assembly inducing protein precursor; LMO00204
<i>aroA</i>	3-deoxy-D-arabino-heptulosonate 7-phosphate synthase; LMO01600
ATCC	American tissue type culture collection
BCG	<i>Mycobacterium bovis</i> BCG
beads	Dynabeads® protein A (Invitrogen)
bp	basepair
CEA	carcinoembryonic antigen
CMV	Cytomegalovirus
DMP	Dimethyl pimelinediimidate dihydrochloride
DNA	deoxyribonucleic acid
dsRNA	double strand RNA
E-cadherin	epithelial cadherin
EGFP	enhanced green fluorescent protein
EGFR	epithelial growth factor receptor
GFP	green fluorescent protein
GST	glutathione S-transferase
h	hour
HBV	Hepatitis B virus
HER2/neu (ErbB2)	Human epidermal growth factor receptor 2
HGF/SF	hepatocyte growth factor / scatter factor
HHV-8	Human herpes virus type 8
HPV	Human papilloma virus
HTLV-1	Human T lymphocyte virus type 1
i.v.	intravenous
<i>inIA</i>	Internalin A; LMO00433
<i>inIB</i>	Internalin B; LMO00434
<i>inIC</i>	Internalin C; LMO01786
<i>inIGHE</i>	Internalin G, H, E; LMO00262/ LMO00263/ LMO00264

<i>int</i>	putative integrase [Bacteriophage A118]; LMO02332
IPTG	Isopropyl β -D-1-thiogalactopyranoside
IRES	internal ribosome entry site
IS	immune system
LD ₅₀	median lethal dose
LDH	lactate dehydrogenase
Lm- <i>aroA</i> ⁺ -spa ⁺	<i>L. monocytogenes</i> Δ trpS/inlA/inlB /int::P _{hly} -spa x pFlo-trpS
Lm-spa ⁻	<i>L. monocytogenes</i> Δ aroA/trpS/inlA/inlB / x pFlo-trpS
Lm-spa ⁺	<i>L. monocytogenes</i> Δ aroA/trpS/inlA/inlB /int::P _{hly} -spa x pFlo-trpS
MAPK	mitogen-activated protein kinase pathway
mcs	multiple cloning site
MET/HGFR	mesenchymal-epithelial transition factor/hepatocyte growth factor receptor
min	minute
M-MuLV RT	Maloney Murine Leukemia Virus reverse transcriptase
n.a.	not assessed
NK	natural killer cells
o/n	over night
p.i.	post infection
P _{actA}	<i>actA</i> promotor
PBS	phosphate buffered saline
PBST	phosphate buffered saline, 0.05 % Tween 20
PBSt	phosphate buffered saline, 0.02 % Tween 20
PCR	polymerase chain reaction
PMSF	phenylmethanesulphonylfluoride
P _{T7}	T7RNAP promotor
qRT-PCR	quantitative real time PCR
RNA	ribonucleic acid
RNAi	RNA interference
rpm	revolutions per minute
RT	room temperature (approximately 23°C)
RTK	receptor-tyrosine-kinase
<i>S. choleraesius</i>	<i>Salmonella enterica</i> serovar choleraesius
<i>S. typhi</i>	<i>Salmonella enterica</i> serovar typhi
<i>S. typhimurium</i>	<i>Salmonella enterica</i> serovar typhimurium
s.c.	subcutaneous
scFv	single chain fragment

SCID	Severe combined immunodeficiency
SDS	sodium-dodecylsulfate
shRNA	short hairpin RNAs
SMAC/DIABLO	second mitochondria-derived activator of caspases
ssRNA	single strand RNA
T7RNAP	T7 RNA polymerase
TAA	tumor associated antigen
<i>trpS</i>	tryptophanyl-tRNA synthetase; LMO02198
u	unit (enzyme amount required to digest 1µmol of DNA per min)
VEGF	vascular endothelial growth factor
wt	wildtype

9.II Publications

"The bacterial virulence factor InlC perturbs apical cell junctions and promotes cell-to-cell spread of *Listeria*."

Rajabian T, Gavicherla B, Heisig M, Müller-Altrock S, Goebel W, Gray-Owen SD, Ireton K. Nat Cell Biol. 2009 Sep 20. [Epub ahead of print]

"Improvement of the live vaccine strain *Salmonella enterica* serovar *Typhi* Ty21a for antigen delivery via the hemolysin secretion system of *Escherichia coli*."

Hotz C, Fensterle J, Goebel W, Meyer SR, Kirchgraber G, Heisig M, Fürer A, Dietrich G, Rapp UR, Gentschev I. Int J Med Microbiol. 2009 Feb;299(2):109-19.

"Regression of advanced human prostate tumors and metastases in nude mice after treatment with the recombinant oncolytic vaccinia virus GLV-1h68."

Ivaylo Gentschev, Elisabeth Hofmann, Ulrike Donat, Stephanie Weibel, Marion Adelfinger, Martin Heisig, Nanhai Chen, Yong A. Yu, Jochen Stritzker and Aladar A. Szalay (in revision)

"Antibody-mediated tumor cell targeting of *Listeria monocytogenes* triggering InlAB independent internalization (of tumor cells)."

Martin Heisig, Alexa Frentzen, Birgit Bergmann, Katharina Galmbacher, Ivaylo Gentschev, Christian Hotz, Christoph Schoen, Jochen Stritzker, Joachim Fensterle, Ulf R Rapp and Werner Goebel (in submission)

"Targeted depletion of macrophages and block of tumor growth by attenuated Shigella in breast cancer."

Katharina Galmbacher, Christian Hotz, Martin Heisig, Joerg Wischhusen, Antoine Galmiche, Birgit Bergmann, Ivaylo Gentshev, Werner Goebel, Ulf R. Rapp and Joachim Fensterle (in submission)

9.III Curriculum Vitae

Personal Data

Name	Martin Heisig
Date of birth	22.03.1980
Place of birth	Fulda, Germany
Nationality	German

Academic Education

Jun 2005 – Sep 2009	PhD thesis (Institute of medical irradiation and cell research, University Hospital Wuerzburg, Germany) Thesis: "Development of Listeria monocytogenes as therapeutic agent for treatment of cancer" Supervisor: Prof. Dr. Werner Goebel
May 2005	Diploma grade: outstanding ("sehr gut")
Sep 2004 - May 2005	Diploma thesis (Department of Microbiology, University of Wuerzburg, Germany) Thesis: "Delivery of therapeutic RNAs into tumor cells by Listeria monocytogenes" Supervisor: Prof. Dr. Werner Goebel
May 1999 – May 2005	Diploma studies of Biology (University of Wuerzburg, Germany) main subject: microbiology minor subjects: biochemistry, cell and developmental biology

10 Acknowledgments

I wish to express my gratitude to the following persons:

- Prof. Dr. Werner Goebel for the opportunity to work on this fascinating project of targeted bacterial tumor therapy. His scientific support promoted the realization of this thesis while still encouraging independent research.
- Prof. Dr. Ulf Rapp for the permission to work in his institute. His suggestions based on the deep knowledge of tumor biology expanded the focus of this thesis. Especially I want to thank for the faith and trust he gave to me in scientific and non-scientific issues.
- PD Dr. Ivaylo Gentshev and Dr. Joachim Fensterle for a multitude of fruitful discussions and meetings. Without your support and advise this thesis would not have developed this way.
- Prof. Dr. Werner Goebel, Prof. Dr. Ulf Rapp and PD Dr. Ivaylo Gentshev for their agreement to review this thesis and being part of my doctorate committee.
- Dr. Birgit Bergmann for her constant support during the thesis. She always found the time to help if necessary. In particular I want to thank Dr. Christian Hotz for critical reviewing of my thesis and plenty discussions dealing with experimental issues. Dr. Katharina Galmbacher for her experimental help.
- Matthias Duechs, Victor Weidmann, Katharina Meder, Susanne Meyer, Sergi Mendoça-Funes and Maureen Menning for their valuable technical assistance.
- Verena Heisig and Biju Joseph for critical reviewing of this thesis. The animal caretakers, especially Markus Schreiber for his willingness to help.
- The members and organizers of the research training group 1141/1 (GCWN) for funding and support, especially Ralf Schreck.
- The whole institute MSZ and the department of microbiology, especially the bacterial tumor therapy unit for the nice working atmosphere.

- Finally I want to express my deep gratitude to my family. Without their education, encouragement and financial support this would not have been possible. Last but not least I want to thank my wife Julia for her constant support. I love you!